TAMPEREEN TEKNILLINEN YLIOPISTO
TAMPERE UNIVERSITY OF TECHNOLOGY

MAHMOOD REAZ SUNNY

SIZING AN ENERGY STORAGE TO BE USED IN PARALLEL WITH A PV INVERTER TO BALANCE THE FLUCTUATIONS IN OUTPUT POWER FROM PV GENERATOR

Master of Science Thesis

Examiner: Professor Seppo Valkealahti
Examiner and topic approved at the
Faculty Council meeting of the
Faculty of Computing and Electrical
Engineering on 5 March 2014

ABSTRACT

TAMPERE UNIVERSITY OF TECHNOLOGY
Master's Degree Programme in Electrical Engineering
SUNNY, MAHMOOD REAZ: Sizing an energy storage to be used in parallel with a PV inverter to balance the fluctuations in output power from PV generator
Master of Science Thesis, 102 pages
September 2014
Major: Smart grids
Examiner: Professor Seppo Valkealahti
Keywords: Photovoltaic system, energy storage, power fluctuations, grid-connected

Photovoltaic (PV) power systems are considered to be a significant part of future electricity generation infrastructure. Widespread implementation of PV power systems is necessary to establish a sustainable and environmentally friendly energy production and consumption system. However, the solar resource is inherently intermittent and the output power from PV generators closely follows the incident solar radiation. As a result, PV generated power can vary greatly and rapidly. Rapid changes in PV generated power can cause serious problems for relatively small power networks with high penetrations of PV generation. Traditional thermal power plants face difficulty to maintain the balance of power, when such rapid changes in power occur. Energy storage systems (ESS) are increasingly being used to integrate the PV power into the electricity grid. Energy storage systems can mitigate issues such as ramp rate deviations, frequency and voltage fluctuations etc. Power quality, network reliability and economic values of PV systems can be greatly enhanced by integrating energy storage systems with grid-connected PV power systems.

In this thesis, an ideal energy storage system of undefined capacity, rating and technology is used to control the output power of a theoretical 1 kW rated PV generator. Solar irradiance data measured with the climatic and electric measurement systems in TUT solar PV research power plant are used to simulate the output power of the 1 kW rated PV generator. The ESS subtracts power from the PV generated power and adds to the PV generated power, whenever necessary, to limit the ramp rate under 10 % of the PV generator capacity per minute. Three main application scenarios of the energy storage system are considered in this thesis. Firstly, the ESS controls the rate of change of PV generator output power when the PV inverter is rated at 100 % of the PV generator capacity. Secondly, the ESS controls the rate of change of PV generator output power when the PV inverter is rated at 70 % of the PV generator capacity (power curtailment is active). Thirdly, the ESS automatically recharges itself using the excess energy when power curtailment is active (inverter operates at 70 % of the PV generator capacity) while controlling the rate of change of PV generator output power. The objective of this thesis is to analyze the operations of the energy storage system in order to size suitable energy storage systems for practical operations.

Periodic (daily) and continuous operations of the ESS have been simulated and analyzed for each application scenario. For example, when the automatic recharging of the ESS is enabled during active power curtailment, the maximum energy stored in the ESS is found to be 1620 Wh during periodic operation. For the same application scenario, the maximum energy deficiency in the ESS is around 568 Wh. The energy balance in the ESS after one year of continuous operation is 77 kWh. The storage system operates for a total of 818 hours in one year. The maximum charging power of the ESS is 960 W and the maximum discharging power is 626 W.

PREFACE

This Master of Science Thesis has been done at the Department of Electrical Engineering of Tampere University of Technology. The supervisor and examiner of the thesis was Professor Seppo Valkealahti.

I would like to thank Professor Valkealahti for providing me with this interesting topic and for his guidance and suggestions. I would also like to thank Diego Torres Lobera and Kari Lappalainen for their help and guidance. Finally, I want to thank my family and friends for their unwavering support throughout my studies.

Tampere 22.06.2014

Mahmood Reaz Sunny

CONTENTS

SYMBOLS AND ABBREVIATIONS

Symbols

B_i	A constant independent of the operating temperature of a solar cell
c	Speed of light
D_{num}	Number of certain days in a year
D_s	Distance between the sun and the earth
E	Energy of an object
E_{coil}	Energy stored in an inductor coil
E_{g0}	Linearly extrapolated zero temperature band-gap of a solar cell semiconductor material
E_p	Energy of a photon
f	Frequency of a photon
F_F	Fill factor of a photovoltaic cell
G	Generation rate of electron-hole pairs per unit volume in a semiconductor material
G_λ	Spectral irradiance
h	Planck's constant
H_{ob}	Height of the vertical object casting a shadow
I	Output current of a photovoltaic cell
I_{coil}	Current flowing through an inductor coil
I_d	Diode current
I_L	Light generated current in a photovoltaic cell
I_{MP}	Current of a photovoltaic cell at the maximum power point
I_o	Dark saturation current of a diode
I_{SC}	Short-circuit current of a photovoltaic cell
k	Boltzmann's constant
L_{coil}	Inductance of a coil
m	Mass of an object
n	Ideality factor of a diode
N	Photon flux
N_s	Total number of solar cells in a series connection
P_{MP}	Power at the maximum power point
P_i	PV inverter capacity
q	Charge of an electron
r	Ramp rate limit
R_s	Series resistance of a photovoltaic cell
R_{sh}	Shunt resistance of a photovoltaic cell
S_{ob}	Length of the shadow cast by a vertical object
T_{abs}	Absolute temperature
T_b	Temperature of a blackbody

V	Voltage applied across a diode
V_{g0}	Linearly extrapolated zero temperature voltage of a solar cell
V_{MP}	Voltage of a photovoltaic cell at the maximum power point
V_{OC}	Open-circuit voltage of a photovoltaic cell
V_s	Voltage across a solar cell in a series connection of solar cells
x	Distance of photons from the surface of the semiconductor
α	Absorption coefficient
λ	Wavelength of a photon
δ	Solar declination
γ	Temperature dependency of remaining parameters of a solar cell
ε	Maximum solar declination
φ	Angle between the sun and the zenith

Abbreviations

AC	Alternating current
AM	Air mass
AM0	Air mass 0
AM1	Air mass 1
AM1.5	Air mass 1.5
AM2	Air mass 2
CAES	Compressed air energy storage
CES	Cryogenic energy storage
CH_4	Methane
DC	Direct current
DER	Distributed energy resources
DMFC	Direct-methanol fuel cell
DMPPT	Distributed maximum power point tracking
DOD	Depth of discharge
ESS	Energy storage system
EU	European union
ECDL	Electrochemical double layer super-capacitors
HT-TES	High temperature thermal energy storage
IEA	International energy agency
$LiCoO_2$	Lithium cobult oxide
$LiMnO_2$	Lithium manganese dioxide
$LiFePO_4$	Lithium iron phosphate
$LiPF_6$	Lithium hexafluorophosphate
$LiAsF_6$	Lithium hexafluoroarsenate monohydrate
$LiClO_4$	Lithium perchlorate
$LiBF_4$	Lithium tetrafluoroborate
$LiCF_3SO_3$	Lithium triflate

LT-TES	Low temperature thermal energy storage
MCFC	Molten carbonate fuel cell
MPP	Maximum power point
MPPT	Maximum power point tracking
N	North
NaS	Sodium sulfur
NbTi	Niobium titane
NH_3	Ammonia
NiCd	Nickel cadmium
NiMH	Nickel metal hydride
NiZn	Nickel zinc
NOC	Normal operating conditions
PHS	Pumped hydroelectric storage
PCM	Phase change materials
PREPA	Puerto Rico Electric Power Authority
PSB	Polysulfide bromide battery
PV	Photovoltaic
RES	Renewable energy sources
RTIL	Room temperature ionic liquids
S	South
SMES	Superconducting magnetic energy storage
STC	Standard test conditions
TES	Thermal energy storage
UPS	Uninterrupted power supply
VRB	Vanadium redox battery
ZnO	Zinc oxide
ZnBr	Zinc bromine

1 INTRODUCTION

One of the most important challenges for the 21st century is to ensure sustainability of the planet while meeting the ever-growing energy demands. Consumption of energy is rapidly increasing due to industrialization of developing countries. Furthermore, growth in electricity demand is rising faster than other primary energy demands. For example, according to International Energy Agency (IEA), electricity energy demand in India may rise as much as 282% by the year 2030. Electricity demand in China could rise up to 195% by the year 2030. Fossil fuels such as oil, coal and gas have been the dominant sources of energy since the up rise in energy consumption began in the late 18th century. In 20th century, nuclear power has been added as a major source of electrical energy.[1]

All these conventional sources of energy pose significant challenges in meeting the future energy demands as well as severely threaten earth's environment. Conventional sources such as oil, coal, gas and uranium, do not regenerate in nature at any significant rate and thus, are considered as finite sources. Depending on the prices, usages, policies and international relations, these conventional fuel reserves will run out eventually. Thus, the current dependence on the fossil fuels for electrical energy production is far from a sustainable practice. Furthermore, emissions from fossil fuel combustions further signify the disadvantages of fossil fuels. Increasing amount of carbon dioxide (CO_2) emissions from fossil fuels into the environment enhances the *greenhouse effect*. Greenhouse effect or global warming is considered as a major environmental problem and energy sector is responsible for two-thirds of the global greenhouse gas emissions. Increasing concentration of greenhouse gasses such as carbon dioxide, nitrous oxides, chlorofluorocarbons and methane in the atmosphere leads to higher amount of radiated heat being trapped inside earth's atmosphere. As a result, surface temperature of the earth increases. During 20th century, earth's surface temperature has increased about 0.6 ˚C and consequently, sea level is estimated to have risen by 20 cm. Due to present trends of fossil fuel consumption, the surface temperature of the earth may increase by 2 to 4 ˚C over the 21st century. Consequently, sea level may rise from 30 to 60 cm by the end of 21st century. Rising of the earth's surface temperature and of the sea level will endanger nature and all of the earth's habitats. Natural disasters may occur more frequently. Flooding of coastal settlements and displacement of fertile lands toward higher latitudes may occur. Availability of fresh water for irrigation and other uses may also be affected consequently. Survival of entire populations could be at risk if preventive measures are not taken in time. In addition to these, catastrophic risk factors are associated with nuclear power plants. Highly radioactive wastages from nuclear power plants

need to be safely contained for a long time, stretching centuries. Moreover, containment failures in reactors of nuclear power plants could result in the release of radioactive materials into the environment, which could destroy human lives and natural ecosystem alike. [1-3]

Renewable energy sources are much more compatible with sustainable development than fossil and nuclear fuels, in terms of both resource limitations and environmental impacts. Renewable energy sources such as wind power and solar power systems can very easily provide the energy needs of the earth's entire population without adversely affecting the natural environment. Thus, widespread implementation of renewable energy sources is now considered a significant part of most sustainable development plans in the world. For example, to implement sustainable energy production and consumption practices, European Union (EU) has set energy and emission targets for the year 2020, known as the "20-20-20" targets. The targets of the energy policy include a reduction in EU greenhouse gas emissions of at least 20% below the levels of 1990, 20% share of renewable energy in EU energy consumption and a 20% reduction in primary energy usage compared to projected levels by improving energy efficiency. EU has also undertaken studies to establish a guideline named "Roadmap 2050". The objective is to reduce the greenhouse gas emission below 80% compared to 1990 levels by the year 2050. In order to reduce the greenhouse gas emissions significantly, it is estimated that renewable energy sources will have to achieve a significant share (40 to 80%) in total energy production by 2050. [3-5]

Solar and wind energies are considered to be the most promising renewable energy sources. There has been spectacular growth in wind energy since the beginning of the 21st century. At the end of the year 2000, global installed capacity of wind power systems was 18 GW. At the end of 2011, the capacity was around 238 GW worldwide. Solar energy is considered to have even more promise compared to wind energy. Based on the method of exploitation, solar energy is generally classified into two categories: *solar photovoltaic* (PV) and *concentrating solar power* (CSP). Solar photovoltaic systems directly convert solar energy into electrical energy using photovoltaic cells made of semiconductor materials such as silicon. Concentrating solar power systems concentrate energy from solar radiation to heat a receiver. This heat is then converted into mechanical energy and then into electrical energy. Solar PV has been the fastest growing renewable power production technology in recent years. Total installed capacity of solar PV systems was around 65 GW at the end of 2011, compared to only 1.5 GW in 2000. In comparison, total installed capacity of CSP systems is around 1.5 GW currently. [6; 7]

Photovoltaic cells, made of semiconductor materials, are the building blocks of photovoltaic systems. PV cells convert the energy of photons in solar radiation, into electrical energy. As the output voltage and current of a PV cell is very low, in most applications, PV cells are interconnected with each other in different combinations and en-

closed in modules, which are referred to as *PV modules*. PV cells inside a PV module are interconnected in series, parallel or in hybrid configurations to increase module output voltage and current. PV generators are in turn created using different series, parallel or hybrid configurations of PV modules. PV generators are thus considered modular systems and can be designed for a wide range of output power.

Solar PV systems can be classified into two categories based on implementation, *stand-alone PV systems and grid-connected PV systems*. In stand-alone PV systems, inverters and energy storages are often used. The output from a PV generator is in the form of *direct current* (DC), which can only drive DC loads. Inverters are used with PV generators to drive *alternating current* (AC) loads. Typically, energy storages are used in stand-alone systems to store energy to be used at night or when additional power is needed. In grid-connected PV systems, inverters are used with PV generators to connect with the electric utility grids. Energy storages are also used in grid-connected PV systems. These energy storages are considered to have potential in many aspects, when used in grid-connected PV systems. Excess energy can be stored during off-peak hours and can be used to provide additional support to meet peak demands. Energy storages can also be used to ensure reliable power quality. PV systems are considered as intermittent energy sources, because the output power from PV generators varies mainly with incident solar irradiance on the modules. For example, incident solar irradiance may vary due to moving clouds. Thus, the output power from a PV generator fluctuates. Energy storages can be used to compensate for the fluctuations. Hence, quality and reliability of the power fed into the utility grid are increased. Energy storage systems can also be used to control the rate of change of PV generator output power to further ensure reliability. Moreover, energy storages can perform additional ancillary services to the grid, such as, voltage and frequency regulation, reactive power provision etc.

The objective of this thesis is to study the application of energy storage systems in grid-connected PV systems to balance the output power of the PV generators. Three main application scenarios of an energy storage system are considered in this thesis. Firstly, the energy storage system (ESS) controls the rate of change of PV generator output power when the PV inverter operates at 100 % of the PV generator capacity. Secondly, the energy storage system controls the rate of change of PV generator output power when the PV inverter operates at 70 % of the PV generator capacity. Thirdly, the ESS recharges automatically when power curtailment is active (Inverter operates at 70 % of the PV generator capacity) while controlling the rate of change of PV generator output power. The ESS subtracts from the PV generated power and adds to the PV generated power, whenever necessary, to control the ramp rates in the PV generated output power. By studying the applications of the energy storage system described above, suitable sizes of the storage systems can be determined for PV generators of different capacities. The grid-connected solar PV research power plant equipped with climatic and electric measurement systems in Tampere University of Technology is used to analyze

the fluctuations in PV generator output power. Solar irradiance data measured and recorded at 10 Hz sampling rate for twenty months are used as input to a theoretical 1 kW rated PV generator to analyze the operation of the theoretical energy storage system.

The thesis is organized as follows: Chapter 2 briefly discusses the properties of the solar radiation and the effect of the atmosphere on solar radiation. In chapter 3, basic properties of semiconductor materials from which the PV cells are made of, are discussed. Electrical properties of PV cells and the effect of operating conditions such as temperature and irradiance on the PV cells are discussed as well. In chapter 4, construction and configuration of PV systems are provided. Interconnected PV cells create PV modules and interconnected PV modules create PV generators. Different configurations of stand-alone and grid-connected PV systems are discussed as well. Important components such as inverters are also discussed in this chapter. In chapter 5, different energy storage technologies are discussed. Potential applications and advantages of energy storage technologies in the field of electrical energy sector are analyzed. At the end of this chapter, general assessment of different storage technologies, in terms of suitability with renewable energy sources, is provided. In chapter 6, the applications of an energy storage system connected to a grid-connected PV generator are analyzed. The simulated long-term operation of the storage unit, where the storage unit operates to balance the PV generator output power, is analyzed. The results of the analyses are also discussed in this chapter. Finally, in chapter 7, conclusions of the thesis are presented.

2 SOLAR RADIATION

The Sun produces energy via nuclear fusion, where hydrogen nuclei are converted into helium nuclei. In accordance with the equation $E = mc^2$, energy is released from this process, because the mass of the helium nuclei that are produced is lower than that of the hydrogen nuclei. The output power of this nuclear reaction is approximately 3.85×10^{17} GW. Hence, solar energy is in fact nuclear energy. [8]

The Earth rotates around the Sun in a slightly elliptical orbit once per year. The orbit has an average distance of 149.6 million kilometers. Solar radiation is distributed evenly in all directions, thus the irradiance at the outer edge of the Earth's atmosphere averages to 1367±2 W/m². This amount varies from a maximum of 1414 W/m² to a minimum of 1322 W/m² due to the slightly elliptical nature of the Earth's orbit. [8]

The amount of solar energy that the Earth receives is over 1000 times higher than the total energy used by the humans. As the fossil fuels continue to run out due to heavy usage, capturing and exploiting the huge amount of solar energy is paramount in importance for a sustainable future. [8]

2.1 Particle-wave duality and blackbody radiation

The current understanding of the nature of light is the result of efforts from the scientists over a few centuries. Newton's mechanistic view of light, where he explained that the light is made up of small particles was prevalent in the late 1600s. By the early 1800s, Young and Fresnel discovered the interference effects in light beams, thus indicating that light was made up of waves. Maxwell's theories of electromagnetic radiation were accepted by 1860s, which defined light as a spectrum of electromagnetic waves with different wavelengths. Electromagnetic radiation has been regarded as both waves and particles after Einstein explained the photovoltaic effect in 1905. Einstein proposed that light was made up of discrete particles or 'quanta' of energy. The complementary nature of electromagnetic radiation is called *particle-wave duality*, which is well accepted now and can be described with the following equation

$$E_p = hf = \frac{hc}{\lambda}, \tag{2.1}$$

where light, of frequency f or wavelength λ, comes in 'packets' or photons, of energy Ep, h is Planck's constant (6.626×10^{-34} Js) and c is the velocity of light (3.00×10^8 m/s). [9]

Thermal radiation is electromagnetic radiation, which is generated by the thermal motion of charged particles in matter. All matters with a temperature greater than absolute zero temperature emit thermal radiation. A 'blackbody' is an ideal absorber, and emitter of radiation. In 1900, Max Planck derived a mathematical expression describing the wavelength distribution of light emitted from a heated object. According to Max Planck, the spectral irradiance of a blackbody can be expressed as

$$G_\lambda(\lambda, T_b) = \frac{2\pi hc^2}{\lambda^5\left[\exp\left(\frac{hc}{\lambda k T_b}\right)-1\right]}, \tag{2.2}$$

where G_λ is the power per unit area per unit wavelength, k is the Boltzmann's constant (1.38065×10^{-23} J/K), and T_b is the temperature of the blackbody.

Because of the massive thermonuclear fusion reaction occurring in the sun, the surface of the sun has a temperature of approximately 5800 K. The energy released by the fusion reaction radiates away from the sun uniformly in all directions, in accordance with equation 2.2. The spectrum of a blackbody radiation at three different temperatures, as observed at the surface of the blackbody, is shown in figure 2.1. [10]

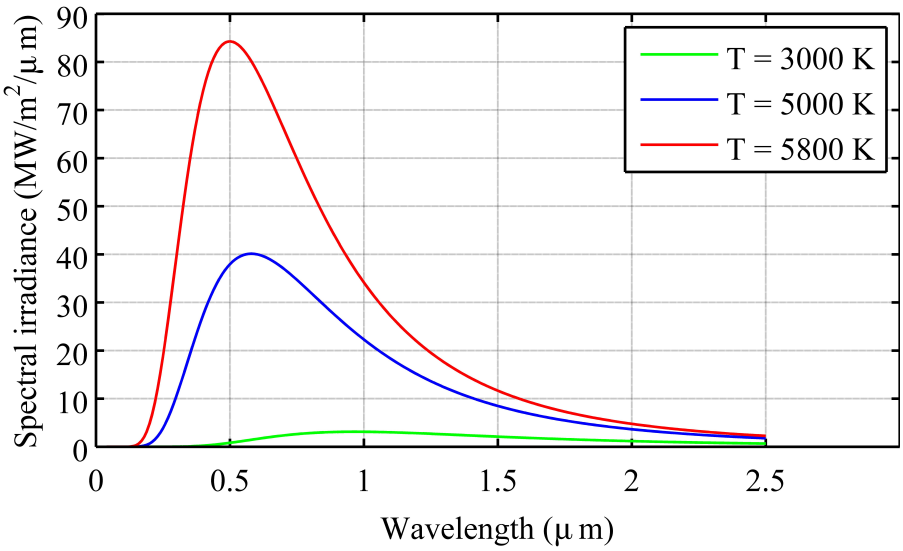

Figure 2.1: *Blackbody radiation spectra are shown for temperatures of 3000 K, 5000 K and 5800 K.*

Typical human eye responds to wavelengths of 390 to 700 nm of electromagnetic radiation, which is referred to as 'visible light'. The lowermost curve in figure 2.1 represents the temperature of 3000 K, where most of the incandescent lamps operate. Only a small portion of emitted energy lies in the visible region, thus making the incandescent lamps very inefficient. The sun, on the other hand, has a surface temperature of approximately 5800 K, and the characteristic white color of the sunlight is obtained due to

the mix of wavelengths in the visible spectral range. Thus, the sun can be reasonably approximated as a blackbody radiator. [10]

2.2 Effect of the atmosphere on solar radiation

The sun is a hot sphere of gas; heated by thermonuclear fusion reactions at its core, with internal temperatures close to 20 million K. This high temperature creates intense radiation from the interior of the sun, but the radiation is absorbed by a layer of hydrogen ions close to the sun's surface. Energy transfers by convection through this layer and then radiates from the outer surface of the sun, called 'photosphere'. The radiation emitted from the surface of the sun is similar to the radiation emitted from a blackbody with a surface temperature of nearly 6000 K. [9]

Radiation from the sun's surface is reasonably constant, but by the time it reaches the earth's surface, it varies due to absorption, scattering and reflection by molecules and objects. Different molecules in the atmosphere affect the radiation differently. Water vapor, carbon dioxide and ozone, for example, have several significant absorption wavelengths. Ozone absorbs a significant amount of radiation in the ultraviolet region of the spectrum while water vapor and carbon dioxide absorb mainly in the visible and infrared parts of the spectrum. [10]

Sunlight that reaches the earth's surface without scattering is called *direct* or *beam radiation*. Sunlight that is scattered is called *diffuse radiation*. If the sunlight is reflected from the ground, then it is called *albedo radiation*. The sum of all three components of sunlight is called *global radiation*. [10]

The maximum radiation reaches the earth's surface when the sky is clear and the sun is directly overhead, thus the sunlight has the shortest path through the atmosphere. This path can be approximated by $1/\cos\varphi$, where φ is the angle between the sun and the point directly overhead. This length of the path is generally referred to as the *Air Mass* (AM). [9] Therefore,

$$AM = 1/\cos\varphi \tag{2.3}$$

Air Mass equals to 1 (AM1) when φ is equal to zero. When φ is equal to 60°, the Air Mass equals to 2 (AM2). AM1.5 is defined as when the sun is at an angle of 48.2° from overhead and is accepted as the standard calibration spectrum for photovoltaic cells. The spectral distribution of sunlight outside the atmosphere (Air Mass Zero or AM0) is essentially unvarying and its total power density, integrated over the spectrum, is called the *solar constant*, with a generally accepted value of 1.3661 kW/m^2. [9]

The Air Mass can be estimated by using the following formula:

$$AM = \sqrt{1 + (\frac{S_{ob}}{H_{ob}})^2}\ , \tag{2.4}$$

where S_{ob} is the length of the shadow cast by a vertical post of height H_{ob}, as shown in figure 2.2. [9]

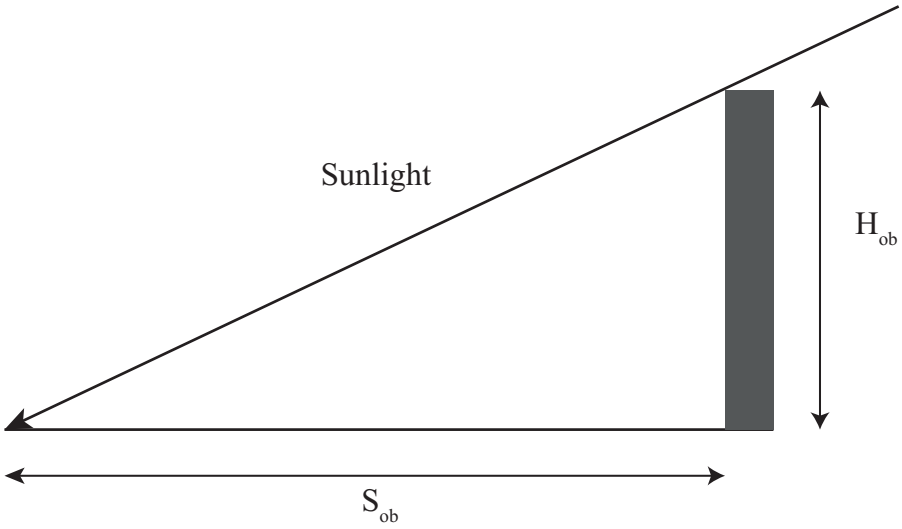

Figure 2.2: *Calculation of Air Mass using the shadow of an object of known height.*

Power density of sunlight is expressed as *irradiance* and is measured in W/m^2. The value of solar irradiance reduces to approximately 1000 W/m^2 when it passes through the earth's atmosphere with a path length of AM1. Spectral content of the radiation is also modified due to atmospheric absorptions. *Irradiation* is the integral of irradiance. Thus, it is the measure of energy density of sunlight and is expressed in kWh/m^2. [10]

Atmospheric gases such as oxygen, ozone, water vapor and carbon dioxide absorbs the sunlight passing through the earth's atmosphere. For example, ozone absorbs wavelengths below 0.3 μm. If the ozone layer in the atmosphere is depleted, more short wavelength components of sunlight come through the atmosphere, which is very harmful to the planet's biological systems. Scattering of sunlight at short wavelengths creates diffuse components of sunlight, which comes from all directions in the sky. Diffuse radiation is primarily at the blue end of the spectrum, thus the sky appears blue to our eyes. AM1 radiation contains 10% diffuse components when the sky is clear. The percentage of diffuse radiation increases with increasing air mass or decreasing sky clarity. Radiation is also attenuated and scattered due to clouds in the sky. Solar radiation can be effectively blocked by low altitude *cumulus* or bulky clouds. However, diffuse radiation helps to recover about half of the blocked radiation by cumulus clouds. *Cirrus* or wispy high altitude clouds also blocks the sunlight but almost two thirds of the direct beam sunlight is converted to diffuse components. Hence, on a cloudy or overcast day with little to no sunshine, most of the radiation that reaches the earth's surface consists of diffuse radiation.[9]

On average, the earth re-radiates the same amount of heat it absorbs daily. This steady state ensures that the earth's average temperature remains constant. This state of delicate balance can be disrupted if the amount of heat absorbed is not equal to the amount of heat re-radiated by earth. For example, volcanoes that fill the atmosphere with fine ash, which reflects the sunlight away from earth, (thus reducing the amount of incident sunlight) can disrupt the temperature balance. The balance can also be disrupted by gases such as carbon dioxide, nitrous oxides, chlorofluorocarbons and methane, which are mostly transparent to short wavelength (visible) radiation, but more absorbing to long wavelength (infrared) radiation. The incident sunlight is mostly composed by short wavelength components, which is similar to radiation from a blackbody (in this case, the Sun) of 5800 K surface temperature. The re-radiated energy has longer wavelength light components, due to the earth's surface temperature being approximately 300 K. As a result, these greenhouse gases restrict the earth from re-radiating at night. It has been observed that average terrestrial temperatures have increased throughout the 20th century. Along with the change in global temperature, the increased variability of climate is also apparent. Extreme climate phenomena such as floods and droughts are also predicted to be increasing in frequency and intensity. [9; 10]

2.3 Apparent motion of the sun

The earth rotates around the sun in an elliptical orbit with the sun at one of the foci, so the distance from the sun to earth can be calculated by

$$D_s = 1.5 \times 10^{11} \left\{1 + 0.017\, sin\left[\frac{360(D_{num}-93)}{365}\right]\right\} \text{ m}, \tag{2.5}$$

where D_{num} is the day of the year, with January 1 as day 1. Since the deviation of the orbit from circular is very small, this distance can be generally expressed in terms of its mean value. [10]

The earth also rotates about its own polar axis once per day. The polar axis of the earth is inclined by an angle of 23.45° to the plane of the earth's orbit around the sun. Due to this inclination, the sun appears to be higher in the sky in the summer than in the winter. Moreover, longer summer daylight hours and shorter winter daylight hours are also caused by the inclination. Figure 2.3 shows the earth's orbit around the sun with the inclined polar axis. The earth is closest to the sun, about 1.47×10^8 km, around January 3rd and farthest away, about 1.53×10^8 km, around July 4th. The angle between the equator and a line drawn from the center of the sun to the center of the earth is called the *declination*, δ. To calculate the declination, angles north of the equator are considered as positive and angles south of the equator are considered as negative. The declination can be found from the following formula:

$$\delta = 23.45° \, sin\left[\frac{360(D_{num}-80)}{365}\right], \tag{2.6}$$

where D_{num} represents the day of the year, with January 1 as day 1. [10]

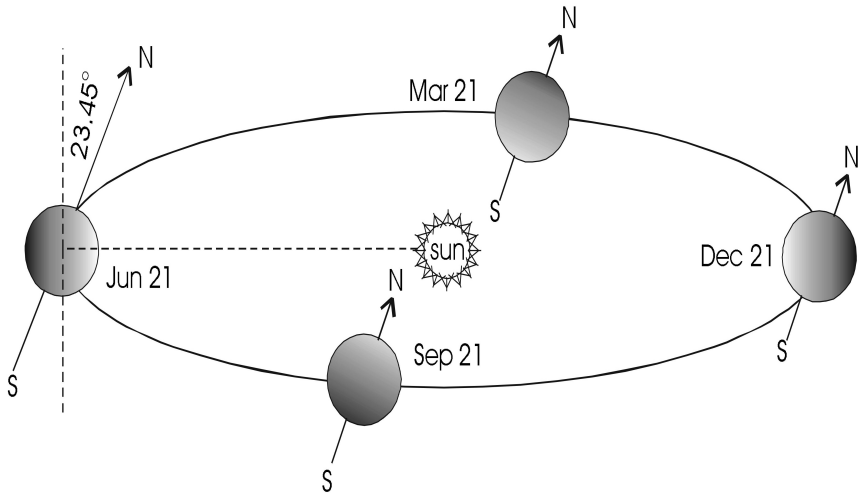

Figure 2.3: *The orbit of the earth, and the declination at different times of the year.* [10]

Solar declination is zero at the equinoxes around March 21st and September 23rd. On these days, the sun rises due east and sets due west. The maximum value of solar declination, ±23.45º occurs at the solstices around June 22nd and December 22nd. The apparent motion of the sun, and its position at solar noon; relative to a fixed observer at latitude 35º S (or N) is shown in figure 2.4.

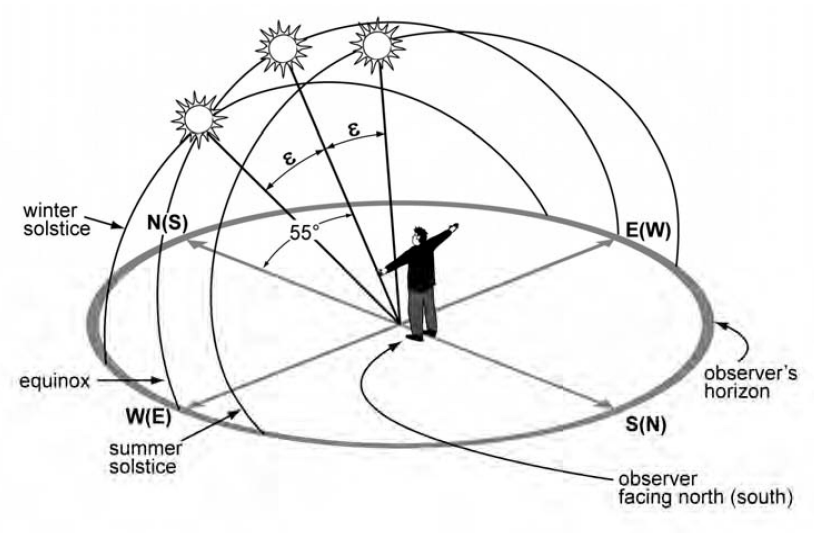

Figure 2.4: *Apparent motion of the sun for an observer at 35° S (or N), where ε is the maximum solar declination.* [9]

It can be observed from figure 2.4 that the sun is never at zenith, in latitudes more than the inclination of the earth's axis, 23.45º S or N. In winter season, the sun is much

lower in the sky than in the summer season, which means that the value of Air Mass is greater on average in winter. The Air Mass is also higher when the sun rises in the morning and sets down in the evening. Solar irradiance spectrum and solar irradiation are both effected by the Air Mass value. [9]

3 PHOTOVOLTAIC CELLS

A photovoltaic cell is a device that converts the energy received from solar radiation into electrical energy. Most PV cells are made of semiconductor materials such as silicon and germanium. Thus, the operation of PV cells can be understood better by studying semiconductor physics briefly.

3.1 Semiconductors and p-n junctions

In 1839, Becquerel observed that certain materials produced electric current when exposed to light. This phenomenon is known as the *photovoltaic effect* and is the basis of the operation of photovoltaic or solar cells. [9]

Solar cells are manufactured using semiconductor materials. Semiconductor materials act as insulators at low temperatures, but when heat or energy is applied, these materials act as conductors. Semiconductor materials belong to group IV of the periodic table, which means that they have four electrons on the outermost shell. Silicon is most commonly used material in PV cells, because of its good light absorption properties and for its mature manufacturing techniques. The electrical properties of semiconductors can be explained using two models, the *bond* and the *band* models. [9]

According to bond model, silicon atoms are joined together by covalent bonds. Figure 3.1 illustrates the bonding and the movement of electrons in a silicon crystal lattice. The bonds remain intact when in low temperatures, thus the silicon acts as an insulator. When at high temperatures, some bonds get broken after receiving external energy from heat and conduction occurs due to free electrons. The electrons from broken bonds become free to move and electrons from neighboring bonds also occupy the ‘holes’ left by the free electrons, thus the ‘holes’ also propagate as apparent positive charges within the material. [9]

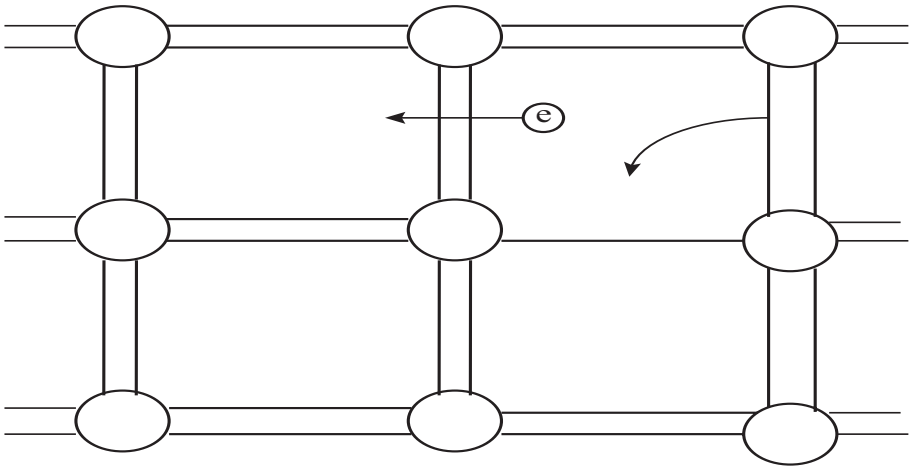

Figure 3.1: *Schematic representation of covalent bonds in a silicon crystal lattice.* [9]

The band model describes semiconductor behavior in terms of energy levels between valence and conduction bands, as can be seen in figure 3.2. The electrons fill the bands from lowest energy to the highest one. The band with the highest energy, which is fully occupied by electrons, is called the valence band. The next band with higher energy than the valence band is called the conduction band. The energy difference between these bands is called the energy gap or the forbidden gap. Electrons in the valence band can absorb necessary energy to jump from valence band to the conduction band, where the electron is free to move around. Consequently, electrons leave 'holes' in the valence band when travelling to the conduction band. Adjacent electrons to the holes can move into it, thus the movement of electrons also occurs in valence band, because of receiving energy from an external source. This movement of electrons in the valence band is generally described as the movement of 'holes', similar to a positive charge. [9]

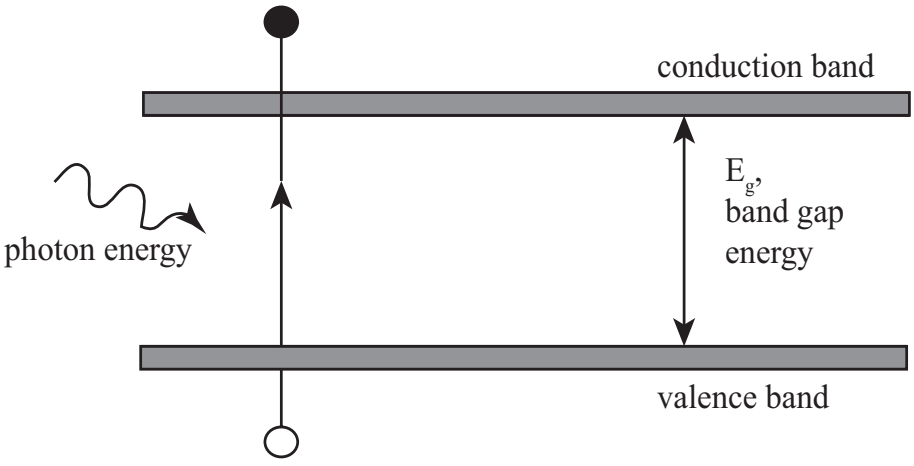

Figure 3.2: *Schematic of the energy bands for electrons in a solid.* [9]

In case of solar cells made by semiconductor materials, when photons in the incident solar radiation possess sufficient energy, i.e. when $hf > E_g$, they are absorbed by the semiconductor materials. The electrons in the material, excited by the received energy

by photons, can make the jump from valence band to conduction band. Photons with energy less than the band gap energy interact only weakly with the semiconductor, passing through it as if it were transparent. Thus, the conductivity of the semiconductor depends on the band gap energy, i.e. the stronger the band gap energy; the fewer electrons move to the conduction band. Photons with higher energy are absorbed closer to the semiconductor surface. The generation rate (G) of electron-hole pairs per unit volume can be calculated using the following formula,

$$G = \alpha N e^{-\alpha x} , \tag{3.1}$$

where N is the photon flux at the surface, α is the absorption coefficient, and x is the distance from the surface. In the absence of light, the electron-hole pairs must disappear to maintain a state of equilibrium. With no external source of energy, the electrons and holes eventually recombine. The average time for recombination to occur after the generation of electron-hole pairs in a semiconductor material is defined as *carrier lifetime* of that material. The carrier lifetime for silicon is typically 1 μs. The average distance a current carrier can move from the point of generation until recombination occurs is defined as the *carrier diffusion length*. Typical diffusion length of silicon is from 100 to 300 μm. [9]

Silicon and other semiconductors have low electrical conductivities. The conductivity of semiconductor materials can easily be modified by introducing impurities into their crystal lattice. The process of adding controlled impurities to a semiconductor is referred to as *doping*. Atoms with one more valence electron than the semiconductor are used to produce 'n-type' material. For example, a silicon atom can be replaced by a phosphorus atom with five valence electrons in the outermost shell. Due to having five valence electrons, one of those electrons will be unable to bond with one of the four adjacent silicon atoms. Thus, the electron can liberate itself from its atomic nucleus and this process creates an electron-hole pair. As the phosphorus atom donates an electron to the crystal lattice, it can be called as a *donor* and the donated electron is called *donor electron*. The energy of the donor electron is only slightly less than the threshold for the conduction band. Thus, only a small amount of energy is needed for the donor electron to move to the conduction band. As the donor electrons are negative charge carriers, these semiconductor materials are called 'n-type' semiconductors. In n-type semiconductors, electrons are called *majority charge carriers* and holes are called *minority charge carriers.* Figure 3.3 demonstrates the doping process for n-type material. [8]

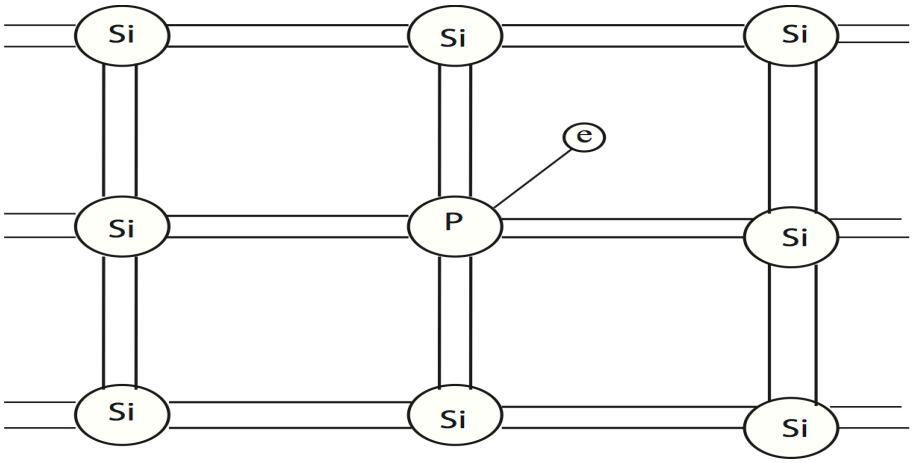

Figure 3.3: *Schematic of silicon crystal lattice doped with phosphorus atom.* [8]

Atoms with one less valence electron than silicon can be used in a crystal lattice structure to produce 'p-type' material. A boron atom, which has three valence electrons in its outermost shell, can be used to replace one of the silicon atoms in the crystal structure. As a result, only three silicon atoms can construct bonds with the boron atom and a hole is created due to the shortage of one electron. An electron from an adjoining atom's valence band can fill this hole since only a small amount of energy is needed and thus, the movement of 'holes' occurs in the crystal lattice. A hole in a valence band can move as freely as a free electron in the conduction band. A boron atom accepts an electron from a silicon atom, so it is referred to as an *acceptor*. A Silicon atom, which donates electrons to boron atom, is thus called a *donor*. Thus, a p-type semiconductor material is produced which consists of positive charge carriers. Figure 3.4 demonstrates the doping process for p-type semiconductor materials. [8]

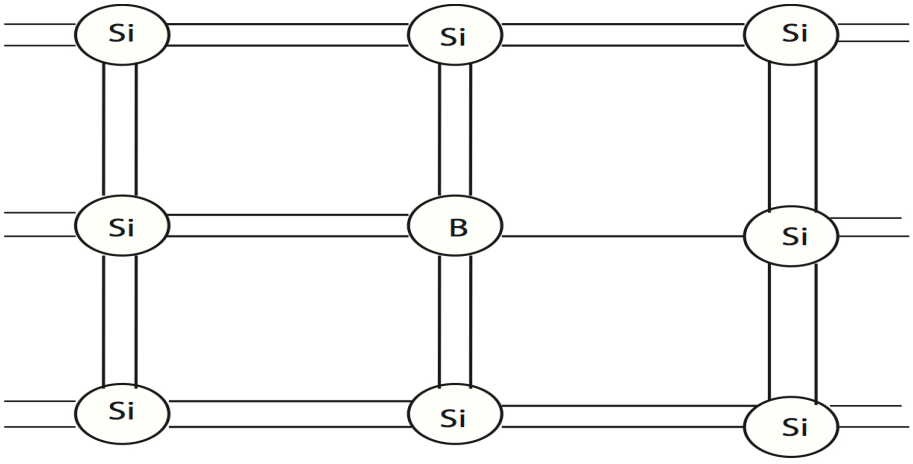

Figure 3.4: *Schematic of silicon crystal lattice doped with boron atom.* [8]

A p-n junction can be formed by joining n-type and p-type semiconductors. Because of the difference in concentration, the excess electrons in n-type material tend to move towards the p-type material. Similarly, excess holes in p-type materials tend to diffuse

towards n-type materials. The electrons leave behind a positive charged region and the holes leave behind a negatively charged region. Thus, a depletion region is formed where an electric field is present to restrict the movement of holes and electrons. The formation of p-n junction is shown in figure 3.5.

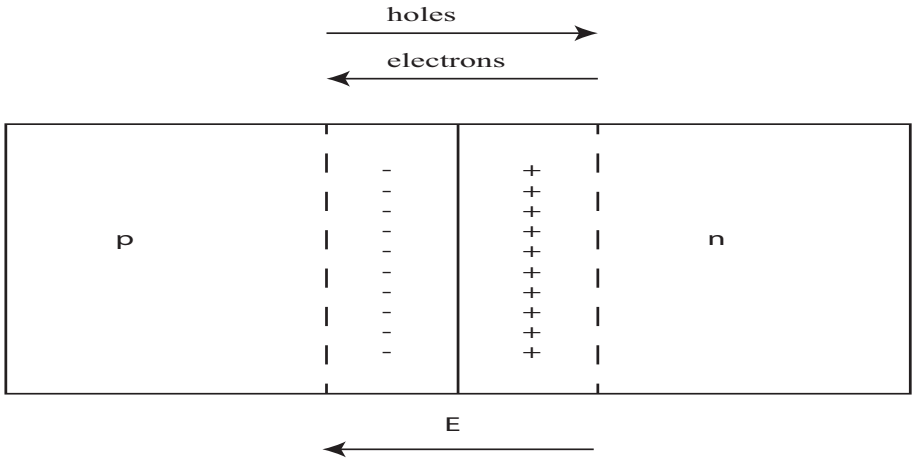

Figure 3.5: *Formation of a p-n junction.* [9]

The voltage due to the formation of electric field can be reduced by applying an external voltage across the material, where the direction of voltage is positive at p-type end. When the electric field in the depletion region is sufficiently reduced, current flow is possible. The application of voltage across a p-n junction is shown in figure 3.6.

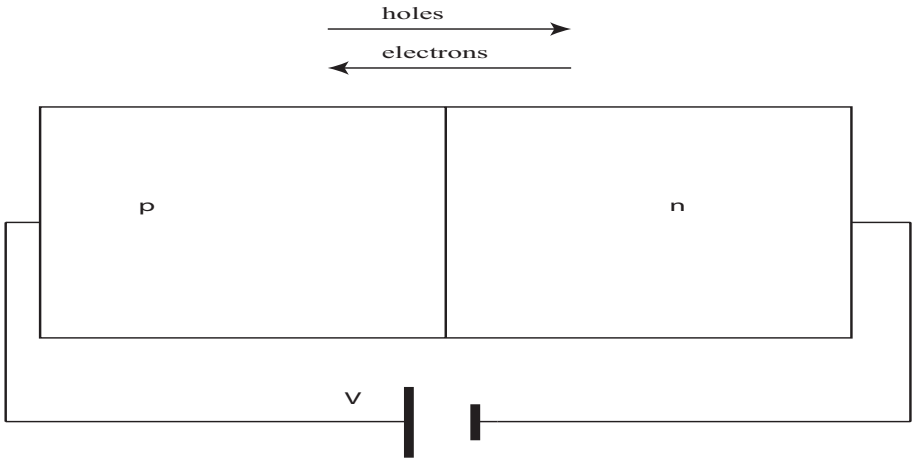

Figure 3.6: *Application of voltage to a p-n junction.*

The current flow increases with increased applied voltage. This phenomenon, called *Ideal Diode Law* can be expressed as

$$I_d = I_0 \left[exp\left(\frac{qV}{kT_{abs}}\right) - 1 \right], \tag{3.2}$$

where I_d is the current produced due to the voltage applied, I_0 is the dark saturation current (the diode leakage current density in the absence of light), V is the applied voltage, q is the charge on an electron, k is the Boltzmann's constant and T_{abs} is the absolute temperature. The dark saturation current, I_0 decreases as the quality of the material increases. I_0 also increases with increased absolute temperature. For actual diodes, the equation 3.2 becomes

$$I_d = I_0 \left[exp\left(\frac{qV}{nkT_{abs}}\right) - 1 \right], \tag{3.3}$$

where n is the ideality factor, which has a value between 1 and 2. The diode law for silicon is illustrated in figure 3.7.

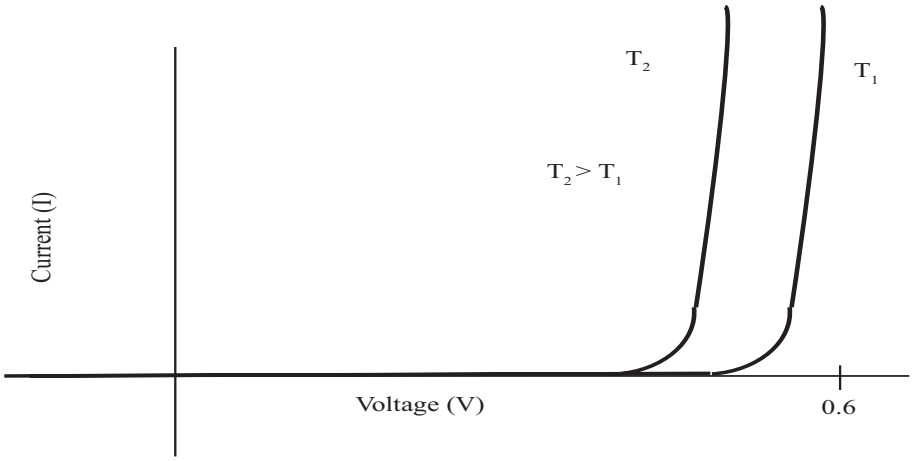

Figure 3.7: *The diode law for silicon: Current as a function of voltage for temperatures T_1 and T_2 ($T_2 > T_1$). For a given current, the curve shifts by approximately 2mV/°C.*

The minimum energy difference between the top of the valance band and the bottom of the conduction band is called band gap energy. In a direct band gap semiconductor, the top of the valence band and the bottom of the conduction band occur at the same value of electron momentum. In an indirect band gap semiconductor, the maximum energy of the valence band and the minimum energy of the conduction band occur at a different value of electron momentum. In direct band gap semiconductors such as gallium arsenide, electrons can absorb the energy from incident photons to travel from the valence band to the conduction band. In indirect band gap semiconductors such as silicon, phonon absorption or emission is required in addition to photon absorptions for the electron to travel from valence band to conduction band. A phonon is the particle representation of lattice vibrations in semiconductor materials. Phonons possess significant momentum but very little energy, which helps the electron to increase its momentum to travel towards the conduction band without increasing too much energy by absorbing phonons. Conversely, by emitting phonons, electrons can decrease momentum without losing high amount of energy. Photon absorption coefficients for indirect band gap semiconductors are relatively lower due to the requirements of phonons with necessary

momentums in the process. As a result, light penetrates more deeply into indirect band gap semiconductors than direct band gap semiconductors. [9]

Although not as dominant as the processes discussed above, there are other light absorption processes possible for both direct and indirect band gap semiconductors. A direct transition is possible in indirect band gap semiconductors, without the assistance of phonons, if the energy of the photon is high enough. Similarly, phonon-assisted transition is also possible in direct band gap materials. [9]

3.2 Electrical properties of photovoltaic cells

A typical photovoltaic cell is a diode that can be constructed by joining p-type and n-type silicon. Typically, the p-type silicon is doped with boron atoms and n-type silicon is doped with phosphorous atoms. The characteristic curve of a silicon diode was shown in figure 3.7 by plotting current I against voltage V when no incident light was available. If a cell is illuminated, a light generated current I_L is introduced in the diode law equation, which is

$$I = I_0 \left[exp\left(\frac{qV}{nkT}\right) - 1 \right] - I_L \,, \tag{3.4}$$

where I_L is the light-generated current. The light shifts the I-V curve down into the fourth quadrant where power can be extracted from the diode. The ideal characteristic curves of illuminated and non-illuminated solar cells are shown in figure 3.8. [9]

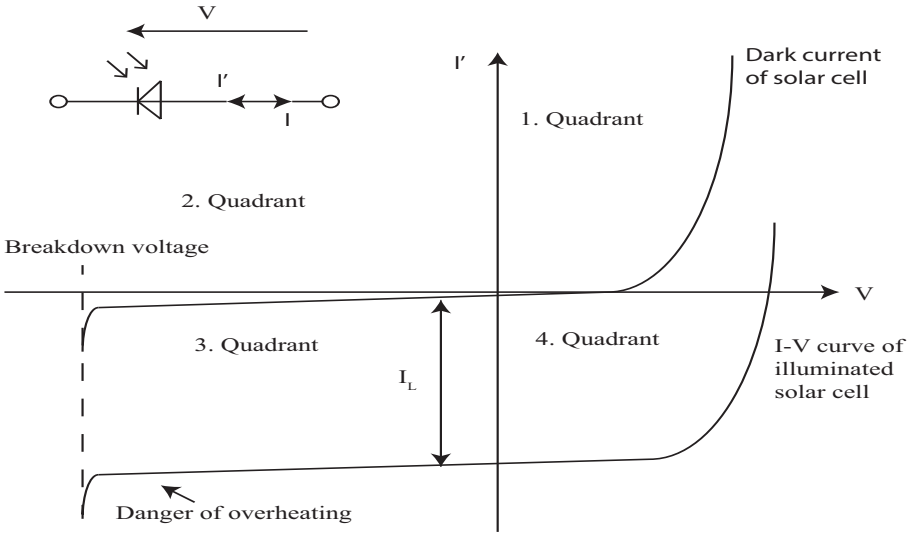

Figure 3.8: *Idealized characteristic curves of illuminated and non-illuminated solar cells.* [8]

The I-V curve is most often shown in reverse, with the output curve in the first quadrant, and can be represented by

$$I = I_L - I_0 \left[exp\left(\frac{qV}{nkT}\right) - 1 \right]. \tag{3.5}$$

The electrical model of the photovoltaic cell can be shown in figure 3.9 below.

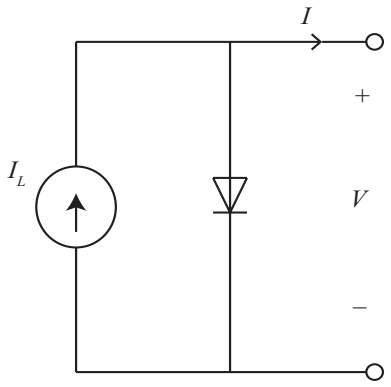

Figure 3.9: *The electrical model of a photovoltaic cell.* [9]

Two limiting parameters are used to characterize the output of photovoltaic cells, short circuit current (I_{SC}) and open circuit voltage (V_{OC}). The maximum current available when the voltage is zero is called the short circuit current. I_{SC} is directly proportional to the incident sunlight to a reasonable approximation. Open circuit voltage is the maximum voltage available at zero current. Due to both limiting parameters, solar cells are not damaged when operating under either open circuit or short circuit conditions. The open circuit voltage is shown by the following equation

$$V_{OC} = \frac{nkT}{q} \ln \left(\frac{I_L}{I_0} + 1\right). \tag{3.6}$$

Power output of a solar cell can be extracted by multiplying the voltage and the current values at each point on the I-V curve. The maximum value of the product of voltage and current provides the *maximum power point*, which can also be graphically extracted from the largest rectangle that could be fitted under the I-V curve. It can be shown as

$$\frac{d(IV)}{dV} = 0\ . \tag{3.7}$$

This leads to the following formula for MPP voltage,

$$V_{MP} = V_{OC} - \frac{nkT}{q} ln\left(\frac{V_{MP}}{(nkT/q)} + 1\right). \tag{3.8}$$

The I-V curve of a photovoltaic cell is shown with open circuit voltage (V_{OC}) and short circuit current (I_{SC}), as well as the maximum power point (V_{MP}, I_{MP}) in figure 3.10.

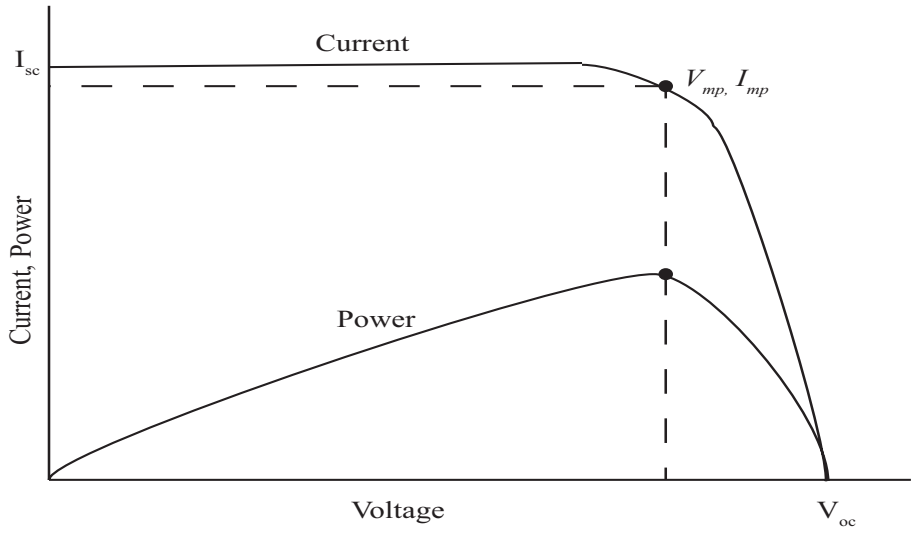

Figure 3.10: *Typical representation of I-V curves, showing open circuit voltage (V_{OC}) and short circuit current (I_{SC}), as well as the maximum power point (V_{MP}, I_{MP}). [9]*

The *fill factor* (F_F) is used to measure the junction quality and performance of a solar cell. It can be used to compare the performances and qualities of different types of solar cells. It is defined as

$$F_F = \frac{V_{MP}I_{MP}}{V_{OC}I_{SC}} . \tag{3.9}$$

Hence,

$$P_{MP=V_{OC}I_{SC}F_F}. \tag{3.10}$$

Higher fill factor value (highest value being 1) of a solar cell means the solar cell is of higher quality. A solar cell's output power is also dependent on the fill factor of that particular solar cell. A solar cell with higher fill factor will produce higher power than a cell with lower fill factor value, if all other parameters are same for both cells. Due to parasitic series and shunt resistive elements in a solar cell, fill factor of that cell decreases. Parasitic resistances of a solar cell can be shown in figure 3.11

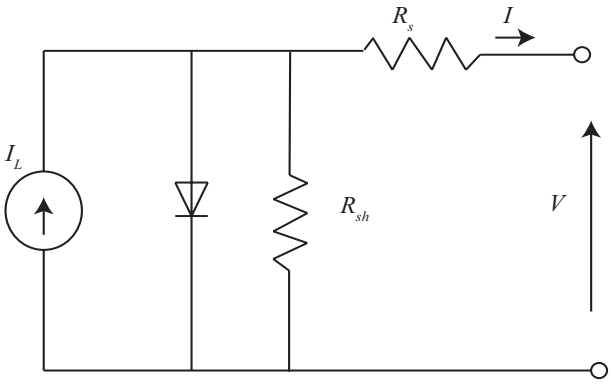

Figure 3.11: *Parasitic series and shunt resistances in a photovoltaic cell.* [9]

Series resistance (R_s) of the solar cells results due to the bulk resistance of the semiconductor material, the metallic contacts and interconnections, carrier transport through the top diffused layer, and contact resistance between the metallic contacts and the semiconductor. Higher values of series resistance can greatly reduce the output power from a solar cell. The effect of series resistance can be shown in the following figure 3.12.

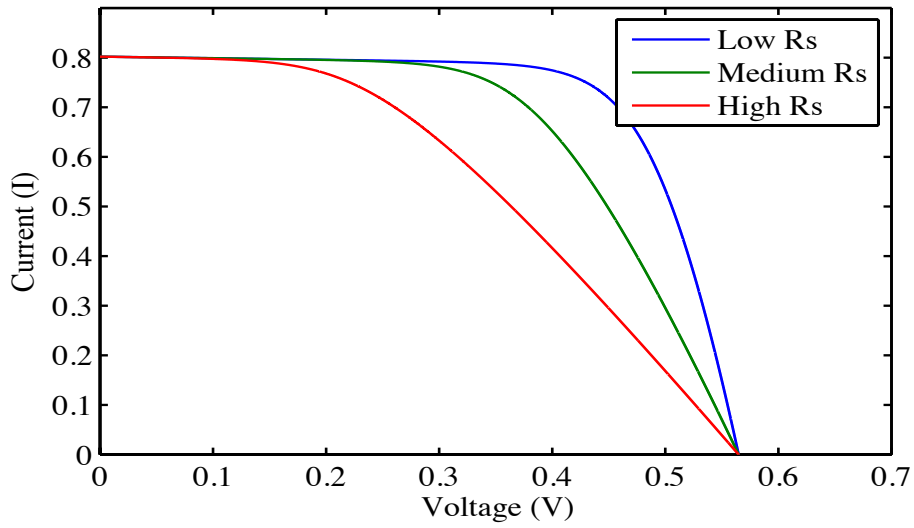

Figure 3.12: *Effect of series resistance on I-V curve of a solar cell.*

The shunt resistance (R_{sh}) can be the result of p-n junction non-idealities and impurities. For a solar cell, it is desirable to have high shunt resistance. Low shunt resistance values decrease the maximum output power of the solar cell. The effect of shunt resistance is shown in the following figure 3.13.

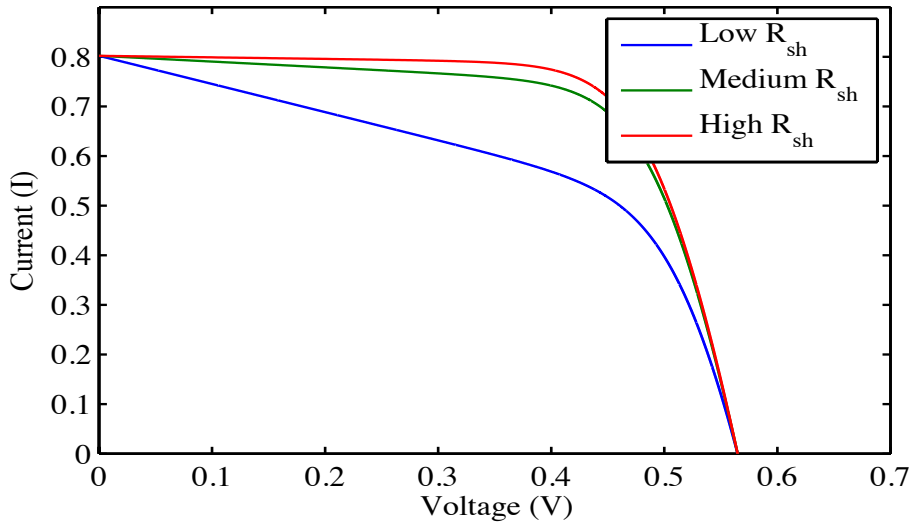

Figure 3.13: *Effect of shunt resistance on I-V curve of a solar cell.*

The I-V characteristic of a solar cell in the presence of both series and shunt resistances can be given by

$$I = I_L - I_0 \left[exp\left(\frac{V+IR_S}{(nkT/q)}\right) - 1 \right] - \frac{V+IR_S}{R_{Sh}}. \tag{3.11}$$

3.3 Effect of operating conditions

Operating conditions such as the temperature of the solar cell and the incident irradiance on the cell, effect the operation of the solar cell. Solar cells are tested and rated using standard test conditions (STC), which refer to 1000 W/m^2 solar irradiance, Air Mass 1.5 and 25°C cell temperature. To better resemble the real world conditions, normal operating conditions (NOC) are also used to test photovoltaic cells. Solar irradiance of 800 W/m^2, ambient temperature of 20°C and the spectral irradiance of AM1.5 constitute NOC.

3.3.1 Effect of temperature

The temperature of solar cell effects the operation of the cell. Operating temperature of a solar cell depends on ambient temperature, solar irradiance, module encapsulation characteristics and wind speed. The dark saturation current I_0 increases with temperature according to the equation

$$I_0 = B_i T^{\gamma} exp\left(\frac{-E_{g0}}{kT}\right), \tag{3.12}$$

where B_i is a constant independent of the temperature, E_{g0} is the linearly extrapolated zero temperature band-gap energy of the semiconductor making up the cell (typical val-

ue of E_{g0} for silicon is 1.15 eV) and γ includes the temperature dependencies of the remaining parameters determining I_0 (with a typical value between 1 and 4). [9]

With increasing temperature, band-gap energy decreases. As a result, more electron-hole pairs are generated by photons and thus the short circuit current I_{sc} increases. However, the effect of cell temperature on short circuit current is quite small. The I_{sc} temperature coefficient for silicon is roughly about 0.04 to 0.05% per Kelvin. In comparison, increase in cell temperature affects the open circuit voltage V_{oc} significantly. Open circuit voltage and fill factor reduce due to increase of cell temperature, hence cell power output also decreases. In silicon photovoltaic cells, V_{oc} decreases by around 2-2.4 mV/K as the temperature decreases. The temperature coefficient of V_{oc} in silicon solar cells are typically from -0.3% to -0.4% per K. The temperature coefficient of maximum power for crystalline silicon solar cells can range from -0.4 to -0.5% per Kelvin. The temperature dependence of V_{oc} and F_F is expressed by the following equations:

$$\frac{dV_{oc}}{dT} = \frac{-[V_{g0} - V_{oc} + \gamma(kT/q)]}{T}, \tag{3.13}$$

$$\frac{1}{F_F}\frac{d(F_F)}{dT} \approx \frac{1}{6}\left[\frac{1}{V_{oc}}\frac{dV_{oc}}{dT} - \frac{1}{T}\right], \tag{3.14}$$

where $V_{g0} = E_{g0}/q$. The effect of temperature on open circuit voltage is much more significant than on short circuit current, as can be seen in figure 3.14. [9]

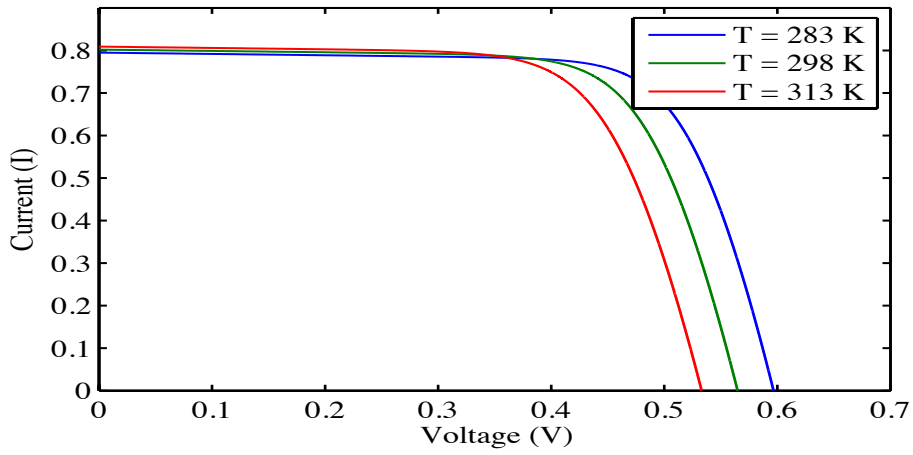

Figure 3.14: *The effect of temperature on the I-V curve of a solar cell.*

3.3.2 Effect of irradiance

The short circuit current is approximately directly proportional to incident irradiance on the cell. However, the effect of irradiance on open circuit voltage is not significant. Open circuit voltage only increases slightly with increasing irradiance. The effect of irradiance on open circuit voltage and short circuit current is shown in figure 3.15.

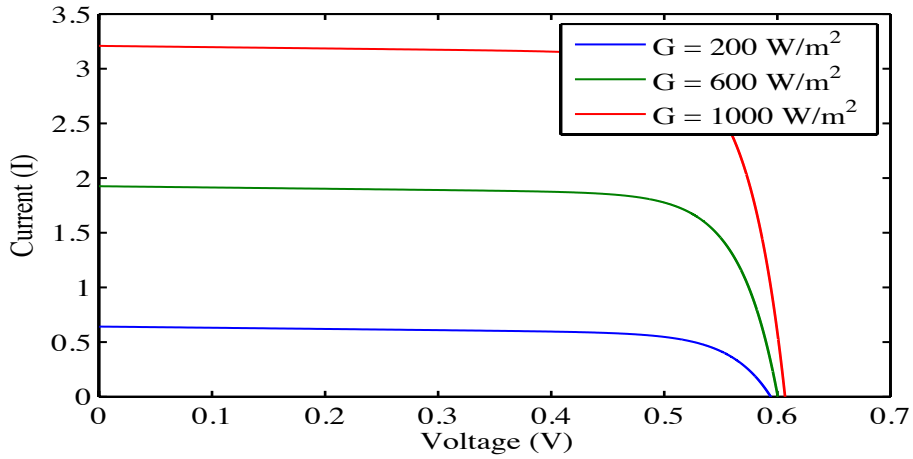

Figure 3.15: *The effect of irradiance on the I-V curve of a solar cell. Temperature of the cell is kept at 25˚C.* [9]

It can be observed from figure 3.15 that change in irradiance effects the short circuit current significantly. The effect of the irradiance on the open-circuit voltage is minimal.

4 PHOTOVOLTAIC SYSTEMS

A typical commercial crystalline silicon solar cell produces open circuit voltage ranging from around 0.55 to 0.72 V at a cell temperature of 25˚C. A solar cell with a cell area of 100 cm^2 can produce short circuit current ranging from 3 to 3.8 A. With higher cell area, the short circuit current of a cell increases. For example, a cell with an area of 225 cm^2 can produce a short circuit current ranging from 6.8 to 8.5 A. To extract optimal power from a cell, the voltage is typically kept at around 0.45 to 0.58 V. Due to the low voltage, individual cells are not used for most applications in general. Usually multiple solar cells are connected in series to produce higher voltage levels. To produce even higher power output, cells connected in series can then be connected in parallel configuration, which results in a series-parallel hybrid configuration of cells. Typically, around 32 to 72 solar cells are interconnected and encapsulated in a single enclosure, which is referred to as a *PV module*. A PV module with 36 cells generally operates at a voltage between 15 to 20 V and can produce an output of 50 to 200 W. [8] PV modules can also be interconnected to create PV arrays. PV modules connected in series configurations are generally referred to as *PV strings*. A PV generator consists of such PV arrays or strings connected in various different configurations to produce desired output power.

PV cells are not identical in practice and each cell exhibits unique characteristics. As such, the I-U curves produced by a module would not be similar to that of the individual cells it contains. The module output is limited by the cell with the lowest output. In a series connection, the output current is limited by the cell with lowest short circuit current and the output voltage is the sum of voltages of all the connected cells. Conversely, voltage output of a parallel connection depends on the lowest open circuit voltage of a cell and the current output is the sum of all the individual cell currents. Thus, the maximum output of the module is usually different from the sum of outputs of all the cells individually. The difference between the sum of maximum output of cells and the module output is referred to as *mismatch loss*. Similar phenomena are true for non-identical PV modules as well.[9]

4.1 Series connection of solar cells

A PV module usually contains PV cells connected in series to achieve higher voltage level. The output current of such series connected cells depends on the current output of the weakest cell. The behavior of series connected solar cells can be easily described using a series connection of only two solar cells, cell A and cell B. It is assumed that the cell B produces lower output, which can be caused by various reasons, such as, by manufacturing defects, degradation or partial shading. Series connection of cell A and B is shown in figure 4.1. The temperatures of both cells are kept the same. Cell B limits the

short circuit current of the series connection to a value close to its own short circuit current. The total output voltage of the series connection is the sum of the voltages of both cells. As the current output from the series connection is limited, the maximum power of the series connection is less than the sum of maximum powers of cells A and B. When the current of the series connection is higher than the short circuit current of cell B, cell B becomes reverse biased and a part of the power produced in cell A is absorbed in cell B as cell B acts as a load. Even when there is no partial shading condition, i.e. both cells are identically illuminated, mismatch losses are still present due to cells being non-identical to each other. PV module manufacturers minimize the mismatch losses by incorporating such cells into a module whose output currents at maximum power point are as similar as possible. Mismatch loss of non-identical series connected solar cells can be observed in figure 4.2.

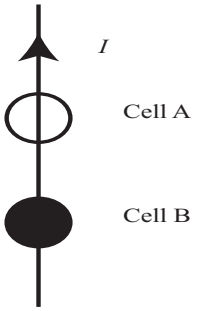

Figure 4.1: *Series connection of two solar cells.*

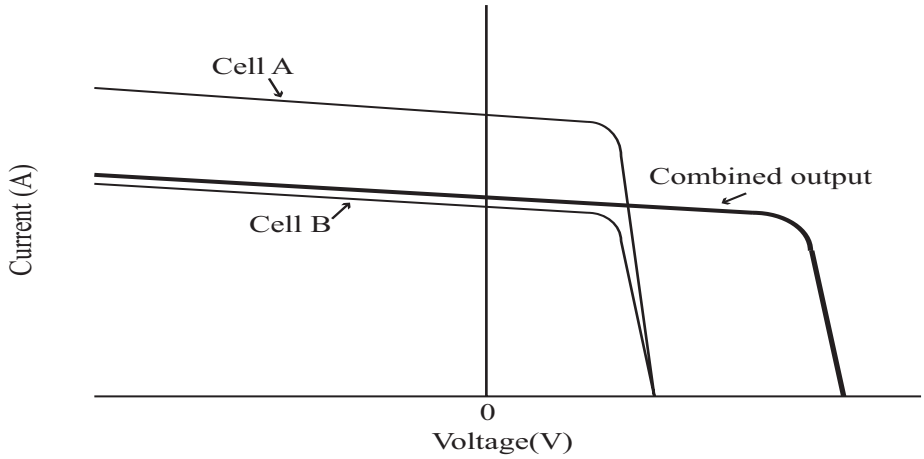

Figure 4.2: *Series-connected mismatched cells and the effect on output voltage.*

In most cases, more than two PV cells are connected in series. If in such a configuration, a cell becomes partially or completely shaded, high power dissipation can occur in that cell, creating a *hot spot*. In case of short-circuit events, all the power produced by the insolated cells can dissipate in the shaded cell. To protect the cells from overheating, anti-parallel connected *bypass diodes* are used. When under normal conditions, each bypass diode is reverse biased and each cell generates power. However, when a

cell becomes shaded, it tends to act as a resistance, thus becomes reverse biased by the other cells. Bypass diode across the shaded cell conducts the current and protects the shaded cell by bypassing it. The effect of a short-circuit event in a partially or completely shaded cell is shown in figure 4.3.

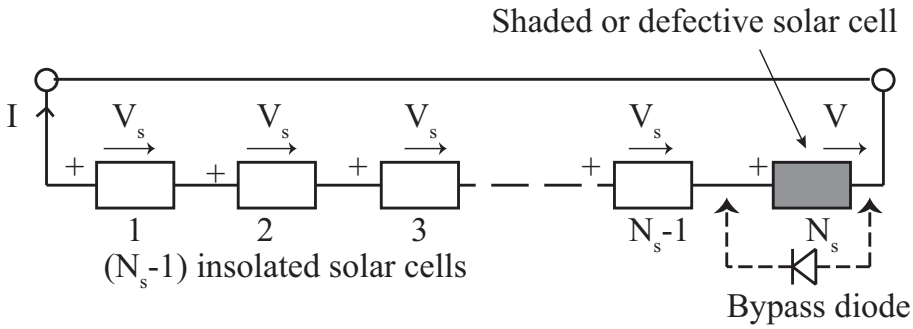

Figure 4.3: *Series connection of a total of N_s solar cells during a short-circuit event.* [8]

It can be seen from figure 4.3 that a shaded or defective cell is subject to the aggregate voltage of all other cells (N_s-1), around $-(N_s\text{-}1)\times 0.5$ V approximately. Bypass diode can be used to reduce the overload voltage substantially. The negative voltage in the shaded cell is only around 0.6 to 0.9 V, and it can be further reduced to a value between 0.3 to 0.5 V by using Schottky diodes. Use of a bypass diode for each cell is very expensive and generally, one diode is used for a group of solar cells. If one cell in a group of cells is shaded, current is bypassed around all the cells of that group. The reverse voltage across the group of cells equals to the *knee voltage* of the bypass diode. Therefore, the shaded cell is reverse biased by the generated voltage of other cells in that group in addition to the diode knee voltage. Thus, using more cells per one bypass diode increases the amount of power dissipation on the shaded cell. For silicon solar cells, usually 10 to 15 cells have one bypass diode, which ensures that no damage is done. The smaller the group of cells under one bypass diode, the less sensitive the module is towards partial shading conditions. The I-U curve of the shaded cell is altered due to the partial shading condition. The voltage drop across a conductive bypass diode is usually the same as the voltage across an insolated cell. Even though power loss due to partial shading is minimized using bypass diodes, a substantial problem is generated. Due to the operation of bypass diodes, multiple maximum power points can be generated for the series connection. As a result, tracking the maximum power point for optimal operation becomes very difficult. [8; 9]

4.2 Parallel connection of solar cells

Solar cells that are manufactured using same technology by the same manufacturer and have similar characteristics are connected in parallel to each other. The output current of the parallel connection is the sum of the currents of all the cells involved in the connection. Output voltage of the parallel connection is the same as the output voltage of an

individual cell in the connection. Due to differences in characteristics among the cells connected in parallel, the maximum output power of the connection is lower than the sum of the maximum powers of all the cells. This mismatch loss is minimized by using solar cells having similar voltage at the maximum power point.[8]

In general, the worst situation occurs when an entire module is operated in open circuit voltage. In that case, the voltage generated by the shaded cells is nearly equal to the open circuit voltage. As a result, the shaded cell receives power from all the illuminated cells adjacent to it. To observe the effect, it can be assumed that two cells (cell A and cell B) are connected in parallel, where both cells are uniformly illuminated. Parallel connection of the two cells is shown in figure 4.4. It can be further assumed that cell A operates at a lower cell temperature than cell B. As a result, the open circuit voltage of cell B is lower than cell A. The voltage of the connection is thus limited by cell B, as shown in figure 4.5. When the voltage of the connection is higher than the open circuit voltage of cell B, the current of cell B becomes negative. Thus, a part of the power produced by cell A dissipates in cell B. In the worst-case scenario, i.e. when the connection is operating at open circuit condition, all of the power produced in cell A dissipates in cell B.

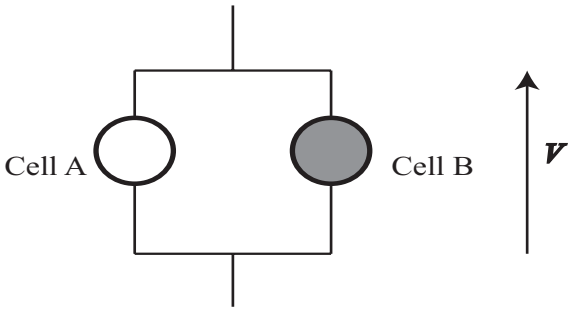

Figure 4.4: *Parallel connection of solar cells.*

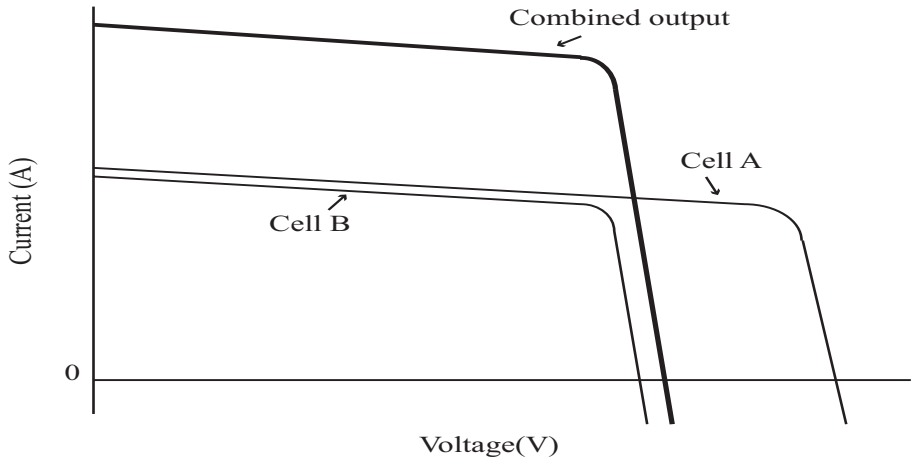

Figure 4.5: *The effect of parallel-connected mismatched cells on output voltage and current.*

Using bypass diodes for PV modules where series-connected cell strings are connected in parallel as shown if figure 4.6, creates a potential problem called *thermal runaway*. In such configurations, one string of bypass diodes can become hotter than the rest, therefore conducting higher share of the current, which in turn makes the diodes even hotter. Therefore, the diodes are rated to be able to conduct parallel current of the module combination. Some modules also employ *blocking diodes*, which ensures that the current only flows in one direction, i.e. out of the module. Blocking diodes, for example, prevents a battery from discharging at night. However, blocking diodes are not universally used because of wasted energy due to their usage.[9]

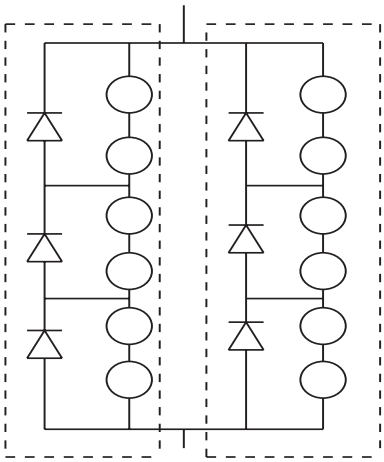

Figure 4.6: *Bypass diodes in parallel-connected cell strings.*

4.3 PV generator configurations

Interconnection of solar modules to build a PV generator requires extensive preventive measures. As PV modules are the building blocks of a PV generator, robust preventive measures are needed due to higher output power of modules compared to cells. A large solar generator is usually subdivided into sections, which can be operated and maintained independently in case of malfunctions in the system. All protective components, such as, fuses, circuit breakers and switches need to be properly rated for DC operation.

Bypass diodes are also used when PV modules are connected in series to form a PV string. When such series connected strings are connected together in parallel, reverse current and overload prevention are also necessary. Different types of preventive components, such as string diodes, fuses and circuit breakers are available to be used. A PV string with various safety features can be seen in figure 4.7. If the PV modules do not have built-in bypass diodes, then bypass diodes need to be integrated into each module as shown in figure 4.7. Fuses and string diodes can be installed in either side of the string.

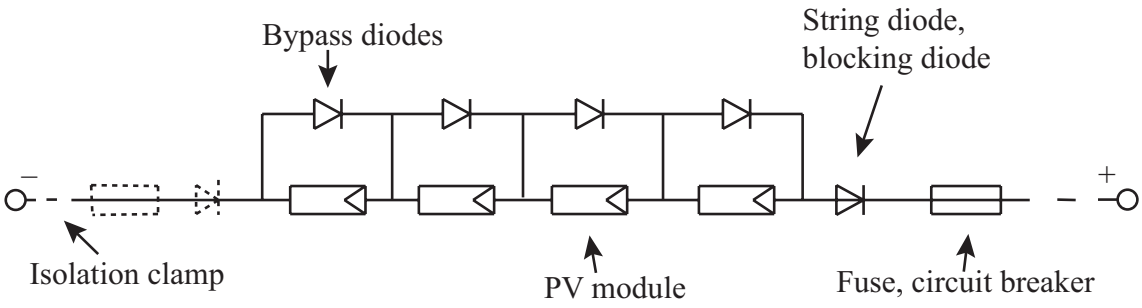

Figure 4.7: *PV string with various safety features.* [8]

A string diode prevents reverse current flow through a string of PV modules, when a malfunction due to shading or other failure occurs. A string diode should have a voltage rating higher than the open circuit voltage of the string, e.g. twice the open circuit voltage. Its current rating should be at least 1.25 times the short circuit current of the modules. As string diodes are prone to atmospheric power surges and higher current flows, e.g. 4 to 6 A, cooling is needed. There is also a voltage drop and consequently power loss associated with using string diodes. Due to the disadvantages of string diodes, the usage of such components is not dominant. In cases of stand-alone PV systems, where nocturnal battery discharge has to be prevented, a diode can be installed near the charge controller or a charge controller with built in preventive functionality can be used. Instead of diodes, DC-compatible fuses can be used to prevent high reverse current flow. Usually a fuse is installed on one side of the string and a disconnect terminal is installed on the other side. Another option is to install circuit breakers instead of fuses. Albeit being a more expensive option, circuit breakers allow a string to be shut down while under load. If unipolar circuit breakers are used, then the installation of a disconnect terminal is necessary on the opposite side of the string.[8]

Solar modules of same technology, open circuit voltage and maximum power point voltage can be used in parallel connection. For relatively large number of parallel-connected modules, e.g. greater than four modules, a fuse with nominal current rating of roughly 1.4 to 2 times the module short circuit current should be series connected with each module to ensure reliable shutdown of a module short circuit. However, due to high cost, such arrangements are a rarity in actual PV systems. When parallel-connected modules are series connected to other parallel-connected modules, a single bypass diode is used for the entire parallel connection. Only a single bypass diode is used to preserve harmonious internal current distribution. The short circuit current rating of the bypass diode should be at least 1.25 times the aggregate short-circuit current of all the modules.[8]

For larger solar generators, parallel-connected series strings are often used. Solar modules are connected in series to produce sufficient string voltage. Those strings are

then connected together in parallel to achieve higher aggregate current. Such configuration of solar generators is shown in figure 4.8.

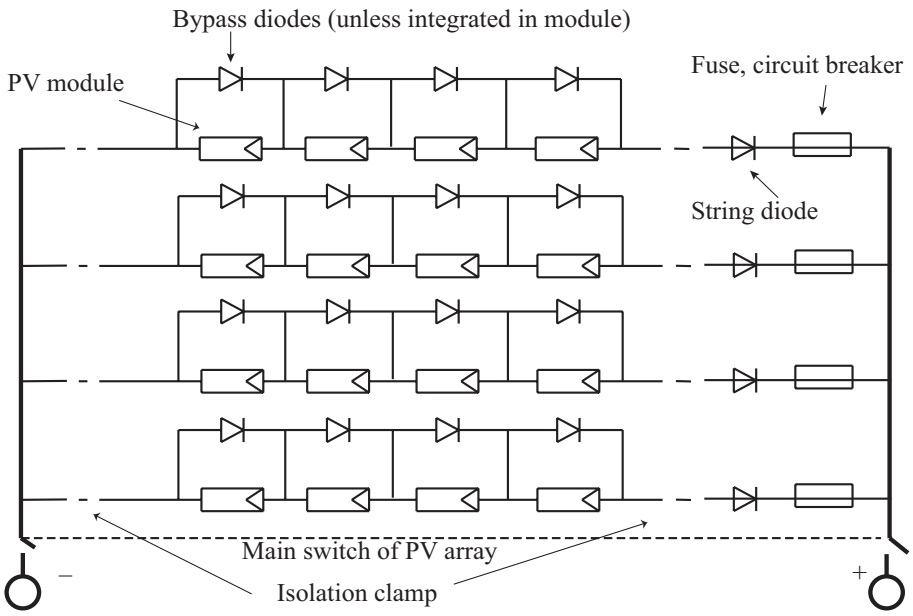

Figure 4.8: *PV generator with parallel-connected series strings.*

Parallel-connected PV strings generally provide the optimal protection against possible anomalies. As shown in figure 4.8, strings are decoupled from each other via string diodes to prevent reverse current flow in functioning string diodes. Due to short circuit conditions, string diodes can fail. In that case, reverse current is limited by circuit breaker as shown in figure 4.8. Costs of such systems can be lowered by using fuses and disconnect terminals instead of circuit breakers. The configuration shown in figure 4.8 also allows current measurements of individual strings. If an individual string experiences severe low current, it can be disconnected from the generator buses using the circuit breakers. Thus, maintenance of the system becomes much easier.

Solar modules are also used in a matrix configuration, as can be seen in figure 4.9. Such intermeshing of series and parallel connections of modules compensates for internal current asymmetries. As a result, power loss due to partial shading of modules is comparatively lower. If the shaded modules (which represents 25% of the total modules) were completely shaded, the power loss would be 25%. If there were no cross-connections present and the generator continues to operate on the original maximum power point voltage, the output power of the generator would decrease to practically zero. However, localizing malfunctions (e.g. module failure) becomes difficult in a matrix configuration of solar modules. As a result, voltage loss due to defective module and to a lesser extent, current loss occurs across the entire solar generator. Moreover, the task of monitoring internal voltages continuously becomes extremely difficult. To localize the defective module in an event of malfunction, the entire generator has to be shut down.

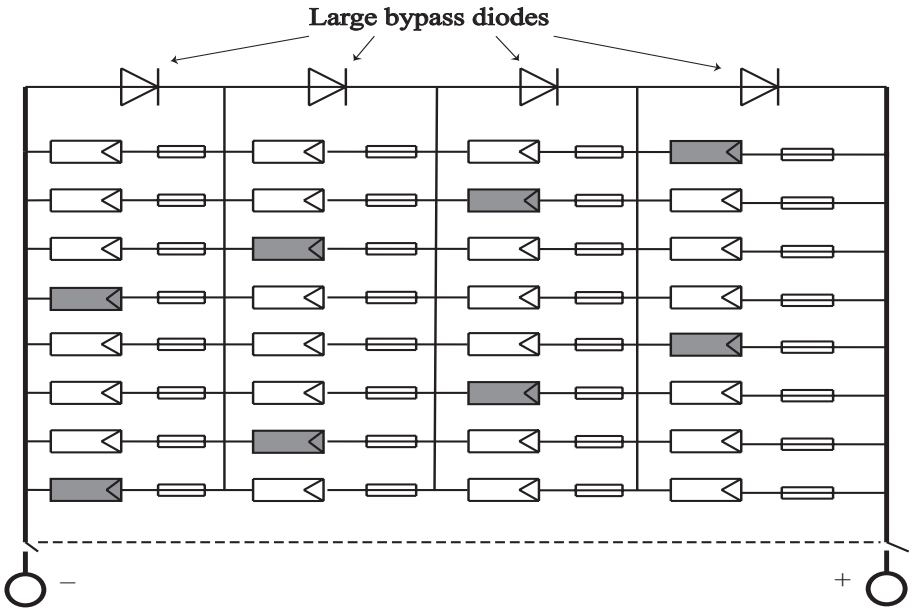

Figure 4.9: *Matrix configuration of solar modules.* [8]

Drastic power loss can occur due to partial or complete shading of modules. Power loss in a series connected string with bypass diodes increases with the number of connected modules. In such cases, voltage in the non-shaded modules increases, thus current starts to flow through the bypass diodes of the partly or fully shaded modules. Similarly to the case of solar cells, using bypass diodes results in multiple maximum power points for solar modules. A PV string of 10 modules operating under uniform irradiance condition and under partial shading conditions can be compared to observe the effect of partial shading on modules. In both cases, the modules operate at a temperature of 25˚C. It can be seen in figure 4.10 that when all the modules operate under a uniform irradiance condition of 1000 W, there is only one maximum power point. In the next scenario, two modules are assumed to be under partial shading conditions. One module experiences an incident irradiance of 500 W and another receives 200 W of irradiance. As a result, there are three maximum power points, all of which are less than the first scenario. Although partial shading conditions typically causes multiple maximum power points, only one maximum power point can occur despite partial shading conditions. Physical properties of PV modules, such as the ratio of MPP current to short-circuit current, power losses in bypass diodes and the value of parasitic shunt resistance of PV cell can determine the number of MPPs in a solar generator under partial shading conditions. Improvement of these PV module characteristics can increase power yield, but the probability of the occurrence of only one MPP can decrease. [11] The effect of partial shading on series-connected PV modules is comparatively higher than on parallel-connected modules. Mismatch losses in series-connected PV generators could be as much as 100 times higher than in parallel-connected generators. [12] Long series-connected arrays are thus generally avoided in building PV generators.

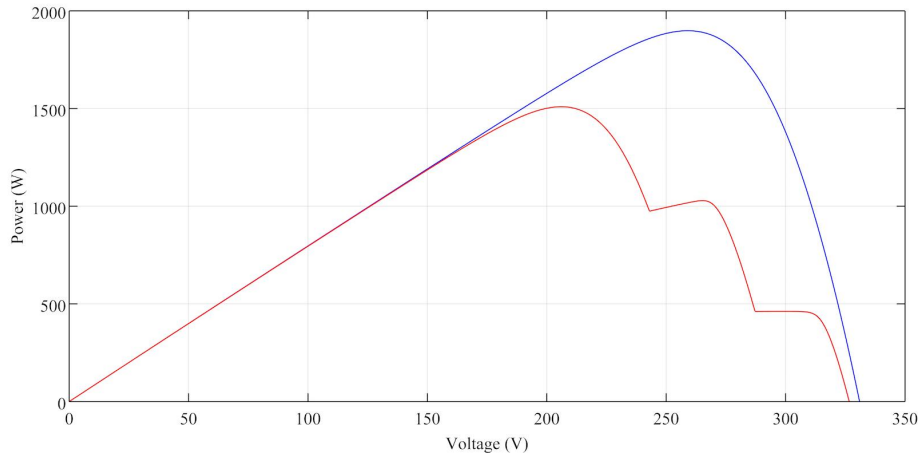

Figure 4.10: *Effect of partial shading on series connected modules. Blue curve represents the power output on uniform irradiance conditions and red curve represents the power output on partial shading conditions.*

Maximum power point tracking (MPPT) techniques are available in order to track the global MPP of a PV generator. As can be seen in figure 4.10, there can be multiple maximum power points when a PV generator operates under partial shading conditions. It is necessary for the generator to operate at the global MPP in order to extract the maximum power out of the system. The energy or power yield from a PV generator can be drastically reduced if the PV generator operates at a local MPP instead of the global MPP. Many MPPT techniques have been developed in order to track the maximum power point, such as, perturb and observe method, parasitic capacitance technique, current sweep technique, incremental conductance, DC link capacitor droop control technique etc. [13] One of the most widely used MPPT algorithms is *perturb and observe*. In this algorithm, output power and change of output power is calculated by sampling both current and voltage. The tracker operates by periodically incrementing or decrementing the voltage, in order to find the change in output power. If after a given perturbation, the output voltage is found to have increased, the direction of the next perturbation is kept in the same direction. The duty cycle is varied and the process is repeated until the maximum power point is found. As a result, the system oscillates about the MPP. The oscillation can be reduced by reducing the perturbation step size, which in turn slows down the process. [14] Moreover, Perturb and observe method may not work properly during time intervals characterized by rapidly changing atmospheric conditions. The possible failure of perturb and observe algorithm in presence of varying irradiance conditions is due to the fact that the algorithm cannot differentiate between the change of power due to duty cycle modulation and the change of power due to irradiance variation. [15] Distributed maximum power point tracking (DMPPT) techniques perform quite well when the PV generator or array is under varying irradiance conditions. In DMPPT technique, each module uses a single MPPT, thus alleviating power mismatch problems. DMPPT technique ensures comparatively higher energy efficiency under varying irradiance conditions. [13]

4.3.1 Stand-alone PV systems

Stand-alone photovoltaic systems are autonomous power generators, which are not connected to the utility grid. These PV generators generally supply certain AC or DC loads only. The simplest form of a stand-alone PV system is the *direct-coupled* system, where the DC output of a solar module or array is connected with a DC load directly.

AC loads can also be connected by using an inverter. Inverters convert DC power to AC power by using switching devices while stepping up the output voltage. PV Inverters usually have built in maximum power point tracking functionality. Inverters in stand-alone PV systems need to supply constant voltage and frequency to the loads. Inverters may also need to absorb or supply reactive power in case of reactive loads. Most inverters have efficiencies of 80 to 85% for loads in the range of 25 to 100% of the inverter rating. Inverter efficiencies can be very low for smaller loads, although this problem is being solved by the newer inverters. For AC loads, it is also desirable that the inverter produces sinusoidal output signal with low total harmonic distortion. The inverter may also need to produce high start-up current (around 2-3.5 times higher than nominal current) for around 300 ms to drive certain loads. Protection against power surge, overload and short-circuit events are also expected from a stand-alone PV system inverter. According to output signal curve characteristics, there are four types of inverters available for stand-alone PV applications.

Those are:

- Rotary converter
- Square-wave oscillator
- Pulse-width-controlled square-wave oscillator
- Sine wave inverter

In a rotary converter, a DC motor drives an AC generator. Rotary converters produce sinusoidal output voltage and can provide high start-up currents due to the energy stored in rotary elements. The disadvantages of these converters are high open-circuit loss, poor efficiency (maximum efficiency around 75 to 80%) and mechanical/electrical wear. Square-wave oscillators are comparatively inexpensive, highly efficient and can withstand overloads to some extents. However, the square-wave output voltage contains high harmonic elements, (around 44%) which causes the build up of heat in load appliances. Pulse-width-controlled square-wave oscillators (also referred to as *modified sine wave inverters*) reduces the total harmonic distortion to under 30% by introducing a third voltage step at 0 V. As a result, pulse-width-controlled square-wave oscillators can be used to drive a wide range of loads over comparatively long periods. Similar to square-wave oscillators, efficiency is quite high, ranging from 85 to 95%. Pulse-width-controlled square-wave oscillators can withstand brief periods of overloads, e.g. 100%

overload for a few minutes and 200-300% overload for a few seconds. Hence, these inverters can drive loads, which need high start-up currents. Moreover, the steepness of switching edges can be reduced without significantly reducing the efficiency of the inverter. Sine-wave inverters produce sinusoidal output voltage with low harmonic distortions, which can drive practically any AC load system. Modern sine-wave inverters can withstand high overloads and thus provide high start-up currents. Sine-wave inverters have efficiencies over 90%.[8]

Stand-alone photovoltaic systems can incorporate energy storage systems in order to store energy to be used at night times or during power outages. Usually battery banks are used with stand-alone PV systems although different storage technologies are available. A comprehensive review of energy storage systems for photovoltaic systems is presented in chapter 5.

4.3.2 Grid-connected PV systems

Grid-connected PV systems are power plants that feed energy into the electricity grid. Grid connected PV systems overtook stand-alone systems as largest global market sector in 2000 for International Energy Agency member countries. [9] PV generators are connected to the utility grid with the help of interfaces such as inverters. The inverter acts as a current source, it produces a sinusoidal output current without regulating its terminal voltage. The inverter may also use maximum power point tracking function to identify best operating voltage for the PV array or generator. [16] The PV generator can be configured in various ways in terms of how it is interfaced with the grid. In the traditional configuration, a central inverter connects a PV generator with parallel-connected strings of modules to the electricity grid. This central inverter configuration, as shown in figure 4.11, is sensitive to partial shading and mismatch losses.

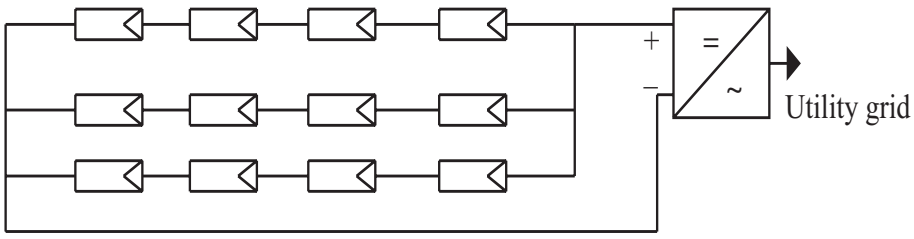

Figure 4.11: *Grid-connected PV generator with central inverter.*

String inverters can be used with individual strings in a configuration where the inverters are then parallel connected on the grid side. PV generator with string inverters is shown in figure 4.12. Such configuration is less sensitive to partial shading and DC power losses are usually lower than in a central inverter system. Despite the fact that DC-AC conversion efficiency in smaller string inverters is lower than larger central inverters, string inverter configuration has similar efficiency level to that of central invert-

er system. String inverter configuration also has better modularity as new strings can be added to the system for expansion of the generator.

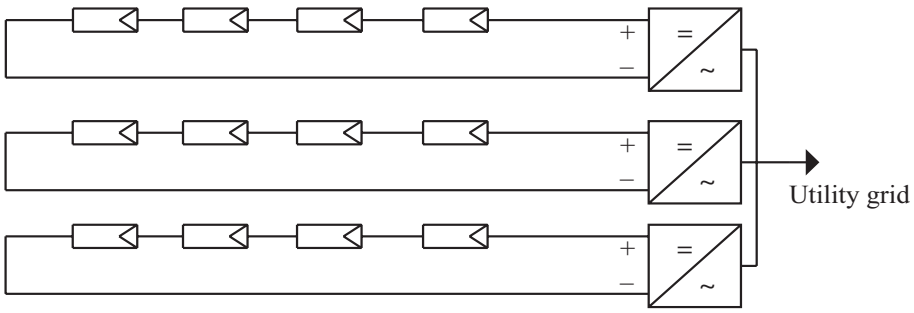

Figure 4.12: *Grid-connected PV generator with string inverters.*

In a multi-string inverter configuration, parallel-connected string inverters can be used in combination with a central inverter. This configuration allows the use of differently configured module strings, where those strings can operate at their own maximum power points. [9] The interfacing of PV generators with the utility grid can be further modified by using module inverters instead of string or central inverters, as shown in figure 4.13. Module-inverters are available for output power ranging from 100 to 400 W. This configuration is modular, upgradeable and has virtually zero DC-side loss.[8]

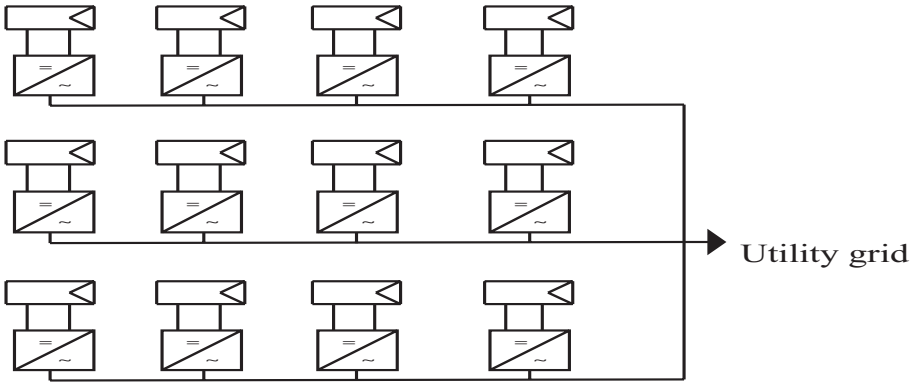

Figure 4.13: *PV generator with module inverters.*

Inverters that tie the PV generators with utility grid have different characteristics than inverters for stand-alone PV systems. Inverters for grid-tied PV systems operate at the grid frequency, i.e. at 50 Hz. These inverters usually have built-in maximum power point tracking capability. These inverters also have the capability to automatically switch on and off depending on the availability of generated PV power. Compared to the inverters for stand-alone applications, the need for production or absorption of reactive power and overload capacity are secondary in importance for grid-tied inverters. Grid-tied inverters can only start up and operate if the grid is operational and in an event of power failure, the inverters must shut down immediately to prevent stand-alone operation. Grid-tied inverters should also exhibit good efficiency in low-load range, low

open-circuit loss and low minimum start-up and shutdown power. Control units of the inverter should be fed from the DC side to minimize power absorption from the grid in a shutdown state. [8]

Two types of inverters are generally used to connect PV systems with electricity grids, *Line-commutated* and *self-commutated inverters*. In line-commutated inverters, grid signal is used to synchronize the inverter with the grid. In self-commutated inverters, intrinsic electronics of the inverter lock the inverter signal with that of the grid. [9] Line-commutated inverters have very little tendency to operate in stand-alone mode in case of grid power failure. Self-commutated inverters use electronic switches, which reduce reactive power consumption and current harmonics. However, due to the switching procedure used in self-commutated inverters, these inverters tend to operate in stand-alone mode following a power failure in the grid, which is not desirable for reasons of safety. Moreover, self-commutated inverters produce high frequency electromagnetic interference without necessary filtering, due to the usage of steep-edge pulses in switching mechanisms. However, the recent trend is towards the use of self-commutated inverters due to low harmonic output current and price reduction.[17]

5 ENERGY STORAGE SYSTEMS

The need for clean and sustainable energy production has led to increased penetration of distributed energy resources (DER) and renewable energy sources (RES) such as PV generators in the electric energy production market. The increasing adoption of renewable energy sources is necessary to minimize the threats of global warming and climate changes. However, these renewable sources of energy such as PV systems are intermittent in nature. The power output from a PV generator depends on the solar irradiance, which varies a lot during the day. Along with the fact that there is no solar irradiance available at night, seasonal changes also effect PV power generation. Energy storage systems such as batteries are usually used with stand-alone PV systems to provide power to the loads at night. Energy storages are also being used with grid-connected PV systems to increase flexibility and reliability of generation. [18]

Traditional electricity generating facilities have little or no storage systems in use due to the fact that in electricity network, generated electricity must be consumed precisely when it is produced. However, as the demand for electricity varies from time to time, the maximum demand could last only for a few hours each year. As a result, inefficient and expensive large power plants are built using fossil resources. Energy storage systems have the potential to help the power plants supplying peak demands. Energy storages can also act as standby reserves and dispatched load, resulting in increased efficiencies of the thermal power plants while reducing emissions. For distributed generation, energy storages are considered as an imperative technology. Distributed energy resources are decentralized power generators and are usually installed at the distribution grid level. DERs typically produce power in the range of a few kW to a few MW. DERs are considered as sustainable, efficient, reliable and environmentally friendly alternative to the conventional power plants. The electrical energy system is in the process of incorporating higher number of distributed sub-systems along with centralized power plants. [19] However, DERs also face disadvantages such as drastic load fluctuations and voltage drops due to smaller capacity and higher possibility of line faults. Energy storage systems can also help in this regard, by providing uninterrupted power supply (UPS) in cases of instantaneous voltage drops in the distributed energy network. Renewable energy sources such as solar photovoltaic, wind power etc. are considered as significant parts of overall electricity energy production industry in the future. As renewable sources of energy are inherently intermittent, storage systems can provide ways to deal with the unpredictability of such generation sources. [20] Nowadays, energy storages store surplus energy when intermittent generation exceeds the demand in the network and discharge energy to the grid when demand is higher than the generation. [21]

5.1 Applications of energy storage systems

Energy storage systems can be used to store bulk energy generated at night to be used later during peak demand periods during the day, thus establishing a more uniform load factor for the electricity network system. Energy storages can also be used in contingencies, where the storages compensate for any failure in power generation facilities. Energy storages can also help to maintain frequency balance in the power network, as both generator-side and load-side equipment can be damaged by large and rapid frequency fluctuations. Energy storage systems can also provide additional power to help generation units to start-up and synchronize with the electricity grid. [21; 22]

In transmission and distribution systems, energy storages can help maintain the stability and synchronized operation. Energy storages can also provide means to regulate voltage and can eliminate the need for additional transmission facilities by shifting energy demand from one time to another. Electricity customers can also benefit from demand shifting as the demand charges reduce. Energy storages also enhance power quality and reliability of service. [21; 22]

Energy storages are needed to facilitate the usage of renewable energy sources in power generation. Storages are needed to mitigate power delivery constraints imposed by inadequate transmission capacity. In many PV and wind power generators, output power is curtailed in order to ensure the reliability and quality of production. Excess power from the generators then can be stored in the energy storage system to be used later. Storing the excess energy when demand is low also helps to achieve a flatter load response. Frequency of the grid can be maintained by using the energy storage as a load or by discharging the stored energy to the grid. Output power fluctuations of intermittent energy sources such as PV and wind power can also be compensated using energy storage systems. [21]

In chapter 6, energy storage systems are used to balance the fluctuations in output power from a PV generator. When PV modules or arrays of a PV generator are shaded due to clouds, the output power drops due to the reduction of incident irradiance. Energy storage system is used to control the rate of change of output power from a PV generator. Restrictions have been imposed on the rate of change of output power from PV generators in many electricity grids. Especially in smaller electricity grids, higher rate of change of power is harmful for grid operation. The storage system stores and discharges energy to keep the rate of change of PV output power under the specified limit. In addition, when power curtailment is implemented by restricting the inverter capacity, excess energy is stored in the energy storage system.

5.2 Classification of energy storage systems

Electrical energy storage systems can be classified based on two basic criteria: function of the storage system and form of storage. Based on the functionality, most storage systems can be divided into two groups, storage systems with high power rating with relatively low energy capacity and storage systems with high energy capacity with low power rating. Storage systems with high power rating but with low energy capacity, such as, super-capacitors, flywheels and batteries are suitable for power quality maintenance operations or UPS operations. Energy storage systems with relatively high-energy capacity, such as, large-scale batteries, fuel cells, pumped hydroelectric storage (PHS) and compressed air energy storage (CAES) can be used for energy management. Based on form of storage, storage systems can be classified into four basic groups, electrical energy storages, mechanical energy storages, chemical energy storages and thermal energy storages. *Electrical energy storages* include electrostatic energy storages such as super-capacitor, and magnetic energy storages such as superconducting magnetic energy storage (SMES). *Mechanical energy storages* include kinetic energy storages such as flywheels and potential energy storages such as PHS and CAES. *Chemical energy storages* include electrochemical energy storages such as lithium-ion batteries, chemical energy storages such as fuel cells and thermochemical energy storages such as solar hydrogen, solar metal, solar ammonia dissociation-recombination etc. *Thermal energy storages* include low temperature energy storages such as aquiferous cold energy storage, cryogenic energy storage and high temperature energy storage such as steam accumulators, graphite, concrete, and latent heat systems (such as phase change materials). [21]

5.3 Characteristics of energy storage systems

Fundamental characteristics of energy storage systems need to be known in order to analyze various storage systems and technologies. One of the most basic characteristics of an energy storage system is its *storage capacity*, which is defined as the quantity of the energy available in the storage system after charging. Capacity of energy storage system is typically measured in watt-hours (Wh), kilowatt-hours (kWh) or ampere-hours (Ah). Ampere-hours is defined as the number of hours a storage unit can provide a current equal to the discharge rate at the nominal voltage of the storage unit.[10] Watt-hour capacity can be measured by multiplying ampere-hour capacity with the nominal voltage of the storage unit. *Discharge rate* of an energy storage system affects the capacity of the storage. If low current is being discharged at a very slow rate, more energy can be extracted from the storage and the capacity is higher. Discharge rates for conventional batteries are usually given as ‘C rate’. For example, a rate of 1 C means that a 1.5 Ah battery would be discharged in one hour at a discharge current of 1.5 A. A rate of 2 C would mean that the battery would be discharged in half an hour with a discharge current of 3 A. *Depth of discharge* or DOD of an energy storage refers to the percentage of

the capacity that can be withdrawn or discharged from the storage during discharging. For example, a battery with 80% DOD rating can discharge 80% of its rated capacity. Batteries are usually categorized as either *deep cycle* or *shallow cycle* batteries. Deep-cycle batteries generally have higher DOD ratings, often as high as 80% or more. *Power rating* of energy storages refers to the maximum power delivered during charging or discharging. *Discharge time* refers to the duration of maximum-power discharge of energy storages. It depends on the depth of discharge and operational conditions of the system. For some applications, discharge time characterizes the adequacy of the storage system. For example, in the case of a pumped hydroelectric storage, storage capacity depends on the mass of water and the height of the waterfall, while the maximum power is determined by the size of the conduits and the power of the reversible turbine-electrical-machine units. Because of the separate power and energy dimensions of the system, optimum time constant for discharge needs to be determined. *Efficiency* of an energy storage system is the ratio between released energy and stored energy. Efficiency of a storage system depends on many factors associated with the system, such as self-discharge loss, energy transfer loss etc. *Self-discharge* refers to the portion of stored energy that has dissipated over a given time. For example, self-discharge rate of lithium ion batteries can be a maximum of 5% of rated capacity per month. *Cycle life* is another important characteristic of a rechargeable energy storage system. One cycle refers to one full charge and one full discharge. Cycle life refers to the number of times an energy storage unit can be fully charged and discharged. For example, some lithium ion batteries can have 1000 cycles before the capacity drops below 80%, at which point the battery should not be in operation. In general, longevity and efficiency of an energy storage system can depend on various factors, e.g. operating temperature, charging and discharging levels etc. *Energy density* refers to the maximum amount of energy accumulated per unit of mass or volume of the storage unit. It is an important factor, which determines size, cost and portability of storage systems among other aspects. Safety, reliability, modularity, effect on environment, cost etc. are also important characteristics associated with energy storage systems. [22]

5.4 Electrical energy storages

Electrical energy storage systems include capacitors and super-capacitors, where electric potential energy can be stored in the electrical field. In superconducting magnetic energy storage (SMES), energy is stored in the magnetic field.

5.4.1 Super-capacitors

A capacitor provides the most basic way of storing electrical energy. Two conducting plates separated by a non-conducting layer called dielectric constitute a basic capacitor. When one plate is charged using a DC source, oppositely signed charge is induced in the other plate, as shown in figure 5.1. Capacitors have very high charging and dis-

charging rates and have very high cycle life with high efficiency. Conventional capacitors have very low energy density because larger dielectric area is required for higher capacity. [21]

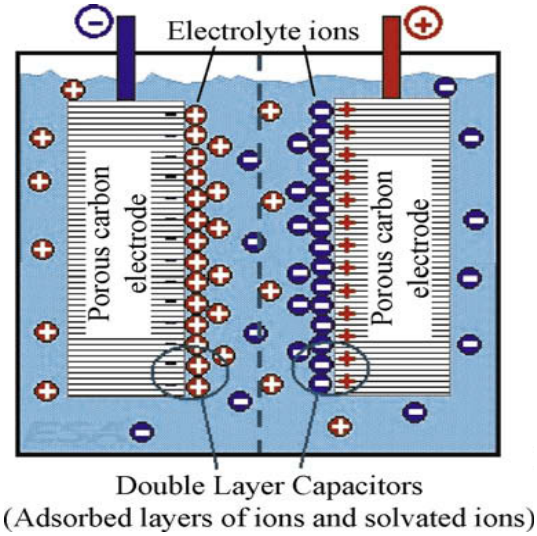

Figure 5.1: *Illustration of capacitors/super-capacitors.* [21]

Super-capacitors are advanced capacitors, which provide very high capacitance in a small package. Super-capacitors use a very thin layer of electrolyte as the dielectric to separate charge. The layer of electrolyte in super-capacitors is measured in fractions of a nanometer, compared with micrometers for most conventional capacitors. Super-capacitors can be classified into two different categories, electrochemical double layer super-capacitors (ECDL) and pseudo-capacitors, depending on the material technology used. There are a few hybrid super-capacitors being developed currently. ECDL super-capacitors are currently the least costly and most used super-capacitors.[18]

The ECDL super-capacitors have a double layer construction. Instead of metal plates similar to conventional capacitors, these super-capacitors contain carbon-based electrochemical electrodes immersed in a liquid electrolyte, which also contains the separator. Porous active carbon is usually used as electrode material. Carbon aerogels and carbon nanotubes are also being used recently as electrode material. The electrolyte can be either organic or aqueous. The organic electrolytes usually use acetonitrile, which can achieve a nominal voltage of up to 3 V. Aqueous electrolytes may use either acids or bases, but can only achieve a maximum nominal voltage of 1 V. An electric field exists between the charged electrodes due to the applied voltage. During charging, charged ions in the electrolyte migrate towards the electrodes of opposite polarity. Thus, two separate charged layers are produced. Since no chemical reaction takes place during the process, typical cycle life of super-capacitors is very high, more than 100,000 cycles at 100% depth of discharge. Self-discharge of super-capacitors is quite high, more than 20% of nominal energy per day. Charging and discharging rates are very fast (from mil-

liseconds to a few minutes) and no thermal or hazardous release is present during discharge. Energy efficiency of super-capacitors can range from 85 to 98%. [18; 21]

Super-capacitors have higher capacitances and higher energy densities than conventional capacitors. This is because super-capacitors have significantly larger electrode surface area, along with much thinner electrical layer between the electrode and the electrolyte. Super-capacitors are currently available with a capacitance of 5000 F and with energy densities up to 15 Wh/kg. Super-capacitors have extremely high power densities, often as high as 10 kW/kg. Cost of super-capacitors is very high currently. Drastic cost reduction is needed for widespread use of the super-capacitors. Super-capacitors are currently used for regenerative braking in vehicles and to provide booster charge in response to sudden power demands. Super-capacitors can be used in combination with high capacity batteries, where fast response time and high power capabilities of super-capacitors compliment higher energy capacity of the batteries. The properties of super-capacitors make them a good candidate to be used with intermittent energy sources such as PV power plants, to compensate for output power fluctuations, which generally last for short durations. Usage of super-capacitors may permit the use of smaller sized batteries and may help extending the longevity of batteries.[18; 21]

Recently the porous, amorphous carbons are being replaced by vertically aligned, single-wall carbon nanotubes. These carbon nanotubes are only several atomic diameters wide. As a result, the surface area of the electrodes is increased. Energy densities of up to 60 Wh/kg and power densities of 100 kW/kg can be achieved with this new technology. Pseudo-capacitors and hybrid capacitors are also showing a lot of promise in delivering higher power and energy densities compared to ECDL super-capacitors. A lot of research is being conducted in these technologies, which promises significant developments in the coming years.[18; 21]

5.4.2 Superconducting magnetic energy storage

Superconducting magnetic energy storage or SMES stores electric energy directly into electric current. DC current flows through an inductor coil made of superconducting cables of nearly zero resistance, usually made of niobium-titane (NbTi) filaments, operating at extreme low temperature of -270 ˚C. The current circulates indefinitely with almost zero loss. Energy is stored as a magnetic field created by the current flow. The inductor is kept at the extreme low temperature by immersing it in liquid helium contained in a vacuum-insulated cryostat. A typical SMES system consists of a superconducting unit, a cryostat system (a cryogenic refrigerator and a vacuum-insulated vessel) and a power conversion system, as shown in figure 5.2. The energy stored in the SMES coil can be calculated by $E_{coil} = 0.5L_{coil}I^2_{coil}$, where L_{coil} is the inductance of the coil and I_{coil} is the current flowing through the coil.[21]

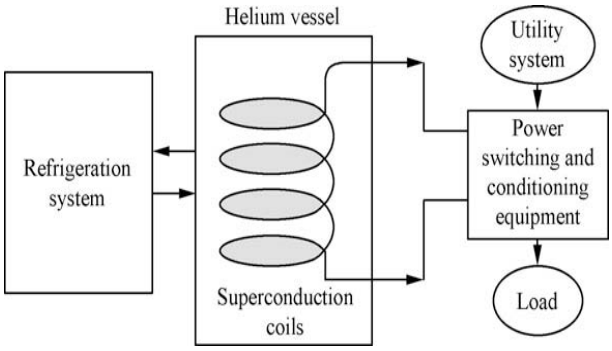

Figure 5.2: *An overview of a SMES system.*[21]

SMES has a high cycle life. Thus, it can be used for constant and continuous full-cycle operations. Efficiency of SMES systems is typically as high as 97%. Response time of SMES systems is also very fast, typically under 100 ms. Thus, SMES is suitable for use in maintaining voltage stability and power quality for electricity network and large industrial systems. SMES systems can provide power ranging from 1 to 10 MW for a very short time, i.e. in order of seconds. Shortcomings of the system also include high cost and environmental impacts associated with strong magnetic fields due to very large coils. To limit infrastructure costs, such systems are preferred to be build underground.[21; 22]

5.5 Mechanical energy storages

Mechanical energy storages include kinetic energy storage systems such as flywheels and potential energy storage systems such as PHS and CAES.

5.5.1 Pumped hydroelectric storage

PHS has been the most widely implemented large-scale electric energy storage system. In a PHS system, there are usually two water reservoirs located at different elevations, as shown in figure 5.3. Water is pumped up into the reservoir situated at higher elevation to store electricity in the form of hydraulic potential energy during off-peak hours. During times of high electricity demands, the potential energy of the water can be converted to electrical energy by releasing the stored water. A turbine is driven by the water returning to the lower reservoir from the higher one. The amount of stored energy is proportional to the difference in height between the two reservoirs and the volume of the water stored. [21]

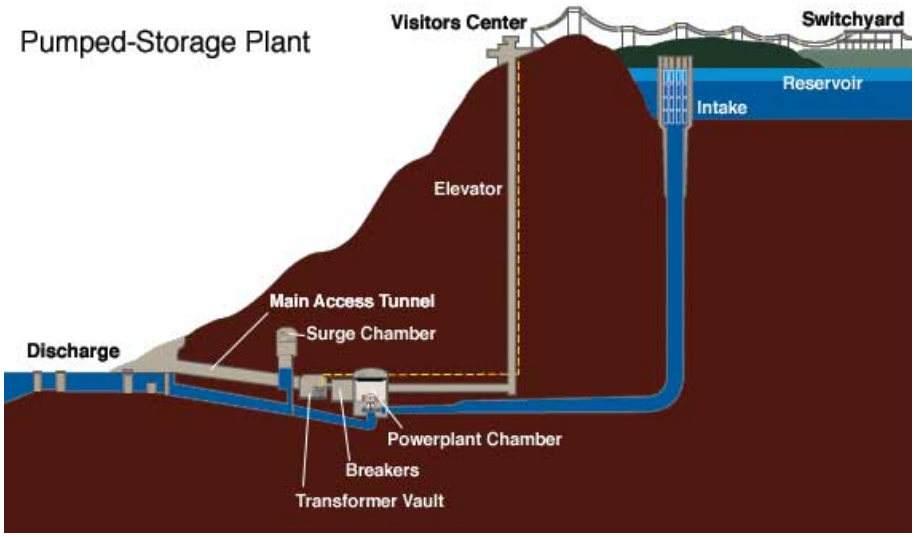

Figure 5.3: *A typical PHS plant.*[18]

Large volume of water can be stored in the higher reservoir for long periods without high amount of wastage due to water evaporation and penetration. PHS is also a technology with high efficiency and relatively low capital cost per unit of energy. The efficiency of a PHS varies from 71 to 85% due to water evaporation and conversion losses. The typical rating of a PHS system ranges from 100 MW to 3000 MW. There are some major disadvantages of PHS technology; for example, it is difficult to find available sites to build the reservoirs and dams. High costs and environmental concerns are also associated with the construction of a PHS system. First use of PHS dates back to 1890s in Italy and Switzerland. PHS systems are generally applied for energy management, frequency control and as a reserve generation system. [21]

5.5.2 Compressed air energy storage

Compressed air energy storage (CAES) can provide for large energy storage needs besides PHS systems. CAES systems are based on the operation of conventional gas turbine generators. The compression and expansion cycles of a conventional gas turbine are separated into two processes in a CAES system. During off-peak hours, electric power is used to compress the air and store it in an airtight space. Energy is stored in the form of elastic potential energy of compressed air. During peak hours, the compressed and stored air is expanded through a high-pressure turbine. The air through the high-pressure turbine is mixed with fuel, combusted with the exhaust and expanded through a low-pressure turbine. A generator is connected with both turbines to produce electricity. The waste heat of the exhaust can be captured using a recuperator before being released. The containers or cavities, where the compressed air can be stored, are usually underground rock caverns, salt mines or depleted gas fields. A typical CAES system is shown in figure 5.4.[21]

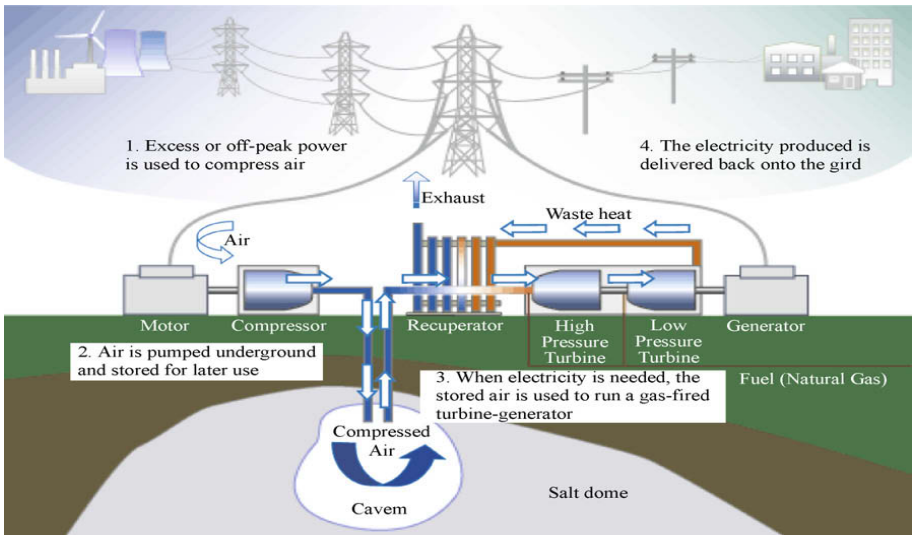

Figure 5.4: *Schematic diagram of a typical CAES system.*[21]

CAES systems can cycle on a daily basis and efficiently respond to changing load conditions due to being sustainable to frequent start-up/shut-down cycles. Typical CAES systems are rated in the range of 50-300 MW. Storage periods of CAES systems can be longer than a year. Storage efficiency of CAES is in the range of 70-89%. Capital costs of CAES systems are relatively low.[21]

The first CAES plant in the world is situated in Huntorf, Germany and has been in operation since 1978. A solution-mined salt dome was converted into a storage cavern of around 310,000 m^3 for compressed air, which is approximately 600 m underground. Compressors rated 60 MW are also used to provide a maximum pressure of 10 MPa. The unit runs on a daily cycle with 8 hours of charging and generates 290 MW for 2 hours. Since CAES system needs to be associated with gas turbine plants situated in suitable geographical locations, improved designs, such as, small-scale CAES with fabricated small vessels are being studied. CAES systems are comparatively less attractive for widespread adaptation due to the requirement of fossil fuel combustion and emission associated with the process.[21]

5.5.3 Flywheels

A flywheel is a mass rotating about an axis, which can store energy mechanically in the form of kinetic energy. The flywheel is charged by spinning it using a motor. Energy is stored in the angular momentum of the spinning mass. The same motor is used as a generator to produce electricity during discharge. The total energy of a flywheel system depends on the size and speed of the rotor, and the power rating is dependent on the motor-generator. A typical flywheel system is shown in figure 5.5.[18; 21]

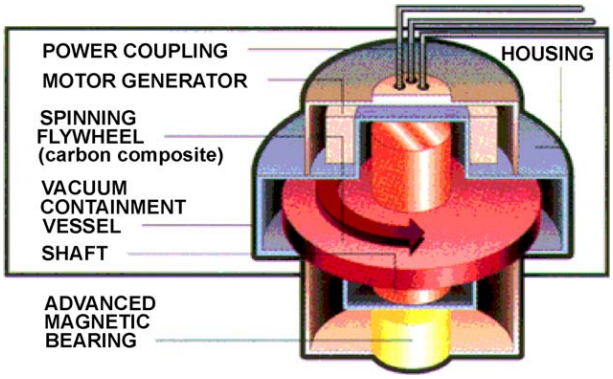

Figure 5.5: *Main components of a flywheel system.*[18]

A flywheel energy storage system typically consists of a rotating flywheel, rotor bearings and power interface. The flywheels can be divided into two categories, low-speed flywheels operates with a maximum speed of 6000 rpm and high-speed flywheels, which operates with a maximum speed of 50,000 rpm. Typical low-speed flywheels are made of steel rotors and conventional bearings. Typical specific energy of low-speed flywheel is around 5 Wh/kg. High-speed flywheels use advanced composite materials for the rotor and ultra-low friction bearing assembly. High-speed flywheels can have specific energy of 100 Wh/kg. Such flywheels also have very little start-up times. High-speed flywheels are either kept in vacuum or in helium filled container to reduce aerodynamic losses and rotor stresses.[18]

Flywheels have very high cycling capability with high charge and discharge rates. Full-cycle lives of flywheels can range from 10^5 to 10^7. Energy efficiency of a flywheel is typically around 90% at rated powers. Flywheel systems have high self-discharge rates, typically at least 20% of the stored capacity per hour. Such high discharge rates make flywheel systems unsuitable for long-term energy storage. Flywheel energy storage systems are best used as standby power systems or to compensate for demand fluctuations throughout the day. When there is excess production than load demand, energy can be stored in the flywheel. Energy can be discharged from the flywheel when insufficient power is generated by the main power source. Flywheels are also suitable to be used with renewable energy sources.[18]

5.6 Chemical energy storages

Chemical energy storages can generally be classified in three categories, electrochemical energy storages, chemical energy storages and thermochemical energy storages. Conventional batteries such as lead-acid, nickel metal hydride, lithium-ion, nickel cadmium, sodium sulfur and flow-cell batteries such as zinc bromine and vanadium redox are examples of electrochemical energy storages. Chemical energy storages include fuel cells, molten-carbonate fuel cells and metal-air batteries. Thermochemical energy stor-

ages include solar hydrogen, solar ammonia dissociation-recombination and solar methane dissociation-recombination.[10; 21]

Rechargeable or secondary batteries are the oldest and most used form of electricity storage. A conventional battery contains one or more electrochemical cells. Each cell contains electrolyte, which can be liquid, paste or solid in form. Inside the cell, a positive electrode (anode) and a negative electrode (cathode) are present. Electrochemical reactions occur at the two electrodes, which creates electricity. Produced electricity is extracted through an external circuit. The electrochemical reactions are reversible, so the battery can be recharged by applying external voltage across the electrodes.[23]

Batteries offer important benefits to electricity utility operations. Batteries generally respond very quickly to load changes and can be operated alongside other power generations systems. Standby losses of the batteries are generally low. Efficiencies of batteries vary from 60 to 95%. Batteries are also modular, making it possible to build large energy storage systems. However, batteries have short cycle life, limited discharge capabilities, and in many cases, low power and energy capacity. In addition, many battery technologies contain toxic materials. Lead acid, nickel cadmium, sodium sulfur, sodium nickel chloride and lithium ion batteries are either currently being used or have potential to be used in utility scale energy storage applications.[10]

5.6.1 Lead acid batteries

Lead acid batteries are the most mature and most widely used rechargeable battery technologies. The battery consists of a lead metal cathode and a lead oxide anode as electrodes. Both electrodes are immersed in an electrolyte made of sulfuric acid solution. Oxygen ions from the anode are exchanged with sulfate ions of the electrolyte at the anode during discharging. At the cathode, sulfate ions from the electrolyte combine with lead ions and form lead sulfate. The acidity of the electrolyte reduces due to the removal of sulfate ions. To maintain charge neutrality, two electrons leave the cathode terminal and two electrons enter the anode terminal via external circuit for each two sulfate ions that leave the electrolyte. Thus, current flows from anode terminal to the cathode terminal. Each oxygen ion released from the anode combines with two hydrogen ions from the sulfuric acid electrolyte and forms water. To charge the battery, a voltage greater than the voltage produced by the reactions at the anode and cathode is applied across the battery terminals. Current now flows into the anode and charge the battery. Two electrons go from anode to cathode to maintain charge neutrality. An oxygen ion replaces the two electrons at the anode and combines with a lead ion, which was created by a sulfate ion entering the electrolyte. A sulfate ion moves from the cathode to the electrolyte when two electrons are added to the cathode. A lead atom is produced at the cathode when those two electrons combine with a lead ion. The sulfate ions liberated from the cathode and the anode to the solution increase the concentration of sulfuric ac-

id in the electrolyte solution. Oxygen ions of the dissociated water molecules remain in the solution. Negatively charged oxygen ions migrate to the anode due to the potential difference and create lead oxide at the anode. Surfaces of the electrodes convert to lead sulfate when discharging and effective surface area of the electrodes can be reduced if excessive lead sulfate builds up. As a result, cell performances may decrease. Thus, full discharge of lead acid batteries is generally avoided. During charging, hydrogen ions may combine with free electrons and produce gaseous hydrogen. When the cathode is fully converted to lead, sulfate ions are no longer present at the cathode. If charging is continued at this point, the electrons entering the cathode can no longer release sulfate ions and instead produce hydrogen gas. This phenomenon is called *gassing*, which is not desirable in order to avoid safety risks. Discharge levels of lead acid batteries are usually limited to a maximum of 50% to minimize *sulfation*, where crystals of lead sulfate grow on electrodes during periods of low state-of-charge, thus reducing battery efficiency and capacity.[10]

Chemical process during discharge at the anode and the cathode can be represented using the following equations 5.1 and 5.2 respectively.[10]

$$PbO_2 + 4H^+ + SO_4^{2-} + 2e^- \rightarrow PbSO_4 + 2\,H_2O \quad (5.1)$$

$$Pb + SO_4^{2-} \rightarrow PbSO_4 + 2e^- \quad (5.2)$$

Chemical process during charging of the battery at the anode and the cathode can be represented using the following equations 5.3 and 5.4 respectively.[10]

$$PbSO_4 + 2\,H_2O \rightarrow PbO_2 + 4H^+ + SO_4^{2-} + 2e^- \quad (5.3)$$

$$PbSO_4 + 2e^- \rightarrow Pb + SO_4^{2-} \quad (5.4)$$

The voltage difference between the electrodes in a lead acid cell is approximately 2.12 V. Cells are usually connected in series to achieve higher voltage levels, for example, six cells are connected in series to produce a nominal voltage of 12 V. Lead acid batteries has low cost, high reliability and high efficiency (ranging from 70 to 90%). Lead acid batteries are generally used to maintain power quality, in UPS operations and spinning reserve applications. Power density of lead acid batteries is typically around 180 W/kg. Due to limited cycle life (ranging from 500 to 1000 cycles) and low energy density (30 to 50 Wh/kg), usage in energy management applications is limited. Cycle life of the lead acid batteries is negatively affected by depth of discharge and operating temperature. Higher temperatures (up to 45 ˚C, which is the upper limit for battery operation) may improve battery performance in terms of battery capacity but reduces battery lifetime and energy efficiency. [18] Lead acid batteries also have poor low temperature performance and therefore usually require thermal management systems. Self-

discharge rates of lead acid batteries are quite low, around 2% of rated capacity per month, at 25 ˚C. [9; 10; 21]

5.6.2 Nickel-based batteries

The nickel-based batteries mainly include nickel-cadmium (NiCd), nickel-metal hydride (NiMH) and nickel-zinc (NiZn) batteries. All three types of batteries use nickel hydroxide as positive electrode and aqueous solution of potassium hydroxide with lithium hydroxide as electrolyte. NiCd uses cadmium hydroxide, NiMH uses metal alloy and NiZn uses zinc hydroxide as negative electrode. The rated voltage of nickel-based batteries is 1.2 V, only NiZn type produces higher voltage of 1.65 V. NiCd batteries has typical energy density of 50 Wh/kg. Energy density of NiMh batteries is comparatively higher, which is 80 Wh/kg. NiZn batteries have energy density of 60 Wh/kg. At deep discharge levels, typical cycle life of NiCd batteries ranges from 1500 to 3000 cycles. NiMH and NiZn batteries have cycle lives similar to lead acid batteries. NiCd batteries are the only ones that are commercially used for industrial UPS applications, for example, in large-scale energy storage applications for renewable energy systems. The main drawback of NiCd batteries is the production cost. Moreover, the efficiency of nickel-based batteries is relatively poor, ranging from 60 to 80%. Self-discharge rate of NiCd batteries is generally high, around 10% of rated capacity per month. Moreover, NiCd batteries contain cadmium, which is a toxic material. As a result, disposal of NiCd batteries has to be done in proper ways. NiCd batteries also suffer from *memory effect*, where the battery can only be charged fully after a series of full discharges. However, this effect can be overcome using proper battery management systems.[9; 18]

NiCd batteries, however, have some advantages over lead acid batteries. NiCd batteries can be overcharged and fully discharged. NiCd batteries are more rugged, have excellent low temperature performances and internal resistance of the batteries is quite low. The charging rates are also higher than for lead acid batteries. Research and development are in progress to overcome disadvantages of nickel cadmium batteries and applications of such batteries for PV applications are being prioritized.[9; 18]

5.6.3 Sodium sulfur batteries

A Sodium sulfur (NaS) battery consists of liquid (molten) sulfur at the positive electrode and liquid (molten) sodium at the negative electrode. A solid beta alumina ceramic electrolyte separates the two electrodes. The electrolyte allows only the positive sodium ions to go through it and combine with the sulfur to form sodium polysulfide. During discharge, positive sodium ions flow through the electrolyte and migrate to the sulfur container. The electrons released by the sodium atoms flow through the external circuit to the electric load and then to the sulfur container. In the container, the electron reacts with the sulfur to form S^- cations, which in turn reacts with sodium ions to form sodium

polysulfide. Sodium level in the cell reduces with the discharging process. This process is reversed during charging. Sodium polysulfide breaks down and releases positive sodium ions, which travels through the electrolyte to recombine as elemental sodium. The heat produced by charging and discharging cycles is around 300 to 350 ˚C and is enough to maintain the process. [18]

NaS batteries have energy efficiency in the range of 75 to 90%. Typical cycle life of a NaS battery is around 2500 cycles. Energy density of the battery is from 150 to 240 Wh/kg and power density is from 150 to 230 W/kg. During discharge, a NaS cell produces 2 V. NaS batteries have the capability to produce power output six times its capacity for around 30 seconds. As a result, NaS batteries are eligible to be used in combined power quality and peak shaving applications. Such applications have been demonstrated in Japan, for example, in the 6 MW/7.25 h unit at the Hitachi plant. High operating temperature (300 to 350 ˚C), which reduces battery performance and high initial costs are major drawbacks of NaS battery technology. [21]

5.6.4 Lithium ion batteries

The cathode of lithium ion batteries is made of various lithiated metal oxides, such as lithium cobalt oxide ($LiCoO_2$), lithium manganese dioxide ($LiMnO_2$), and lithium iron phosphate ($LiFePO_4$). The anode is made of graphite carbon with a layer structure. The electrolyte is made up of lithium salts dissolved in organic solvents such as ethylene carbonate or diethyl carbonate. Lithium salts may include lithium hexafluorophosphate ($LiPF_6$), lithium hexafluoroarsenate monohydrate ($LiAsF_6$), lithium perchlorate ($LiClO_4$), lithium tetrafluoroborate ($LiBF_4$) and lithium triflate ($LiCF_3SO_3$). Lithium polymer batteries are another type of lithium based battery, which are similar to lithium ion batteries, except the lithium salt electrolyte is kept in solid polymer composite such as polyethylene oxide or polyacrylonitrile instead of in an organic solvent. Pure lithium is highly reactive with water. Thus, non-aqueous electrolytes are typically used and the battery is kept in a sealed container to prevent moisture from entering. When the battery is charged, the lithium atoms in the cathode become ions and migrate towards the anode through the electrolyte. Lithium ions combine with external electrons to form lithium atoms and stays between the carbon layers in the anode. This process is reversed during discharging. [18; 21; 24; 25]

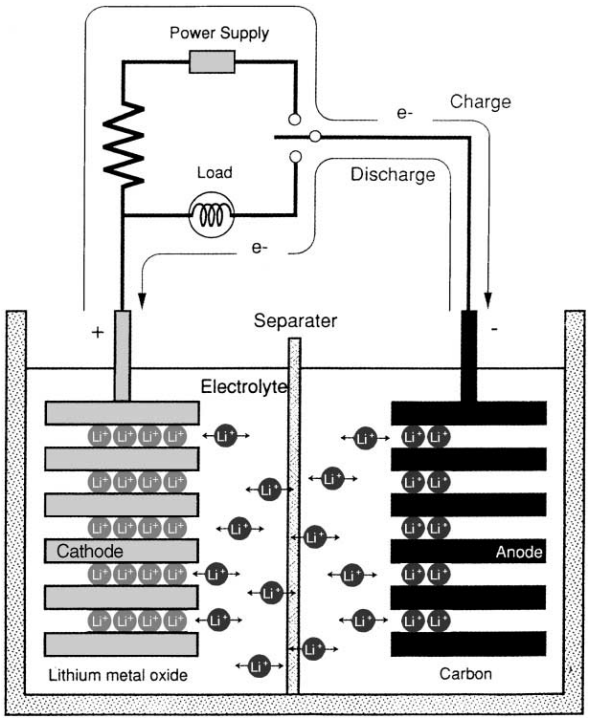

Figure 5.6: *Operation principle of a typical lithium ion battery.*[25]

Lithium ion batteries are extensively used in consumer electronics such as laptops and mobile phones. Lithium ion batteries are also being used in electric vehicles and are considered as one of the most promising battery technologies. Lithium ion batteries have high energy density, high efficiency, low self-discharge rate and require very low maintenance. Lithium ion cells with nominal voltage of 3.7 V have energy densities ranging from 80 to 150 Wh/kg. Energy efficiencies may range from 90 to 100 %. Power density for lithium ion cells ranges from 500 to 2000 W/kg. Power density of lithium polymer batteries ranges from 50 to 250 W/kg. Self-discharge rate of lithium ion batteries can be a maximum of 5% of rated capacity per month. Battery cycle life may reach more than 1500 cycles. However, the cycle life of the battery depends on temperature. High operating temperature and deep discharges can significantly reduce the lifetime of a lithium ion battery. A protection circuit is required with the battery to control the voltage of the cells during charging and discharging. The protection circuit also prevents overheating of the battery. Overheating and overcharging of the battery may lead to explosion or fire. Lithium polymer batteries have lower cycle life, around 600 cycles and have narrower operating temperature ranges avoiding lower temperatures. However, lithium polymer batteries are generally lighter and safer with minimum self-inflammability. [18; 21; 24; 26; 27]

Breakthroughs in lithium battery technology are expected through innovations in electrode and electrolyte components. Most lithium ion batteries are currently produced using carbon graphite as anode and lithium cobalt oxide as cathode. Worldwide research and development efforts are focused toward the replacement of present battery compo-

nents with materials having higher performance in terms of energy, power, cost, reliability, lifetime and safety. Replacements are being tested for graphite and lithium cobalt oxide with alternative materials, which provide higher capacity and lower cost. Researches into replacing the organic carbonate liquid electrolyte solution with safer electrolyte systems are also ongoing. Promising cathode materials include lithium iron phosphate ($LiFePO_4$), which offers better energy capacity, lower cost, better safety and higher operating temperature range. Lithium titanate is another promising material to replace graphite as anode materials because it offers better safety, better operating temperature range and higher charging rate. Polymer electrolytes are being considered to replace the conventional $LiPF_6$ organic carbonate solution among other alternatives. Lithium ion batteries are being used in large-scale energy storage applications for electric power industry. As an example, Department of Energy in the United States has sponsored a project undertaken by companies such as Saft batteries and SatCon Power Systems to design and construct two 100 kW/1-min lithium ion battery energy storage systems. The application of these energy storages is to provide power quality for grid-connected micro-turbines. Lithium ion batteries offer plenty of advantages and promises. Lithium based batteries are very suitable to be used with renewable energy sources such as PV generators to maintain power quality, although cost reduction and improvement in waste management of the batteries are needed. [24; 26; 27]

5.6.5 Fuel cells

Fuel cells are electrochemical energy conversion devices. Fuel flows in from external sources in the anode and reacts with the oxidant in the cathode. The reaction takes place in the presence of an electrolyte. Generally, the reactants flow in and reaction products flow out, while the electrolyte remains in the cell. [28; 29] As long as the necessary flows are maintained, a fuel cell can maintain its operation continuously. The difference between a fuel cell and a battery is that, a fuel cell consumes reactants, which need to be resupplied, while batteries store electrical energy chemically in a closed environment. In addition, the electrodes in a fuel cell are catalytic and relatively stable, where as electrodes in batteries generally react and change during charging and/or discharging. Many combinations of fuels and oxidants are possible. A hydrogen fuel cell uses hydrogen as fuel and oxygen as oxidant, as shown in figure 5.7. A reversible hydrogen fuel cell can also be built using electricity and water to produce hydrogen and oxygen. Other fuels include hydrocarbons, alcohols and metal. Oxidants include air, chlorine and chlorine dioxide. [21; 22]

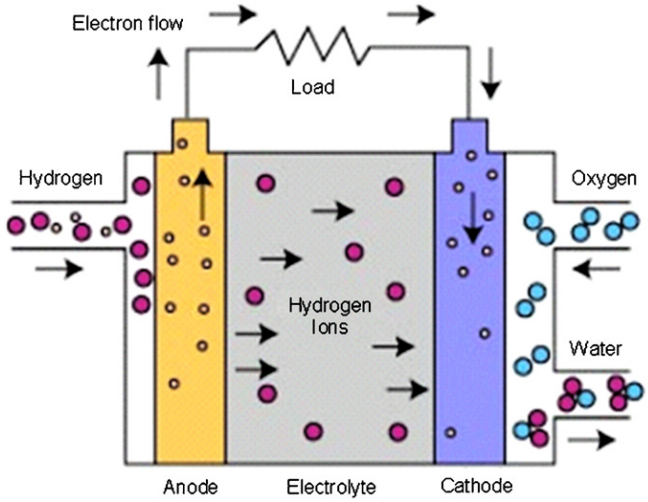

Figure 5.7: *Illustration of a hydrogen fuel cell.*[22]

There are many fuel cell technologies currently being studied and implemented. Hydrogen-based fuel cells have good potential to be used with renewable energy sources. Hydrogen fuel cells have high energy density (600 to 1200 Wh/kg). Hydrogen fuel cells have modular characteristics. These systems can be implemented in different capacity ranges, from kW to multi-MW systems. Hydrogen fuel cells also have independent system charge rate, discharge rate and storage capacity. Presently, hydrogen fuel cells have very low efficiency (20 to 50%) and high costs. Direct-methanol fuel cell (DMFC), has very high energy density and is being researched for implementations in the future. Molten carbonate fuel cells (MCFCs) are another type of fuel cells, which show a lot of promise in large-scale industrial processes, due to high power generation capabilities. Solid oxide fuel cells can have efficiency of around 60% and these could be used for generating electricity and heat. Metal-air battery is another type of fuel cell, which uses metal as the fuel and air as the oxidant. Metal-air batteries typically use common metals with high energy densities, such as aluminum or zinc that release electrons when oxidized. Metal-air batteries are very compact in nature, environmentally safe and potentially the least expensive. However, the electrical recharging of these batteries is very inefficient and difficult. As a result, consumed metal is usually replaced instead of electrical recharging. Rechargeable metal-air batteries, which are currently under development, have only a few hundred cycle-life and the efficiency is below 50%. [21]

5.6.6 Solar fuels

The basic concept of solar fuels can be described as follows. Diluted sunlight is concentrated over a small area using parabolic mirrors. The energy of the concentrated radiation is captured using suitable receivers and reactors. The energy is used as heat to carry out an endothermic chemical transformation and a storable and transportable fuel is produced. That fuel is then used to create electricity. [21; 30]

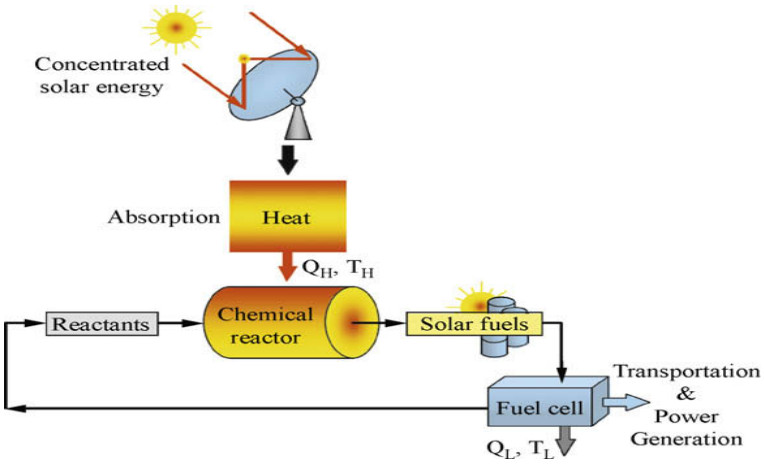

Figure 5.8: *Operating principle of a typical solar fuel energy storage system.* [31]

When concentrated solar radiation is used to create solar hydrogen, different chemical sources can be used. Besides water, fossil fuels can also be used to produce hydrogen using different processes. In metal-air fuel cells, metal oxides, such as Zinc oxide (ZnO), are created as products of chemical reactions. Instead of using carbothermic and electrolytic processes to extract metal from the metal oxides, concentrated solar energy can be used to provide the process heat. Conventional carbothermic and electrolytic processes need high energy and create environmental pollution. Moreover, solar thermal dissociation of ZnO is very promising due to low temperature requirement for the reaction. In another potential application, heat generated from concentrated solar radiation can be used to drive an endothermic reversible reaction in a solar chemical reactor. The products of the reaction can be stored and can be later used as exothermic reverse reaction. Thus, equivalent heat can be generated from the stored solar energy. The heat may be used to produce electricity. The chemical products from the reverse reactions are the original products, which can be returned to the solar reactor to be used again. CH_4 reforming methanation and NH_3 dissociation synthesis are such reversible reactions that have been extensively investigated for this purpose. [21; 32]

5.6.7 Flow batteries

A flow battery is a type of batteries in which the electrolyte contains one or more dissolved electro-active components flowing through a reactor or power cell, in which the chemical energy is converted to electricity. Energy is stored by driving electrochemical reactions, e.g. by electrolysis of metal salts. Additional electrolyte is stored externally and is usually fed through the cell of the reactor. The reaction in the flow battery is reversible. Flow batteries are considered as the intermediate technology between conventional batteries and fuel cells. Unlike conventional batteries, the energy is stored in the electrolyte in flow batteries. The energy capacity of a flow battery is a function of the quantity of the electrolyte. Power rating is dependent on the battery chamber size (i.e. active area of the cell stack). Flow batteries can release energy continuously at a high

discharge rate for up to 10 hours. Flow batteries differ from fuel cells in terms of operation. For example, flow batteries drive the electrolyte flows through the reactor, where as in fuel cells, electrolyte remains within the reactor at all times. Flow batteries are rechargeable batteries with reversible chemical reaction; hence, the electro-active materials do not need to be replaced. [9; 21; 33]

Currently there are three types of flow batteries available: vanadium redox battery (VRB), zinc bromine battery (ZnBr battery) and Polysulfide bromide battery (PSB), based on the type of electrolyte used. In PSB, solutions of sodium bromide and sodium polysulfide are used as electrolytes. Both electrolytes flow to the reactor, where a polymer membrane separates the electrolytes. Only positive sodium ions are allowed to go through the polymer membrane. As a result, about 1.5 V is generated across the membrane. Cells are usually connected in series and parallel to achieve higher voltage and current levels. The battery operates in room temperature. The operation of a PSB is shown in figure 5.9. [21; 22]

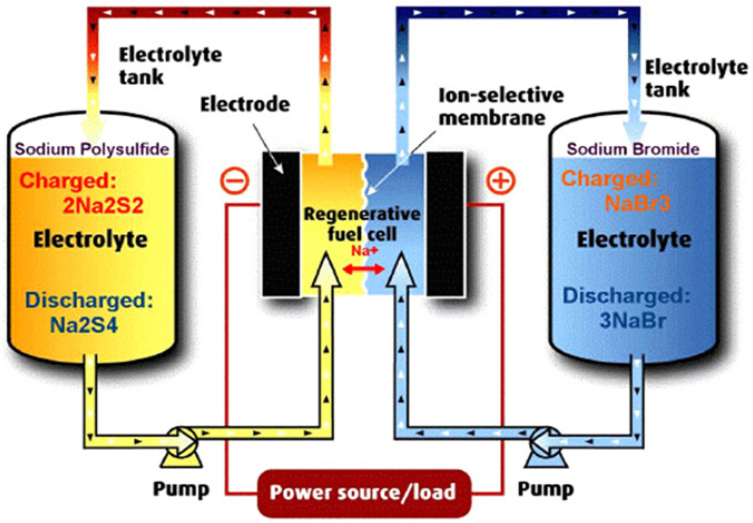

Figure 5.9: *Illustration of a polysulfide bromide battery.* [22]

Cell voltage of flow batteries ranges from 1.4 to 1.8 V. The efficiency of flow batteries ranges from 75 to 85%. Flow batteries have long cycle life, quick response times and are environmentally quite safe. These batteries also need low maintenance and are tolerant to over-charge and over-discharge. In addition, self-discharge of flow batteries is very low. On the negative side, flow batteries have relatively low energy density and need additional system components such as pumps, sensors, control units etc. Flow batteries are suitable for a wide range of applications, such as, power quality maintenance, load balancing, UPS, peak shaving and supply reliability enhancement. VRB can also be integrated with renewable energy systems to compensate for fluctuating power outputs. [21; 33]

5.7 Thermal energy storage

In Thermal energy storage or TES systems, materials are kept at either high or low temperatures in insulated containments. Electricity is generated using heat engine cycles when the heat or cold is recovered. Low-temperature TES (LT-TES) systems have operating temperature lower than the room temperature. High-temperature TES systems (HT-TES) operate at temperatures higher than the room temperature. TES can be further categorized based on operating temperature into industrial cooling system (below -18 ˚C), building temperature system (at 0 to 12 ˚C), building heating system (at 25 to 50 ˚C) and industrial heat storage (higher than 175 ˚C). The Overall efficiency of TES systems is from 30 to 60%. [21; 34]

5.7.1 Aquiferous low-temperature TES

Water is cooled using a refrigerator during off-peak hours and stored to be used for cooling needs during peak hours. The amount of the stored energy is dependent on the temperature difference between the cooled stored water and the warm return water from the heat exchanger. Aquiferous storage systems are useful for peak shaving commercial and industrial cooling loads during the daytime, which allows lower air conditioning operating costs and lower peak demand charges. [21]

5.7.2 Cryogenic energy storage

Cryogenic energy storage or CES systems use off-peak power or renewable energy sources to generate cryogen (e.g. liquid nitrogen or liquid air). During peak hours, liquid is heated by surrounding environment and the heated cryogen is used to create electricity using a cryogenic heat engine. Wasted heat from power plants can also be used by CES. CES can also provide direct cooling and refrigeration.[35]CES systems have relatively high energy density (around 100 to 200 Wh/kg), low capital cost per unit energy, long storage period and are safe for environment. However, CES systems have low efficiency, ranging from 40 to 50%. CES systems are still in development in various universities worldwide. [21]

5.7.3 Room temperature ionic liquids

Room temperature ionic liquids or RTILs are organic salts with negligible vapor pressure in the relevant temperature range and a melting temperature below 25 ˚C. Such liquids can be stored at extremely high temperatures without any decomposition. Such technology is still in the development and testing phase. [21]

5.7.4 Phase change materials

Phase change materials or PCMs are those materials, which change phases (usually from solid to liquid) at a temperature equal to the thermal input source. The latent heat from a phase change is high, which may result in higher energy densities compared to systems with non-phase-changing high-temperature materials. Storage based on PCM is still in early development phase. [21]

5.8 Assessment of energy storage technologies

Energy storage systems differ from each other based on technical maturity. PHS and lead acid battery can be considered as matured technologies, which have been used for over 100 years. CAES, NiCd, NaS, flow batteries, SMES, flywheels, super-capacitor, Al-TES and HT-TES can be considered as developed technologies. Although technically developed and commercially available, actual applications of these technologies may not be widespread yet. Moreover, continued research and development promise further improvement of these technologies. Fuel cells, metal-air battery, solar fuel and CES are developing technologies. These technologies have great potential, especially in terms of environmental impacts and energy costs. [21; 22]

PHS, CAES and CES are suitable for applications in scales above 100 MW with hourly to daily output durations. Energy management applications such as load leveling, load following and spinning reserve are appropriate for these storage technologies. Flow batteries, fuel cells, solar fuels, CES and TES are suitable for medium-scale energy management applications with a capacity of 10-100 MW. Flywheels, batteries, SMES and super-capacitors have fast response times (milliseconds) and are suitable for power quality applications, such as instantaneous voltage drop, flicker mitigation and short duration UPS. Typical power required for such applications is generally less than 1 MW. Batteries, flow batteries, fuel cells and metal-air batteries have fast response times of less than one second. These storage technologies also have long discharge times (hours). Therefore, these technologies have potential to be used as buffer and emergency storages. [21; 22]

PHS, CAES, fuel cells, metal-air batteries, solar fuels, flow batteries have very small discharge rates and can be used for long term energy storage applications. Lead acid batteries, NiCd batteries, lithium ion batteries, TES and CES systems have good self-discharge rates and can be used to store energy for medium terms, e.g. for weeks. NaS, SMES, super-capacitors have high self-discharge rates and can generally be used to store energy for duration of few hours. Flywheels have 100% self-discharge rate per day. As a result, flywheels are generally used to store energy for only a few minutes. [21; 22]

Super-capacitors, lithium ion batteries, flywheels and SMES have very high efficiencies, generally higher than 90%. PHS, CAES, flow batteries and other types of batteries generally have efficiencies in the range of 60 to 90%. Metal-air batteries, solar fuels, fuel cells, TES and CES usually have efficiencies lower than 60%. [21; 22]

CAES, metal-air batteries, PHS, TES and CES generally have low costs per kWh. Costs of batteries and flow batteries are gradually decreasing with the advancement of technology. Reduction of costs of storage technologies is one of the major focus points in current research activities. [21; 22]

Fuel cells, metal-air batteries and solar fuels have very high energy density, typically around 1 kWh/kg. Energy densities of batteries, TES, CES and CEAS are relatively lower. PHS, SMES, super-capacitors and flywheels have very low energy densities, generally below 30 Wh/kg. However, power densities of SMES, super-capacitors and flywheels are very high. Hence, SMES, super-capacitors and flywheels are suitable for power quality applications due to high power rating and fast response times. NaS and lithium ion batteries have higher energy densities compared to other types of rechargeable batteries. [21; 22]

Lifetime and cycle life of SMES and super-capacitors are very high. Cycle lives could be as much as 100,000 and lifetime could stretch beyond 20 years for SMES and 500 years for super-capacitors. PHS, CAES, flywheels, TES and CES systems also have very long lifetimes and cycle lives. For example, flywheels have a cycle life of over 20,000 cycles. PHS, CAES, CES systems can have lifetimes of 40 years or more. Cycle lives of batteries, flow batteries and fuel cells are not as high as other systems. For example, NaS batteries have cycle life of 2500 cycles. Metal-air batteries have even lower cycle life, ranging from 100 to 300 cycles. [21; 22]

Solar fuel systems use solar radiation to produce electricity and store energy in the form of hydrogen, which is a green fuel. Thus, solar fuel systems reduce the use of fossil fuels and help the environment. CES systems can remove contaminants in the air during charging process, which helps the environment. PHS, CAES, batteries, flow batteries, fuel cells and SMES negatively affect the environment for various reasons. Construction of PHS destroys green lands and associated ecological systems. CAES requires gas turbine plants and thus fossil fuels are used. Batteries contain toxic materials and require proper disposal. SMES generates strong magnetic fields, which are harmful for humans. [21; 22]

Many improvements are anticipated in energy storage technologies in the near future. Performance, storage capacity and cycle life are expected to increase where as costs are expected to decrease. The usage of lead acid, NiCd and lithium ion batteries is also expected in the field of large-scale electricity industry. Usage of energy storage systems with renewable energy sources is also expected to increase.

Conventional batteries such as lead acid batteries, nickel-based batteries, sodium sulfur batteries and lithium ion batteries have properties that generally suit the applications with PV power systems. Super-capacitors are also very suitable to be used along with PV systems. In table 5.1, approximate values of power and energy densities, self-discharge rates, efficiencies and cycle lives of these storage technologies are presented.

Table 5.1: *Characteristic properties of conventional batteries and super-capacitor.*

Type of ESS	Power density (W/Kg)	Energy density (Wh/Kg)	Self discharge per day (%)	Efficiency (%)	Cycle life
Lead acid battery	75 – 300	30 – 50	0.1 – 0.3	70 – 90	500 – 1000
Nickel-based batteries	150 – 300	50 – 80	0.2 – 0.6	60 - 80	2000 – 2500
Sodium sulfur battery	150 – 230	150 – 240	0	75 - 90	2500
Lithium ion battery	150 - 315	75 – 200	0.1 – 0.3	90 - 100	1000 – 10,000
Super capacitor	500 – 10,000	2.5 - 15	20 – 40	85 - 98	100,000

Lead acid batteries are the most commonly used battery technology due to the maturity of the technology and low cost. Lead acid batteries also have low self-discharge rate, long lifespan and fast response time. However, these batteries are very sensitive to the operating environment. Changes in operating temperatures greatly shorten the lifespan of the battery. Battery cycle life also reduces for high depth of discharge. In addition, typical charge-to-discharge ratio is 5:1 and the battery cell would be damaged if faster charging rates are applied. Nickel-based batteries have higher self-discharge rates than lead acid batteries and can withstand relatively higher operating temperature. Nickel-based batteries can also have very high cycle lives if the depth of discharge is kept small, i.e. approximately 10 % of the capacity. However, these batteries suffer from memory effect. Moreover, cadmium, which is used in nickel-cadmium batteries is a toxic material and poses a great threat to the environmental safety. The main advantage of sodium sulfur battery is the pulse power capability, where the battery can produce power six times its rated power for around 30 seconds. However, the operating temperature needed for the battery is from 300 to 350 ˚C. Hence, challenges are associated with maintaining the high temperature and ensuring safety. Lithium ion batteries have excellent efficiency, good cycle life and relatively high energy density. Research and development efforts are ongoing to reduce the costs and improving the safety of lithium ion batteries among other factors. Super-capacitors have very high cycle life and

can produce very high amount of power. Compared to the batteries, super-capacitors do not degrade due to deep discharges, do not produce heat and do not involve any toxic materials. However, energy density of super-capacitors is very low. Hence, high costs are associated with using super-capacitors in large-scale operations. In table 5.2, major advantages and disadvantages of these energy storage systems are presented. [21; 36-38]

Table 5.2: *Advantages and disadvantages of conventional batteries and super-capacitor.*

Type of energy storage	Advantages	Disadvantages
Lead acid battery	• Mature technology • Low self-discharge	• Sensitive to environmental factors • Sensitive to charge rate
Nickel based batteries	• Long life • Tolerate high temperatures	• Memory effect • Disposal
Sodium sulfur battery	• Pulse power capability • Demonstrated technology	• Requires high temperature • Harsh chemical environment
Lithium ion battery	• High energy density • High efficiency • Long life	• High cost
Super capacitor	• Long life • High power density	• Low energy density • High self-discharge rate

From above discussions, general comprehension can be achieved regarding the potentials of different energy storage technologies to be used with PV power systems. Different energy storage technologies offer different advantages and disadvantages; and with the help of continuous research, storage technologies can only be improved further.

6 BALANCING PV GENERATOR OUTPUT POWER USING ENERGY STORAGE

Renewable sources of energy offer tremendous advantages compared to conventional energy sources. Renewable energy sources such as solar photovoltaic and wind power systems need to replace conventional energy sources in order to establish a sustainable model of energy production and consumption. However, growing rate of adaptation of renewable energy sources poses significant challenges. Inherent intermittency of renewable sources such as PV and wind power systems is one of such challenges. Output power from wind and PV power plants can vary greatly and rapidly. Fluctuations in generated power from these renewable sources can create serious problems to the electricity network.

As a prominent renewable energy source of the future, Photovoltaic (PV) power plants are being adopted in increasing rate day by day. In smaller electricity networks or in comparatively weak network sections, high penetration rate of PV generators could pose serious problems to network reliability due to the variability in generated output power. [39] The output power from PV generators closely follows the incident solar radiation on the generator modules. Due to natural variability of solar radiation, along with the shading effects of moving clouds, the rate of change of output power from PV generators can be very high. Although the aggregation of geographically dispersed PV power plants can create a smoothing effect in the generated power, the smoothing effect is intrinsically limited. [40] Thus, in smaller electricity grids where the share of PV generated power is high, such fluctuations in PV generated power can create serious consequences for the electricity grid. Several grid operators around the world have imposed new regulations, which limit the variability of PV generated output power. For example, Puerto Rico Electric Power Authority (PREPA) recently imposed a regulation that the rate of change of PV generator output power cannot exceed the limit of 10 % per minute of the generator's nameplate capacity. This regulation is equally applicable to cases where the rate of change of power is positive and negative. This limitation is also applicable when curtailment of output power is active. [41]

Output power from large-scale grid-connected PV power plants can vary up to 90 % per minute, which is far beyond the limitation imposed by PREPA. [42] Energy storage systems can be used to control the rate of change (ramp rate) of PV generator output power. In such application, the energy storage charges and discharges itself to control the ramps in the output power. The energy storage system charges by subtracting power from PV generated power. The energy storage discharges by adding power to the PV generated power. Because of this operation, the rate of change of output power remains within the given limit and compliance with the regulation is ensured. In this thesis, ap-

plications and operations of energy storage systems (ESS) are analyzed, where the energy storage systems control the ramp rates in PV generator output power for different periods.

A 1 kW rated (in Standard Test Condition) PV generator is assumed in this thesis. It is assumed that the generator consists of 5 series connected PV modules. Each module produces 200 Watts of power with a voltage of 25 volts. The surface area of each module is assumed to be 1 square meter. Moreover, it is also assumed that the PV generator's output power is directly proportional to the incident solar irradiance. An energy storage unit with undefined technology, capacity and rating is used to limit the rate of change of PV generator's output power. The ramp rate limit, R_{lim} is defined as 100 W/min or 1.6667 W/sec (which is 10 % of the generator capacity per minute) for this PV generator. The PV generator is theoretically connected with the electricity grid by a central PV inverter. The energy storage system operates in parallel with the PV inverter.

6.1 Observations of ramp rate fluctuations

Daily solar irradiance data for one month (July 2013), measured at 10 Hz sampling frequency have been used to simulate the output power of the assumed 1 kW rated PV generator. A moving average of 5 seconds is applied to the solar irradiance data to get rid of the noises in the signal. The rate of change of output power is generally calculated based on the following formula:

$$\frac{dP}{dt} = \frac{\Delta P}{\Delta t} = \frac{[P(t) - P(t - \Delta t)]}{\Delta t} \quad , \tag{6.1}$$

where $\frac{dP}{dt}$ is the rate of change of PV generated output power. The rate of change of PV generated output power can be defined as *ramp rate*, R = $abs\left[\frac{dP}{dt}\right]$.

The ramp rate limit R_{lim} is defined as 10 % of the PV generator capacity per minute. As the capacity of the PV generator is 1 kW, hence the ramp rate limit is 100 W/min or 1.6667 W/sec. The rate of change of output power or the ramp rate R, then can be compared with the ramp rate limit R_{lim} to count the times when the fluctuations exceed the ramp rate limit, as shown in equation 6.2.

$$R > R_{lim} \, . \tag{6.2}$$

At first, different sampling times (such as 1 s, 2 s, 4 s, 10 s, 20 s, 60 s, 120 s) have been used and the results were compared with each other. It was observed that using sampling times of less than 8 seconds produced better results than higher sampling times. Obviously, using 1 second sampling time produced the best results. Hence, the decision was taken that 1 second sampling times would be used when analyzing the op-

erations of the energy storage system. Equations 6.1 and 6.2 are applied to find out the total time when the rate of change of output power exceeded the specified ramp rate limit in each day of July 2013. The results are shown in figure 6.1.

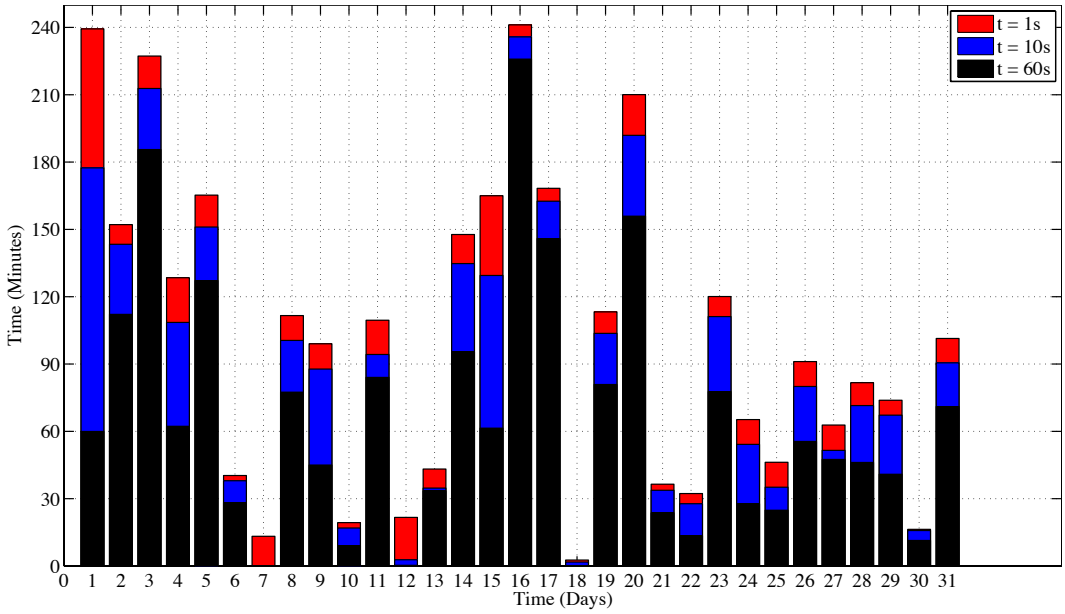

Figure 6.1: *Observed time of ramp rates higher than the ramp rate limit in each day of July 2013 are shown. Sampling times of Δt = 1 s, Δt = 10 s and Δt = 60 s have been used.*

Sampling times of 1 s, 10 s and 60 s have been used to calculate the rate of change of output power. It was observed that the daily times when the rate of change of output power was higher than the specified limit were rather high. It can be observed from figure 6.1 that the PV generator output power exceeds the ramp rate limit throughout the month. When sampling time of 1 second is used to measure the time of ramp rates, up to 4 hours exceeding the ramp rate limit were found for a single day. It can also be determined from figure 6.1 that higher sampling rates should be used to measure ramp rates, as that produces more observations of ramp rates. High ramp rates occur less during clear sky days, as can be seen for 7th of July 2013, which was a clear sky day. On 7th of July 2013, ramp rates higher than R_{lim} occurred for less than 20 minutes. Ramp rates occur more in days where cloud activities and movements are more prominent, such as on 16th of July 2013. On 16th July, high ramp rates occurred for more than 4 hours. Solar irradiances on 7th and 16th July 2013 are shown in figure 6.2.

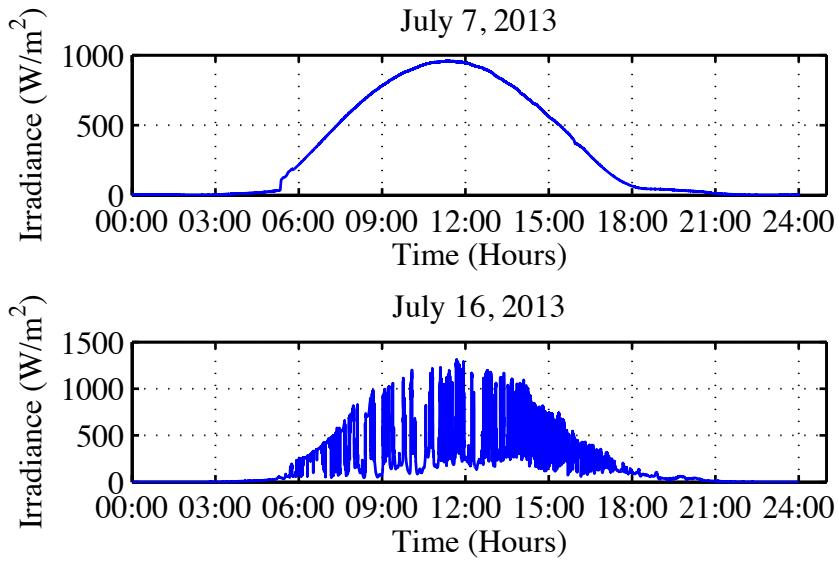

Figure 6.2: *Solar irradiance measured on 7th of July (top) and on 16th of July (bottom).*

It can be seen from figure 6.1 that high ramp rates occurred quite significantly during the month of July 2013. On average, high ramp rates occurred for about 101 minutes every day during the month of July 2013. The total time of deviations for the month is slightly more than 52 hours. To observe the ramp rates for longer times, solar irradiance data measured every day for the whole of the year 2012 have been analyzed from experimental data. In figure 6.3, daily times of high ramp rates can be observed for the year 2012 in ascending order.

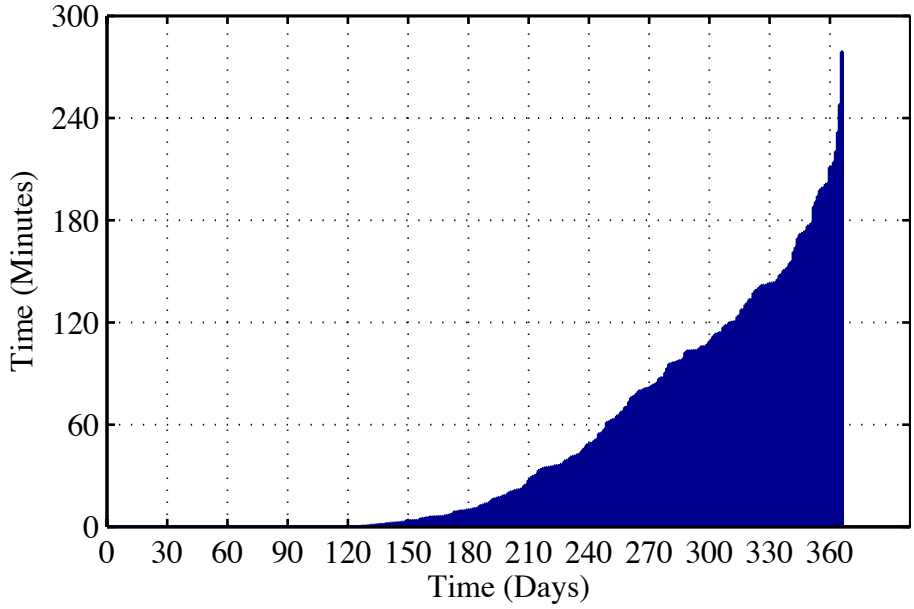

Figure 6.3: *Times of daily ramp rates higher than R_{lim} are shown for the year 2012 in ascending order.*

During the 366 days of the year 2012, ramp rates were lower than R_{lim} for 32 % of the days. Daily total time, when ramp rates were higher than R_{lim}, varied from 1 second to 1 hour for 37 % of the days in the year 2012. High ramp rates occurred for times ranging from 1 hour to 2 hours for 17 % of the days in the year 2012. High ramp rates occurred for times ranging from 2 hours to 3 hours for 11 % of the days and in only 3 % of the days of the year, high ramp rates occurred for more than 3 hours. Total time when ramp rates were higher than R_{lim} was 289 hours in the year 2012. In figure 6.4, monthly averages of times when the ramp rates were higher than R_{lim} are shown.

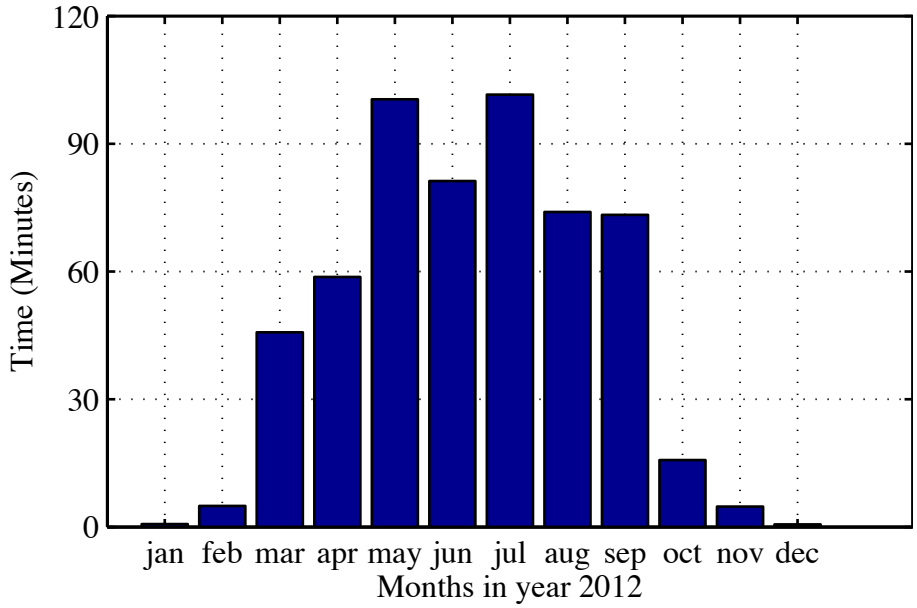

Figure 6.4: *Monthly average daily times of ramp rates exceeding R_{lim} in 2012.*

It can be observed from figure 6.4 that high ramp rates occurred more prominently during the months of summer. The daily average times of high ramp rates were higher than 1 hour for the months of May, June, July, August and September in the year 2012. Daily average times of high ramp rates were higher than 90 minutes in the months of May and July in the year 2012. Daily average times of high ramp rates were less than 15 minutes in the months of January, February, October, November and December in the year 2012. From figure 6.4, an observation regarding the operating times of an energy storage unit can be made. The need for an energy storage system having a long cycle life and continuous operability is quite apparent from the observations.

6.2 Inverter operating at 100 % of PV generator capacity

An energy storage system (ESS), without any defined technology, capacity and rating is theoretically used to balance the output power from the PV generator. As established earlier, the specified ramp rate limit is r = 1.6667 W/s. When the rate of change of output power from the PV generator doesn't exceed the ramp rate limit, the ESS does not

interfere with the PV generator output power. It is considered as normal condition of operation and the output power from the PV inverter goes directly to the electricity grid. The control system in the ESS actively checks the rate of change of inverter output power in every second. When the rate of change of PV generator output power does exceed the specified ramp rate limit, the ESS is activated. If the output power increases at a rate, which exceeds the ramp rate limit, it is referred to as *increasing ramp*. Similarly, when the power decreases at a rate higher than the specified ramp rate limit, it is referred to as *decreasing ramp*. During increasing ramp, the ESS stores as much power as needed (by subtracting from the PV generated power) to maintain a steady ramp of 1.6667 W/s. During decreasing ramp, the ESS discharges and adds power to the PV generator output to maintain a steady ramp of 1.6667 W/s. The operation of the storage system can be observed in figure 6.5 for the whole day of 1st of July 2013 and in figure 6.6 for 20 minutes during the morning on the same day.

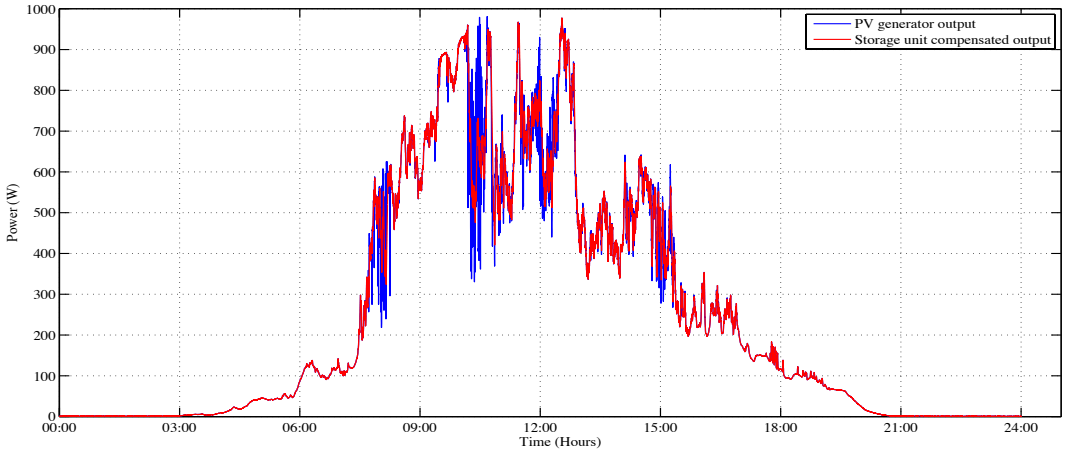

Figure 6.5: *The operation of the energy storage system on 1st of July 2013.*

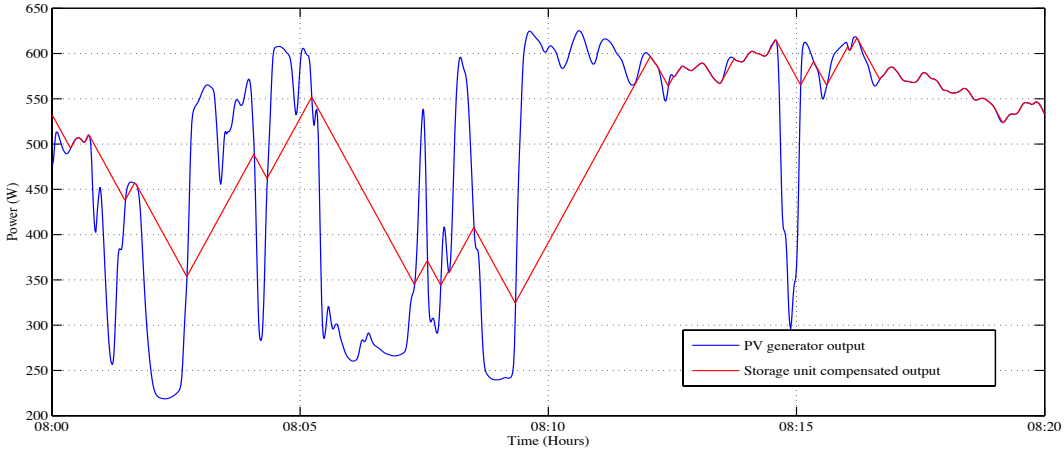

Figure 6.6: *The operation of the energy storage system for 20 minutes in the morning on 1st of July 2013.*

When the inverter output power doesn't exceed the specified ramp rate limit (i.e. during normal operating conditions), the ESS doesn't store or discharge any energy. The following figure 6.7 shows power values either charged or discharged by the ESS on 1st of July 2013. In figure 6.7, blue lines represent positive power values during each second, when energy is stored in the ESS and black lines represent negative power values during each second, when energy is discharged by the ESS.

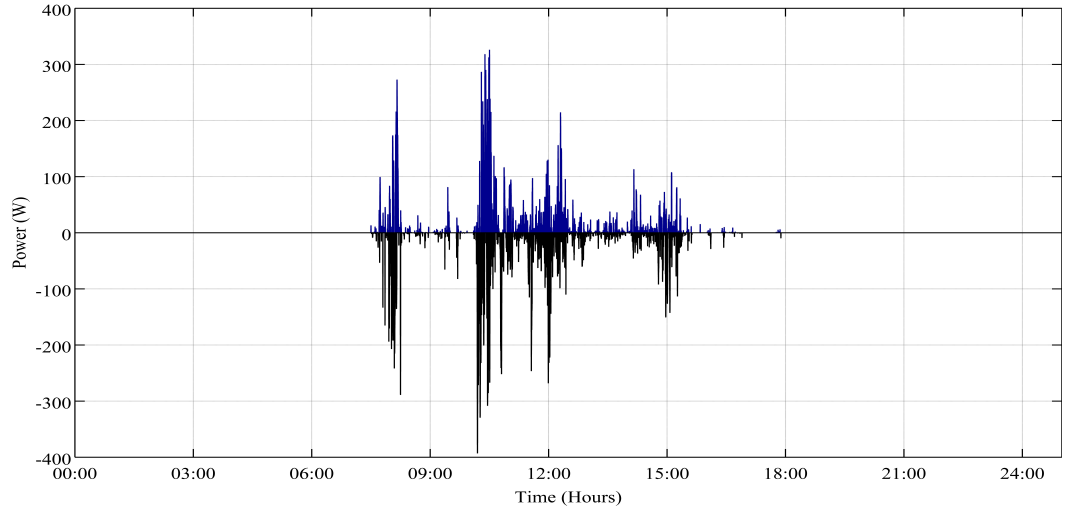

Figure 6.7: *The charging (positive values, in blue) and discharging (negative values, in black) of power of the ESS throughout the day (1st of July 2013).*

Status of energy in the ESS during one day of operation (on 16th of July 2013) can be seen in figure 6.8. Net discharged energy from the ESS is represented by negative energy values in figure 6.8. Net positive values of energy represent the energy stored by the ESS.

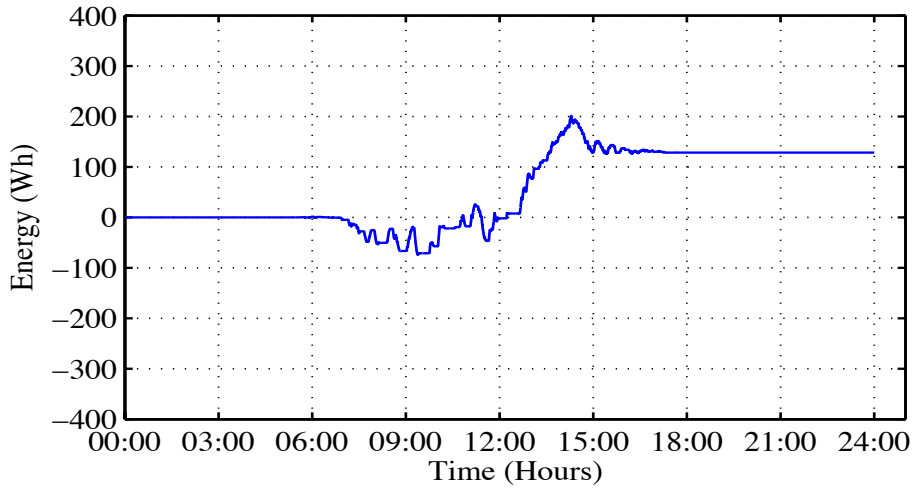

Figure 6.8: *Energy balance of the ESS during operation, on 16th of July 2013.*

It can be observed from figure 6.8 that for that particular day, the ESS discharged more energy than it charged early in the day but had around 128.36 Wh of energy stored at the end of the day. From figure 6.8, it is apparent that the ESS reaches certain maximum and minimum points of energy capacity during one day of operation. The capacity of an ESS thus need to be determined by observing the maximum energy capacity (by storing energy) reached by the ESS or the minimum capacity (in negative energy terms, due to discharging actions) reached by the ESS. Highest amount of energy either charged or discharged by the ESS during one day may indicate the needed capacity of the ESS if the ESS is recharged every night. On 16th of July 2013, the maximum stored energy in the ESS was 201.21 Wh and the maximum energy deficiency in the ESS was 74.5 Wh during the day. The maximum stored energy, the maximum energy deficiency and the energy remaining at the end of the daily operation, vary greatly from one day to another.

6.2.1 Periodic operation of the ESS

The operation of the ESS has been simulated for each day of the year 2012 to gather information regarding the maximum charged and discharged energy and the energy remaining at the end of each day. In these simulations, an ESS of undefined capacity has been used. Therefore, the state of energy in the ESS is set to zero at the start of each day. In figure 6.9, the daily maximum energy values charged by the ESS for each day of 2012 are shown in ascending order of the energy values. In figure 6.10, histogram of maximum energy stored by the ESS in each day of the year 2012 is shown.

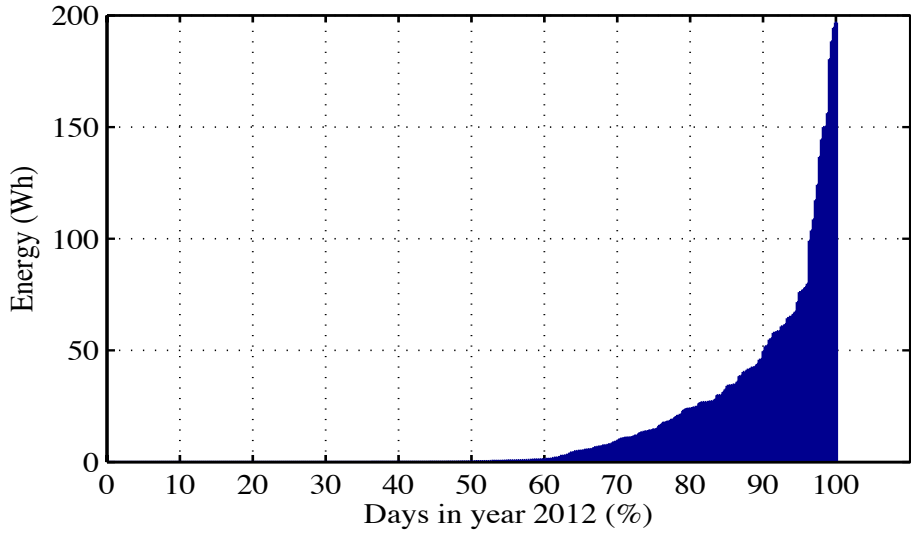

Figure 6.9: *Daily maximum energy stored by the ESS, in each day of 2012, shown in ascending order.*

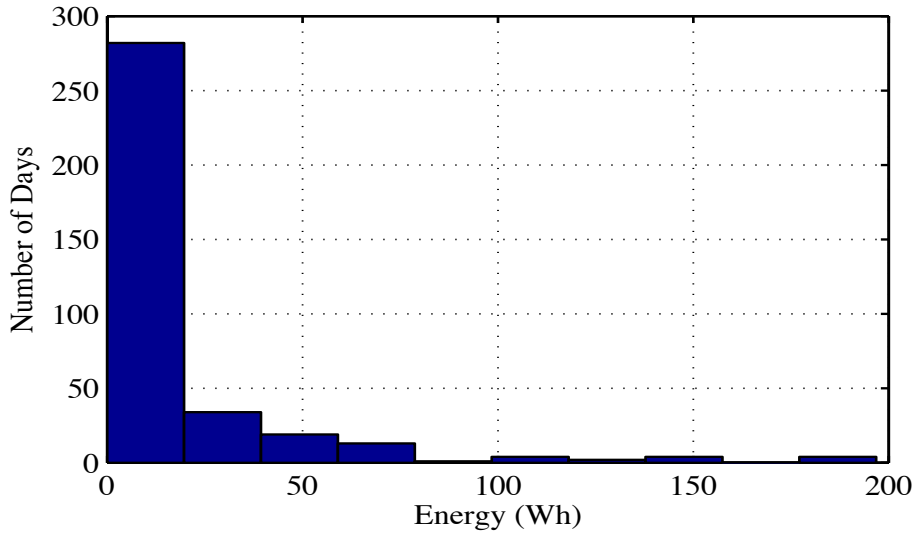

Figure 6.10: *Histogram of daily maximum energy stored by the ESS in each day of 2012.*

In the year 2012, the ESS did not store any energy in 132 days. For 80 % of the days, the maximum energy capacity reached by the ESS was around 20 Wh, as seen in figure 6.9. In only 10 % of the days, the maximum energy capacity reached by the ESS was higher than 50 Wh. The maximum stored energy capacity reached by the ESS was 197 Wh, as can be seen in figure 6.10. In figure 6.11, the daily maximum energy deficiencies due to discharging of the ESS are shown for the year 2012.

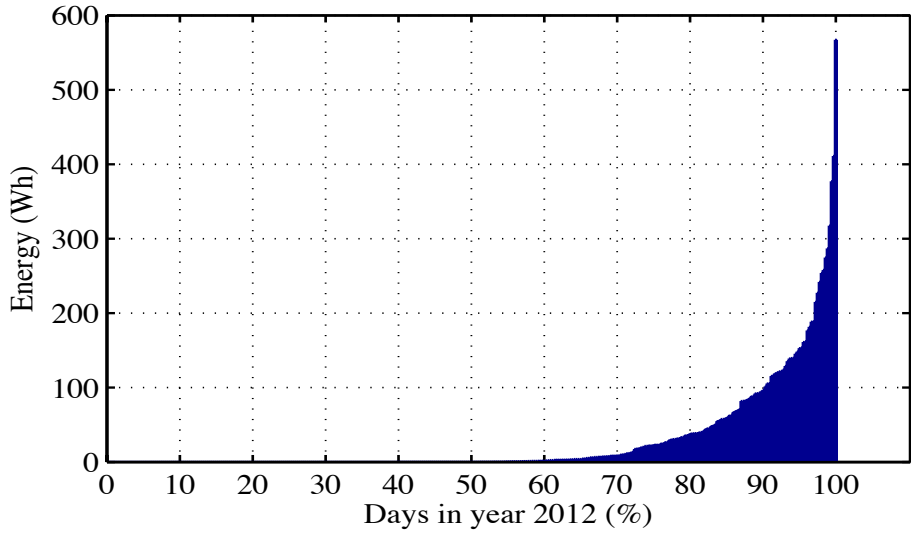

Figure 6.11: *Daily maximum energy deficiencies in the ESS in each day of 2012 are shown in ascending order.*

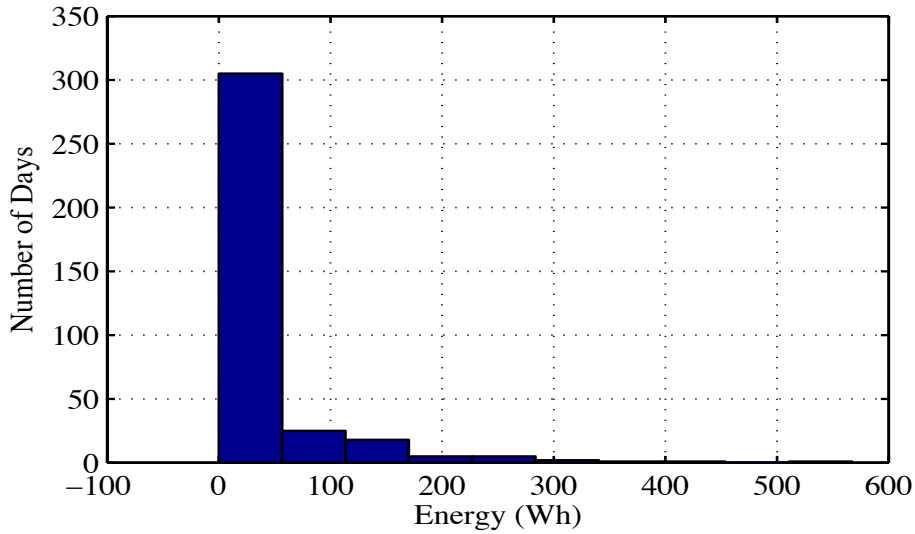

Figure 6.12: *Histogram of daily maximum energy deficiencies in the ESS in 2012.*

It can be observed from figures 6.11 and 6.12 that the ESS did not discharge any energy during 40 % of the days in the year 2012. For 90 % of the days in year 2012, maximum energy deficiency was below 100 Wh. Maximum energy deficiency by the ESS was 568 Wh in year 2012. In figure 6.13, the energy remaining in the ESS in each day of the year is shown in ascending order. In figure 6.14, histogram of the energy remaining in the ESS at the end of each day in year 2012 is shown.

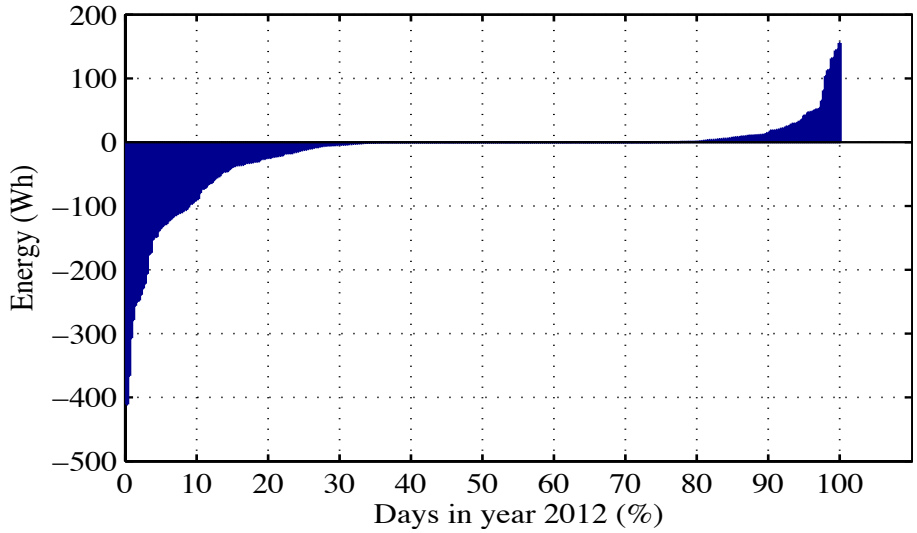

Figure 6.13: *Energy remaining in the ESS at the end of operation, in each day of 2012, shown in ascending order.*

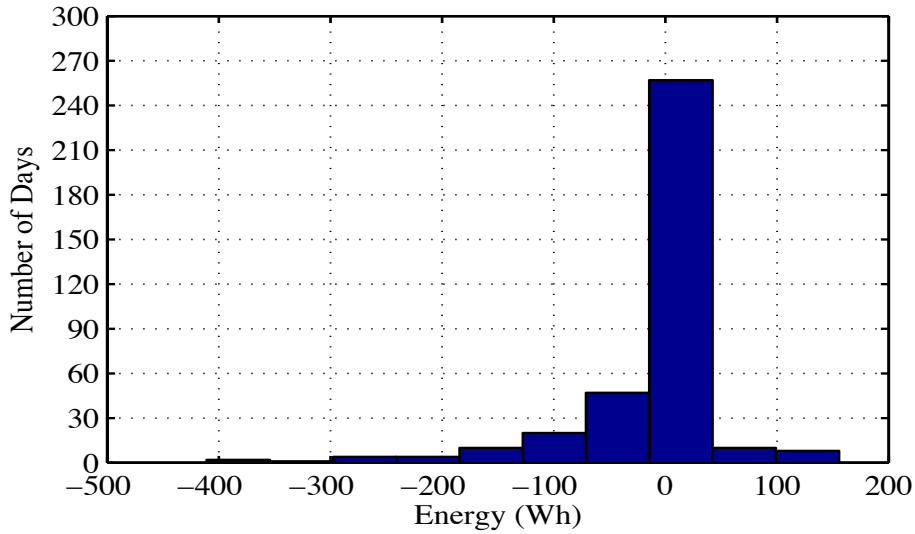

Figure 6.14: *Histogram of energy status in the ESS, at the end of each day in 2012.*

For around 45 % of the days in 2012, almost zero energy remained in the ESS. In 35 % of the days, the ESS had deficiency of energy. Deficiency of energy in the ESS is represented by negative energy values. During its daily operation, the ESS may discharge more energy than the energy it charges. As a result, at the end of the operation, the ESS has a deficiency of energy. In terms of capacity determination, the ESS should be sized according to the maximum capacity reached by the ESS, by either charging or discharging actions. In 20 % of the days in 2012, energy remained in the ESS at the end of daily operation. It can be concluded that the ESS discharges more energy than it charges during its day-to-day operations. The maximum energy deficiency in the ESS was 411 Wh and the maximum remaining energy in the ESS was 156 Wh, as shown in figures 6.13 and 6.14.

Similar simulations have been carried out for 8 months (245 days) of the year 2013, from May to December. In figure 6.15, daily maximum energy stored by the ESS is shown in ascending order. In figure 6.16, daily maximum energy deficiency in the ESS is shown in ascending order. In figure 6.17, energy remaining in the ESS at the end of each day is shown in ascending order.

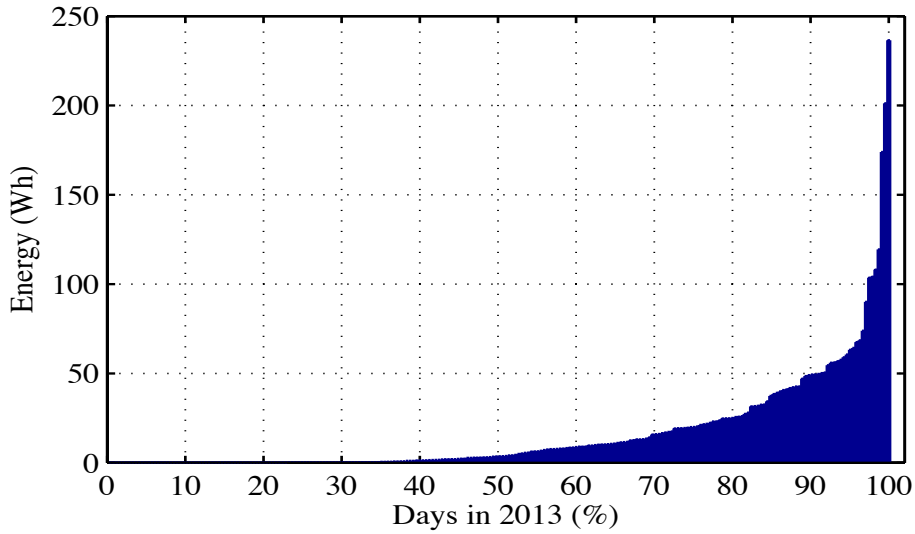

Figure 6.15: *Daily maximum energy stored by the ESS, in each day of 2013 from May to December, shown in ascending order.*

The maximum energy charged by the ESS was 237 Wh. For 90 % of the days, the maximum stored energy was less than 50 Wh. For only 10 % of the days in 8 months of the year 2013, the maximum charged energy exceeded 50 Wh, as seen in figure 6.15.

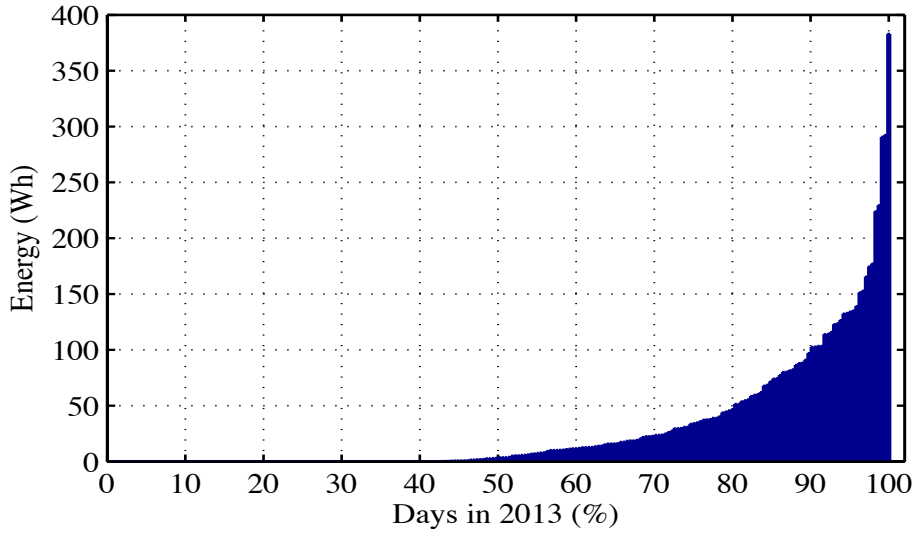

Figure 6.16: *Daily maximum energy deficiencies in 2013 from May to December are shown in ascending order.*

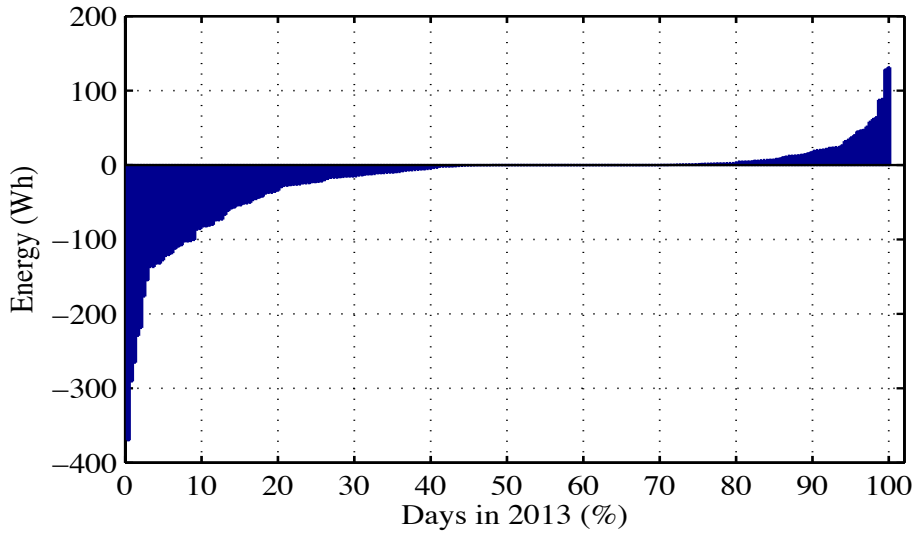

Figure 6.17: *Energy status in the ESS, at the end of operation in each day of 2013 from May to December, shown in ascending order.*

The maximum energy deficiency in the ESS was 383 Wh, as can be seen in figure 6.16. For more than 40 % of the days, zero energy remained in the ESS. For 90 % of the days, maximum energy deficiency was less than 100 Wh. Negative energy remained in the ESS for about 40 % of the days, as seen in figure 6.17. Positive remaining energy was found for around 25 % of the days. The maximum remaining positive energy was 132 Wh. The maximum negative energy in the ESS was about 370 Wh. Similar to the observations in 2012; the amount of discharged energy was higher than charged energy.

6.2.2 Continuous operation of the ESS

A simulation of the operation of the energy storage system has been done, where the energy storage remains active without any recharging for a full year. PV generator output power has been simulated for the year 2012 using measured solar irradiance data. The energy storage unit charges and discharges itself as described earlier to keep the ramp rate of PV generator output power under the limit of 1.6667 W/s.

From figure 6.18, it can be seen that the battery loses very little energy during the winter months of January, February, October, November and December in the year 2012. The discharge of the battery is significant in summer months of May, June, July and August. The energy of the battery was near 0 kWh at the start of May and the energy of the battery was around -6 kWh at the end of August. At the end of December 2012, the state of energy in the battery was around -6.12 kWh.

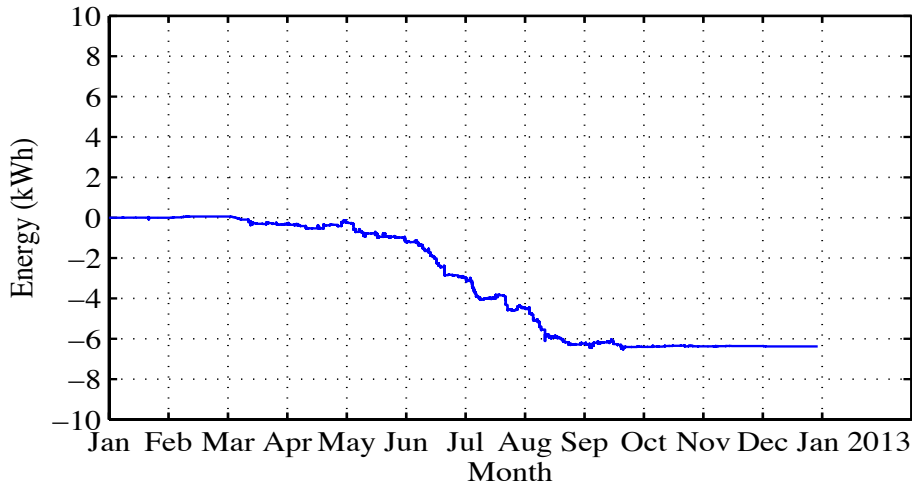

Figure 6.18: *Continuous operation of the energy storage system, throughout the year 2012.*

Similar simulation has been conducted for 8 months in 2013, from the month of May to the end of December. Solar irradiance data for the first four months of 2013 weren't available, which is why the simulation has been done for the later months. The battery loses energy throughout the summer months of 2013, and at the end of August, the state of energy in the battery was around -4.6 kWh, as can be seen in figure 6.19.

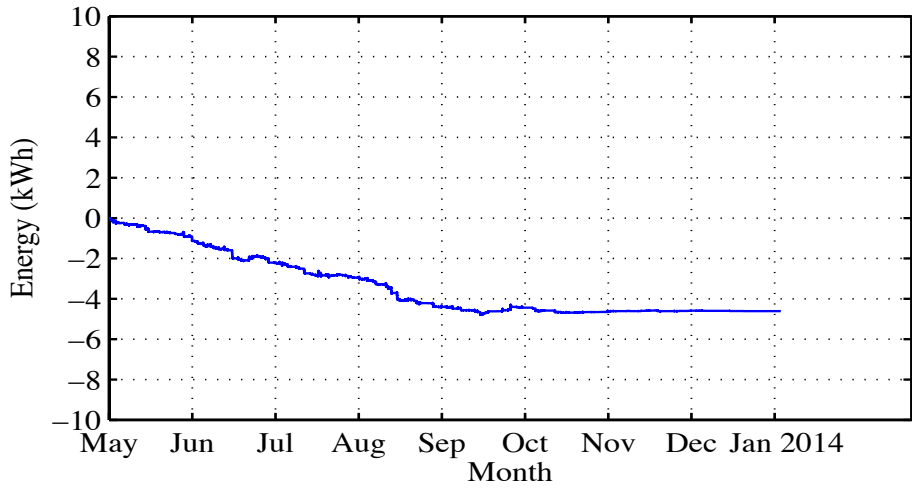

Figure 6.19: *Continuous operation of the energy storage system, from May 2013 to the end of December 2013.*

The required power rating of the ESS can also be determined by analyzing the continuous operation of the ESS. The power values of the ESS during charging for the entire year of 2012 are shown in figure 6.20 in ascending order. The discharging power values for the entire year of 2012 are shown in figure 6.21 in ascending order.

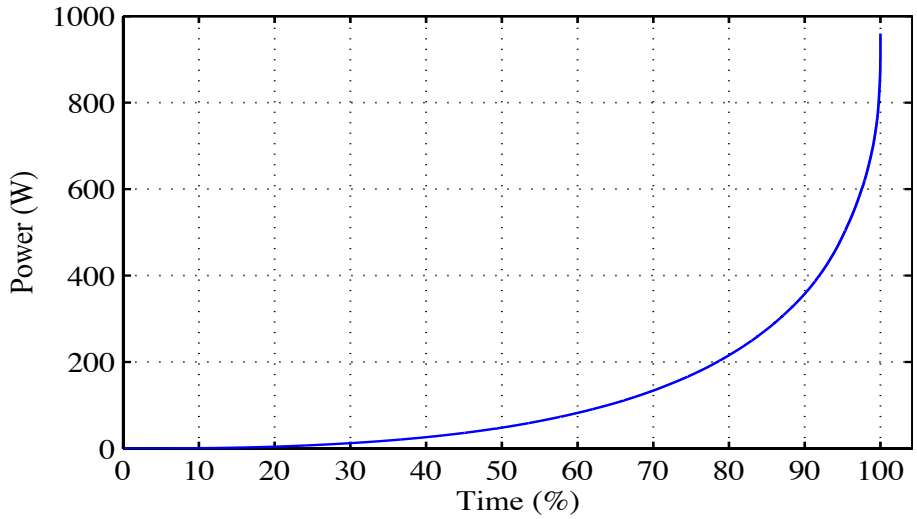

Figure 6.20: *Charging power of the ESS in ascending order, during continuous operation (total 267 hours of charging) throughout the year 2012.*

In 2012, the ESS operated for a total of 546 hours. In that period, Maximum charging power of the ESS was 960 W, as shown in figure 6.20. Average charging power of the ESS was 120 W. For 80 % of the time, the charging power was less than 200 W. The charging power exceeded 600 W for less than 5 % of the time during 2012.

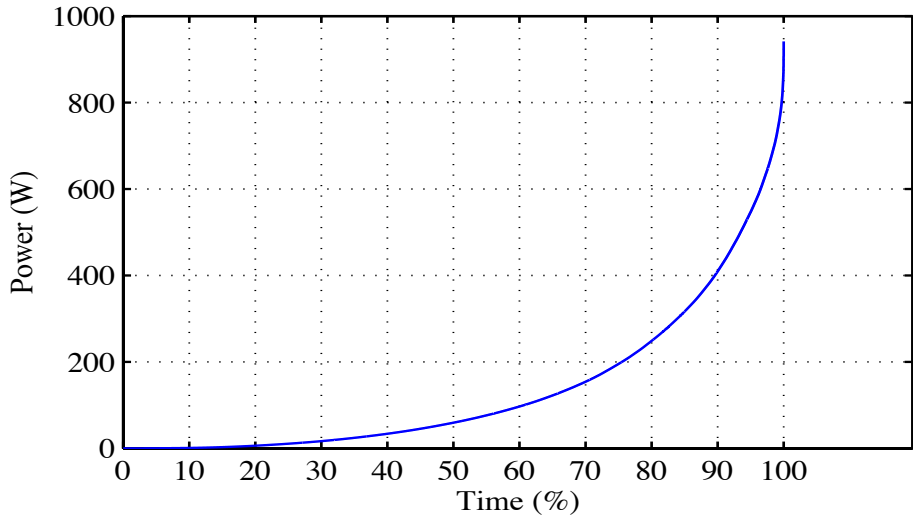

Figure 6.21: *Discharging power of the ESS in ascending order, during continuous operation (total 279 hours of discharging) throughout the year 2012.*

Maximum discharging power was 942 W, as shown in figure 6.21. Average discharging power was around 137 W. The discharging power was less than 220 W for 80 % of the time in 2012, as can be seen in figure 6.21. Discharging power exceeded 600 W for only 5 % of the time. Similarly, the ESS operated for a little more than 420 hours during 8 months of continuous operation in 2013. Charging and discharging power val-

ues are shown in ascending order for 8 months in 2013 in figure 6.22 and 6.23 respectively.

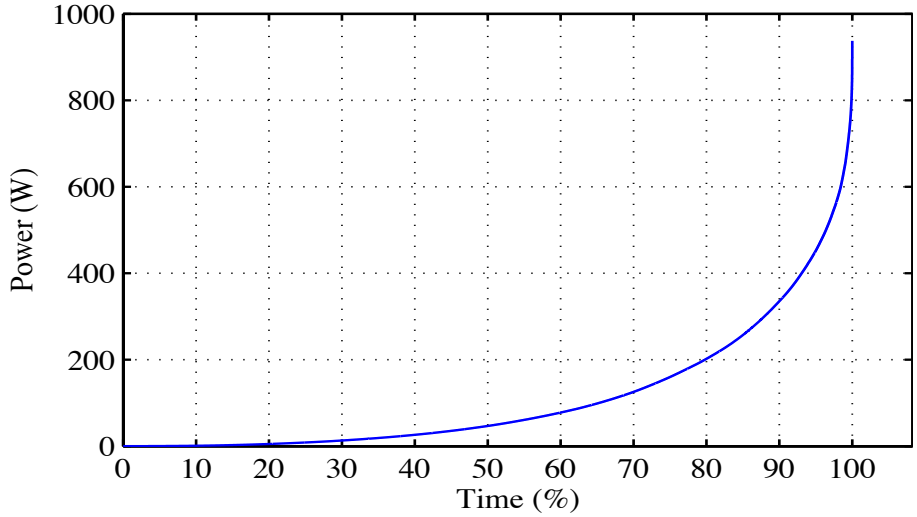

Figure 6.22: *Charging power of the ESS, in ascending order, from May to December in 2013.*

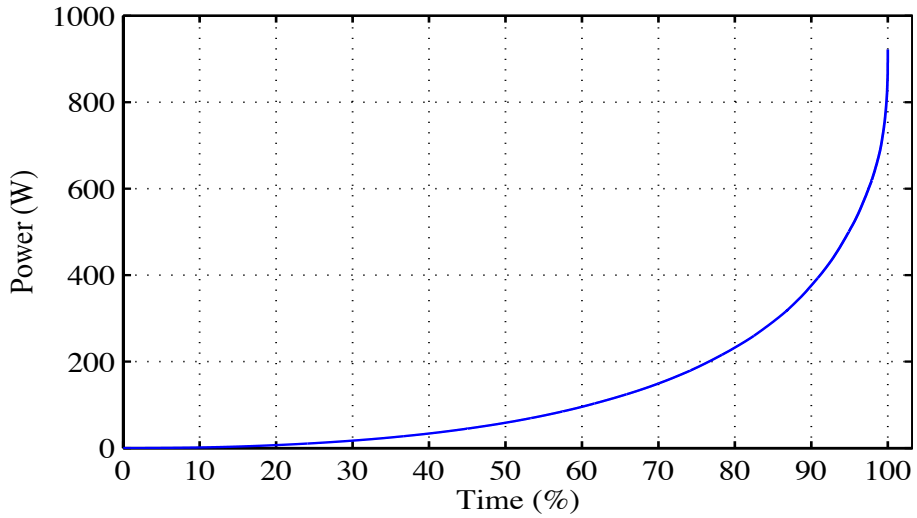

Figure 6.23: *Discharging power of the ESS, in ascending order, from May to December in 2013.*

The ESS was charging for more than 205 hours and was discharging for more than 215 hours. Maximum power during charging operation was about 938 W. Average power during charging was around 113 W. Highest power during discharging of the ESS was around 922 W. Average power during discharging was around 129 W. The charging power was less than 200 W for 80 % of the time, as can be seen in figure 6.22. The discharging power was around 220 W for 80 % of the time, as observed in figure 6.23.

6.3 Inverter operating at 70 % of PV generator capacity

In this section, similar simulations are carried out to analyze the operations of the energy storage system. However, in this section, it is assumed that the PV inverter is rated at 70 % of the PV generator capacity. This method is undertaken to reflect the imposed regulations in many places in the world. In case of grid-connected PV generators, power curtailments are applied due to the intermittent nature of the PV systems. Power curtailments are achieved by using PV inverters having less capacity compared to their respective PV generators. For example, in this case, the PV inverter is rated at 70 % of the PV generator capacity. Thus, the inverter does not inject more than 700 W of PV generated power in to the electricity grid. The ESS operates the same way as in the previous sections. Similar to the previous section, the ESS controls the ramp rates of the PV generator output power. The operation of the ESS is shown in figure 6.24.

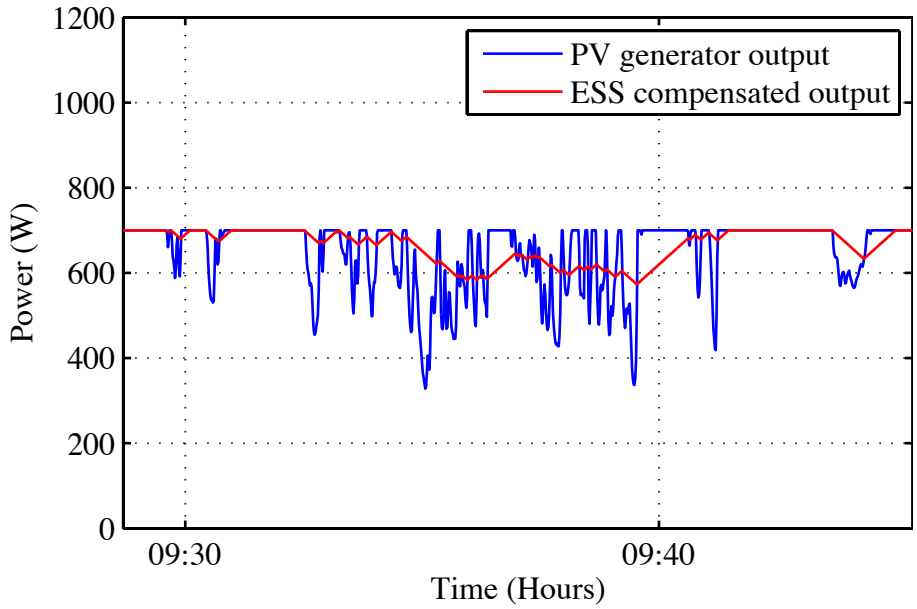

Figure 6.24: *Operation of the ESS, when inverter is rated at 70 % of the PV generator capacity (on 9th of May 2012).*

The required capacity of the ESS in this section should be different from the capacity required when the inverter was operating at 100 % of the generator's capacity. As the inverter flattens the maximum output power at 700 W, the ESS should operate for less time. Moreover, the energy needed for charging and discharging actions should be comparatively lesser.

6.3.1 Periodic operation of the ESS

The ESS operates for each individual day in the year 2012. The state of energy in the ESS is set to zero at the start of each day. In figure 6.25, the daily maximum charged energy values of the ESS in 2012 are shown in ascending order. In figure 6.26, daily

maximum energy deficiencies in the ESS in the year 2012 are shown in ascending order. In figure 6.27, the energy status of the ESS at the end of each day in the year 2012 is shown in ascending order.

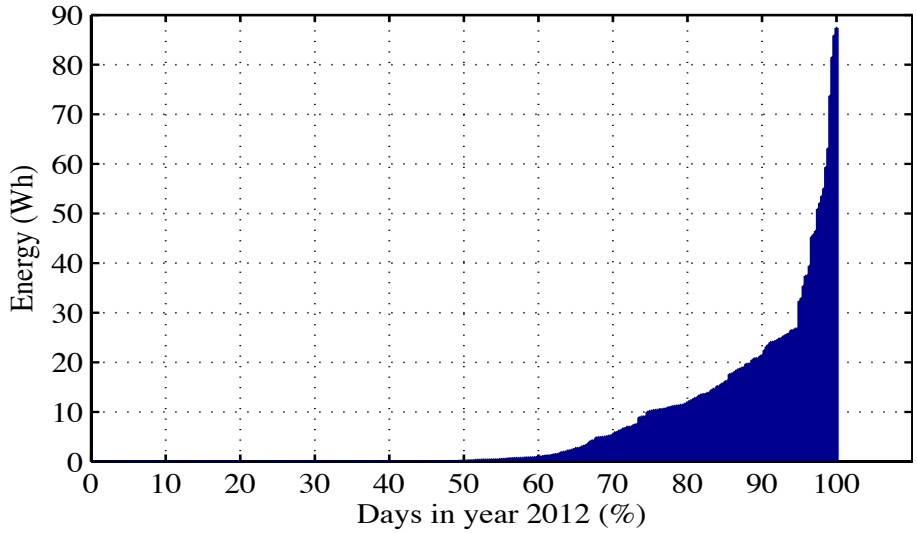

Figure 6.25: *Daily maximum energy charged by the ESS in each day of 2012, in ascending order.*

Maximum energy charged by the ESS was around 87 Wh, as can be seen in figure 6.25. The ESS did not charge any energy for almost 50 % of the days. The maximum energy charged by the ESS was less than 12 Wh for 80 % of the days. Maximum charged energy was higher than 30 Wh for only 5 % of the days.

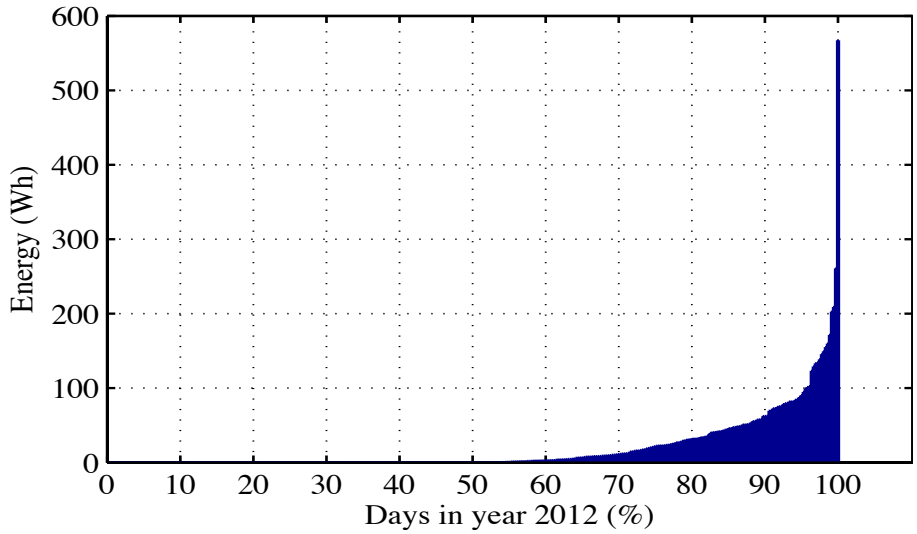

Figure 6.26: *Maximum energy deficiencies in the ESS in each day of 2012, in ascending order.*

Maximum energy deficiency in the ESS was around 567 W, as can be seen in figure 6.26. The ESS did not discharge any energy for almost 45 % of the days. For almost 95 % of the days, the maximum energy deficiency in the ESS was less than 100 Wh.

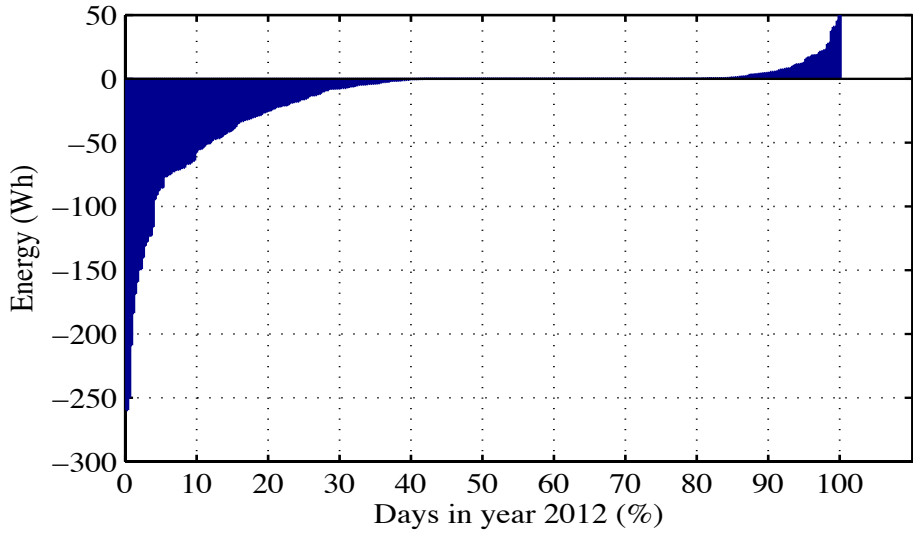

Figure 6.27: *Status of energy in the ESS, at the end of each day in the year 2012, in ascending order.*

The ESS had energy deficiencies for about 40 % of the days in the year 2012, as seen in figure 6.27. Energy remained in the ESS in around 20 % of the days. The maximum remaining energy was 50 Wh. The maximum energy deficiency in the ESS was about 260 Wh.

Similar observations can be made for 245 days (8 months) in the year 2013. In figure 6.28, the daily maximum charged energy values by the ESS during 8 months in 2013 are shown in ascending order. In figure 6.29, the daily maximum energy deficiencies in the ESS during 8 months in the year 2013 are shown in ascending order. In figure 6.30, energy remaining in the ESS at the end of each day in 8 months of the year 2013 is shown in ascending order.

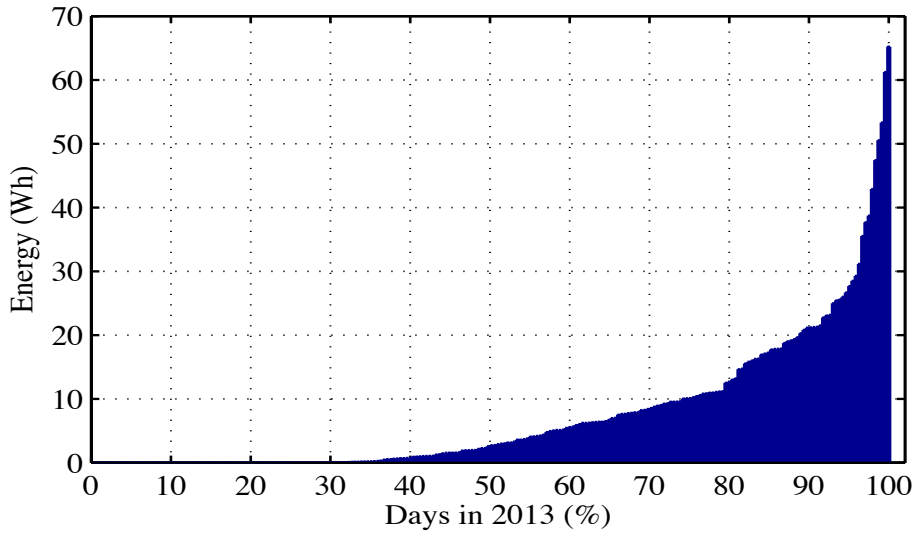

Figure 6.28: *Daily maximum energy stored by the ESS in each day of 8 months in 2013 is shown in ascending order.*

Maximum daily energy charged by the ESS was around 65 Wh in 8 months (245 days) of 2013, as can be observed in figure 6.28. The maximum charged energy was less than 12 Wh in 80 % of the days. The maximum charged energy exceeded 30 Wh in only 5 % of the days. The ESS did not charge at all for almost 25 % of the days.

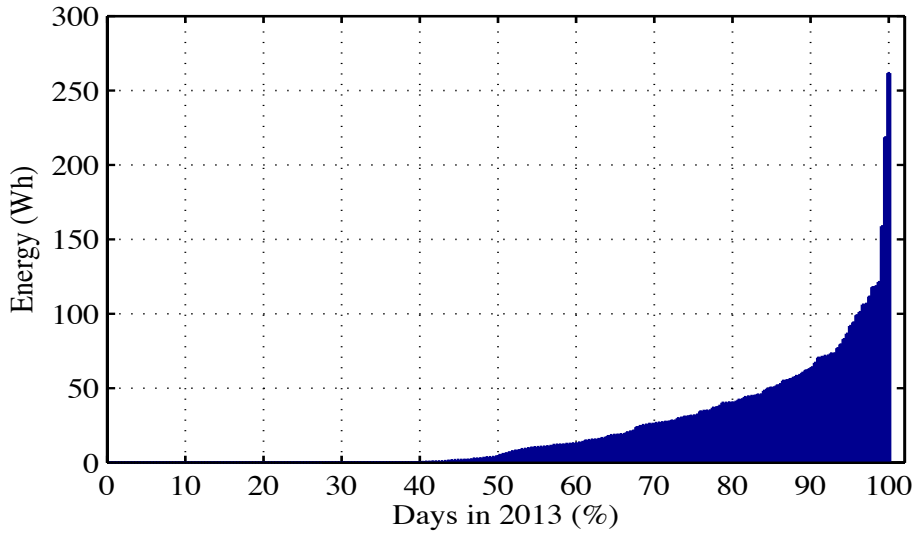

Figure 6.29: *Daily maximum energy deficiencies in the ESS during 8 months in 2013 are shown in ascending order.*

Maximum daily energy deficiency in the ESS was around 262 Wh during 245 days of 2013. The maximum deficiency was less than 50 Wh in 85 % of the days, as can be seen in figure 6.29. The maximum deficiency exceeded 100 Wh in only 5 % of the days. The ESS did not discharge at all for 27 % of the days.

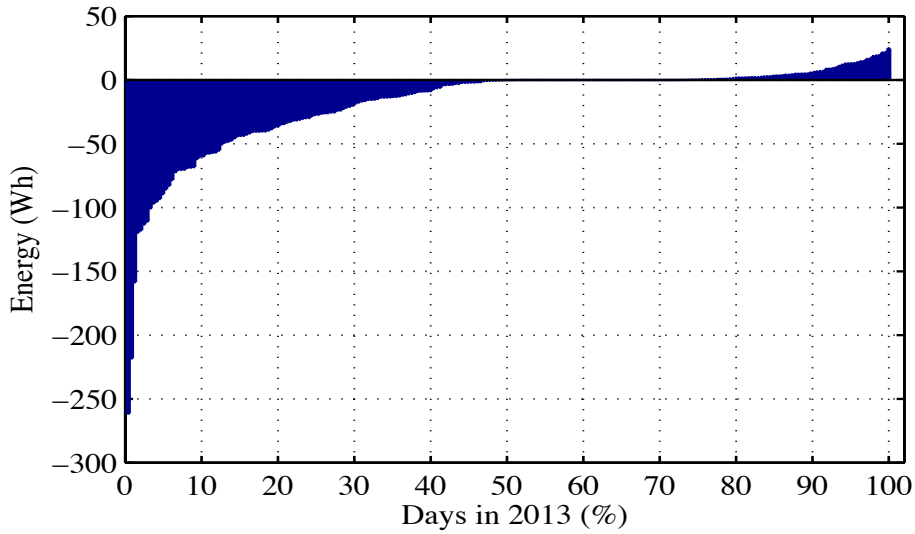

Figure 6.30: *Status of energy in the ESS at the end of each day of 8 months in year 2013, shown in ascending order.*

In almost 30 % of the days, energy remaining in the ESS was zero. Energy was deficient in the ESS in about 50 % of the days, as can be seen in figure 6.30. The maximum energy deficiency in the ESS was around 262 Wh. The maximum energy remaining in the ESS was around 25 Wh. Energy remained in the ESS for around 25 % of the days. Similar to the observation made for year 2012, the number of days when energy was deficient is twice than the number of days when energy remained in the ESS at the end of daily operation.

6.3.2 Continuous operation of the ESS

Continuous operation of the ESS throughout the year 2012 is shown in figure 6.31. Continuous operation of the ESS for 245 days in 2013 is shown in figure 6.32. The energy storage system begins the operation with 0 kWh and continuously operates to keep the ramp rate of the PV output power under control. At the end of the year 2012, the ESS had almost -5.24 kWh of energy. At the end of the year 2013, the energy in the ESS was around -4.34 kWh.

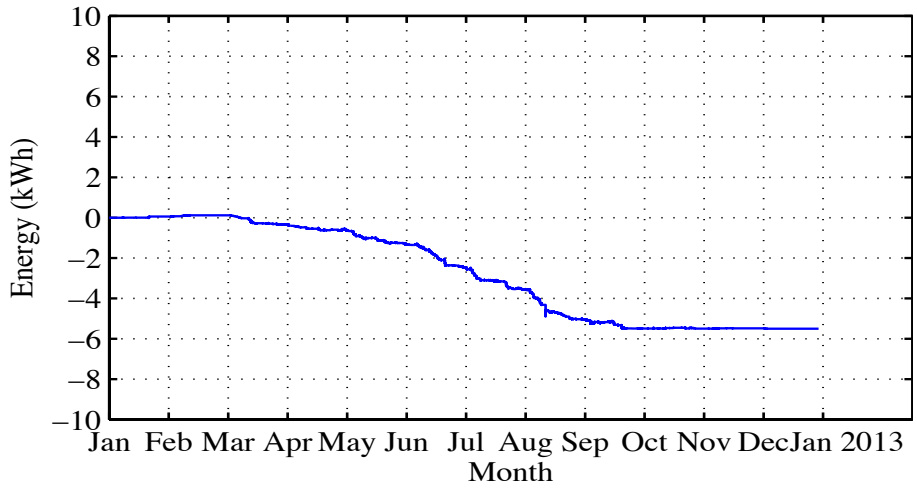

Figure 6.31: *Continuous operation of the ESS, throughout the year 2012, when inverter is rated at 70% of the PV generator capacity.*

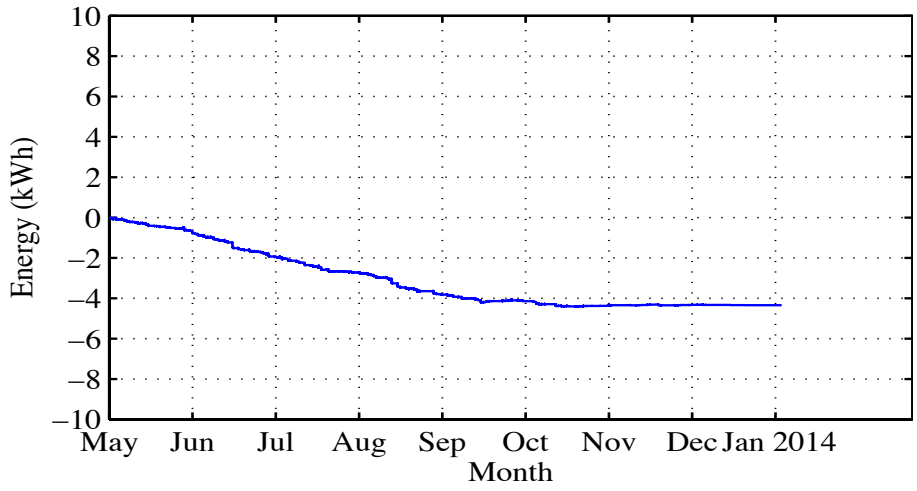

Figure 6.32: *Continuous operation of the ESS for 8 months in the year 2013, when inverter is rated at 70% of the PV generator capacity.*

The charging and discharging powers of the ESS during the year 2012 are shown (in ascending order) in figure 6.33 and 6.34 respectively. During 2012, the ESS was charging for a total of 216 hours. Maximum power during charging was around 578 W. Average charging power was 93 W. The ESS was discharging for a total of 228 hours. Maximum discharge power of the ESS was 626 W. Average discharge power of the ESS was around 112 W.

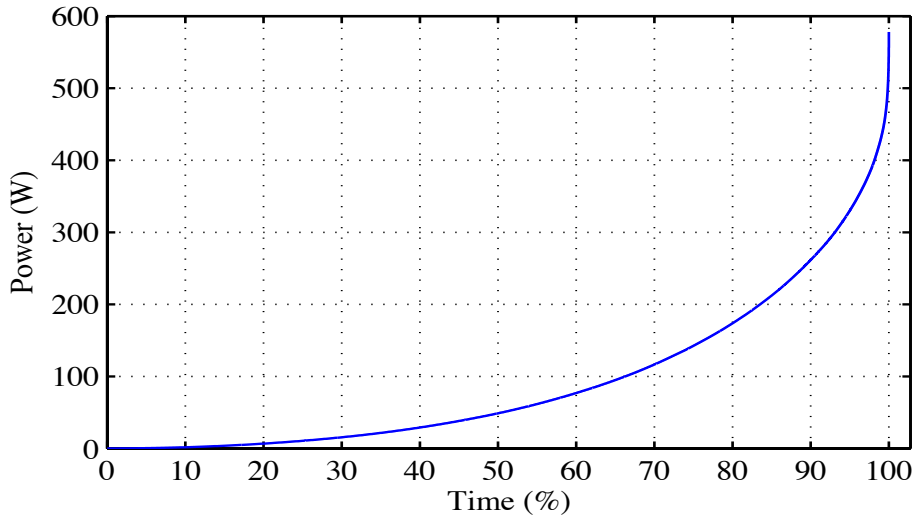

Figure 6.33: *Charging power of the ESS, in the year 2012, shown in ascending order.*

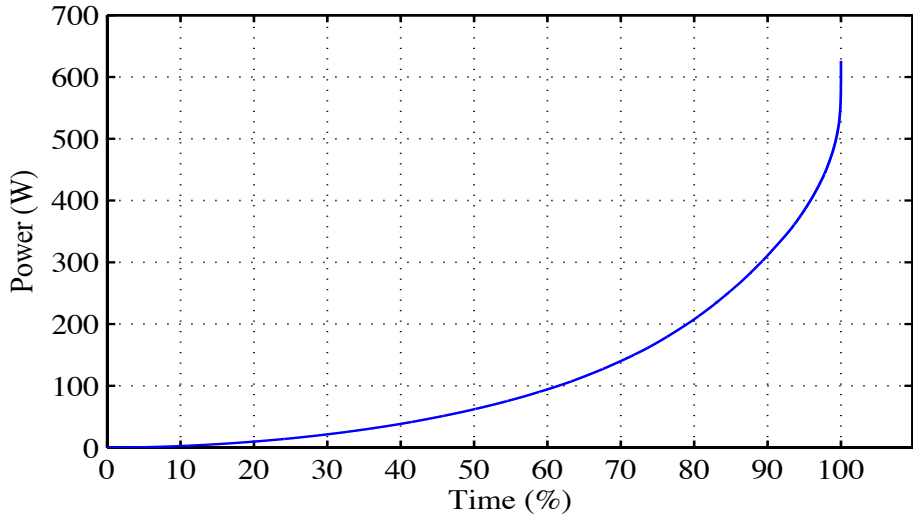

Figure 6.34: *Discharging power of the ESS, in the year 2012, shown in ascending order.*

During the year 2012, the charging power was lower than 250 W for almost 90 % of the time. The charging power was less than 50 W for 50 % of the time. The discharging power was lower than 300 W for almost 90 % of the time. The discharging power was around 60 W for almost 50 % of the time. The charging and discharging powers of the ESS during 8 months in the year 2013 are shown (in ascending order) in figures 6.35 and 6.36 respectively.

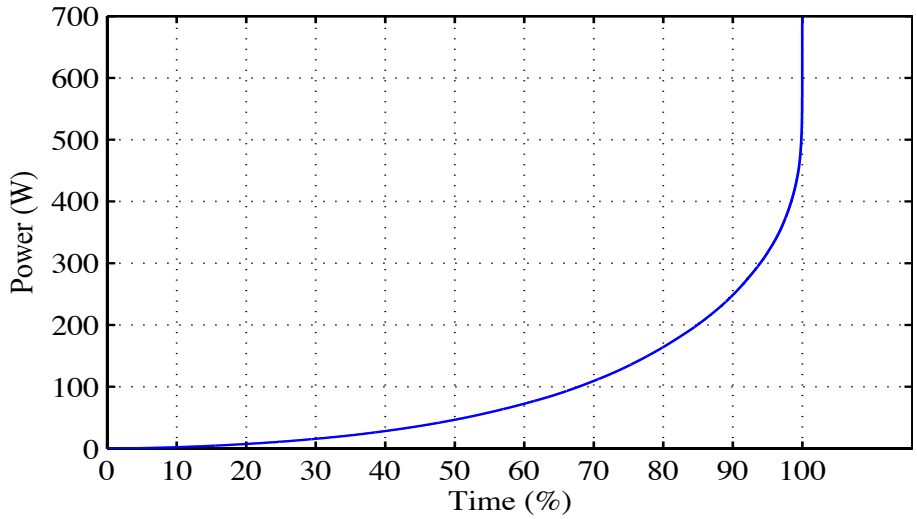

Figure 6.35: *Charging power of the ESS, in the year 2013, shown in ascending order.*

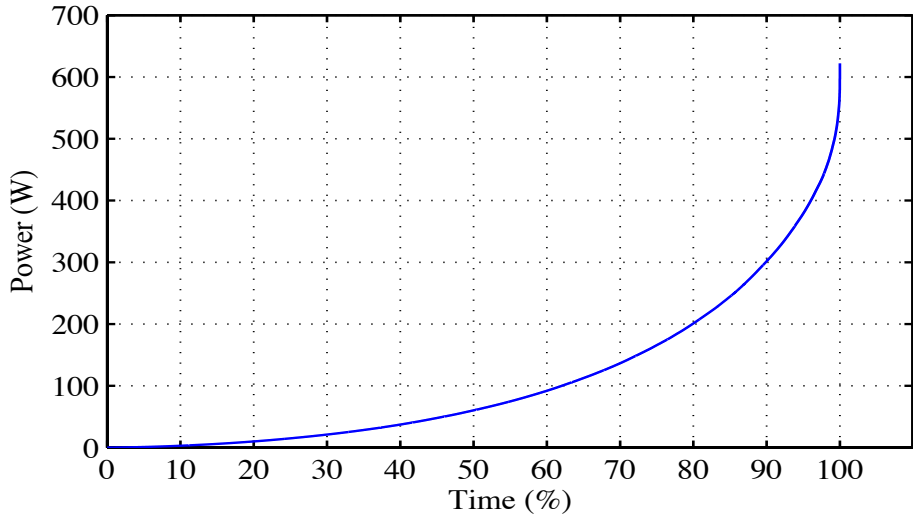

Figure 6.36: *Discharging power of the ESS, in the year 2013, shown in ascending order.*

The maximum charging power was 698 W during 168 hours of charging in 8 months of 2013. The maximum discharging power was 622 W, during 177 hours of discharging. The maximum charging power was less than 250 W for 90 % of the time. The maximum discharging power was less than 300 W for 90 % of the time.

6.4 Automatic recharging of the ESS when power curtailment is active

In section 6.3, the inverter was rated at 70 % of the PV generator's capacity. As a result, the inverter only injected PV generated power lower or equal to 700 W in to the elec-

tricity grid. Whenever the PV generator produced power more than 700 W, that excess power was wasted by the system.

However, in this section, the simulations of the operation of the ESS are carried out based on the premise that the excess energy, which is cut off by the inverter is stored in the energy storage system. Every time the PV generator produces power more than the rated capacity of the inverter, the excess energy is stored by the ESS. Similar to the previous section, the inverter is rated at 70% of the PV generator's capacity. The objective of such arrangement is to better use the generated power and to enhance the capabilities of the energy storage system. In most electricity networks, power curtailment is either always active or active for short periods. For example, in Germany, a PV generator system with a capacity of less than 30 kW can only inject power up to 70% of its rated capacity into the electricity grid. In such cases, energy storages can be used to store the excess energy produced by the PV generator along with the ramp rate control operation.

6.4.1 Periodic operation of the ESS

The ESS operates for each individual day in the year 2012. The state of energy in the ESS is set to zero at the start of each day. In figure 6.37, the daily maximum energy charged by the ESS is shown in ascending order, for the year 2012. In figure 6.38, the daily maximum energy deficiencies in the ESS are shown in ascending order, for the year 2012.

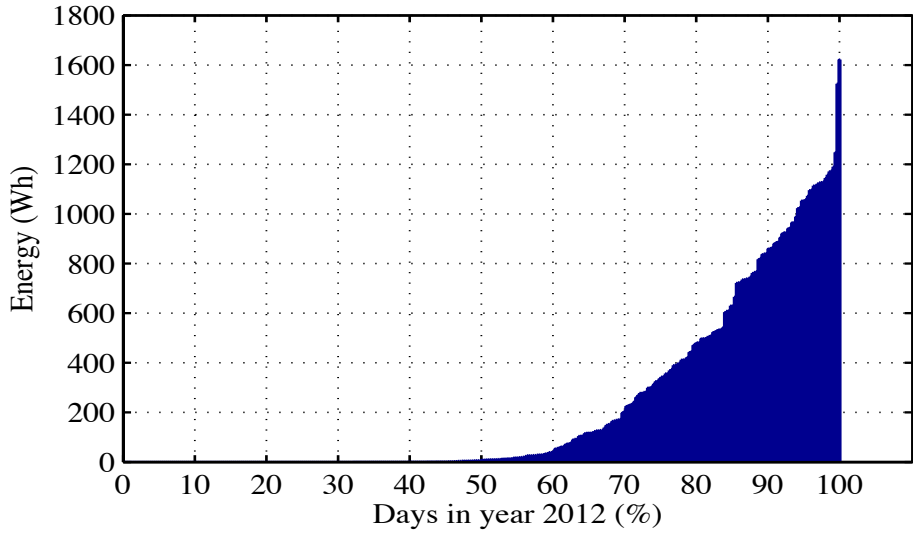

Figure 6.37: *Daily maximum energy charged by the ESS in each day of 2012, shown in ascending order.*

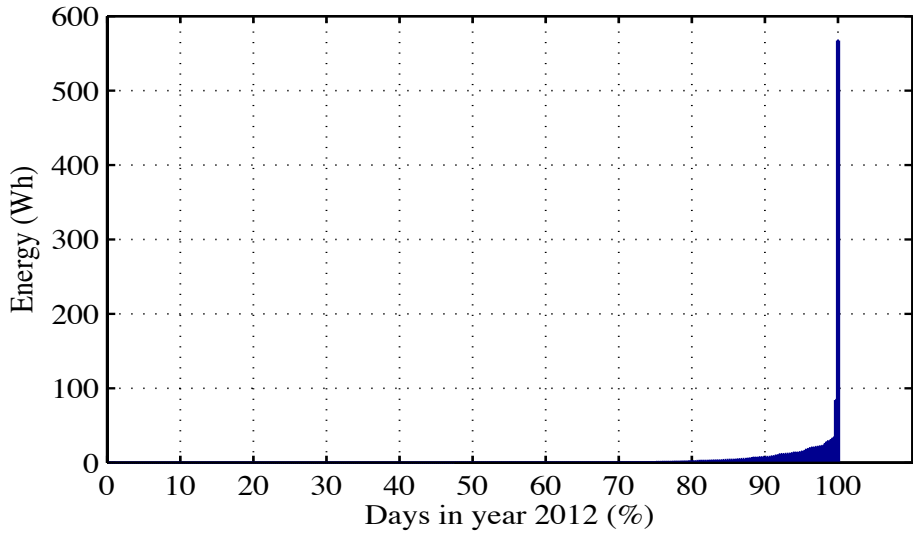

Figure 6.38: *Daily maximum energy deficiency in the ESS in each day of 2012, shown in ascending order.*

Maximum energy charged by the ESS was around 1.62 kWh, as can be seen in figure 6.37. Maximum charged energy was less than 800 Wh for around 90 % of the days in 2012. Maximum energy deficiency in the ESS was around 568 Wh, as can be observed in figure 6.38. However, the maximum energy deficiency was less than 8 Wh for around 90 % of the days in 2012. In figure 6.39, the status of energy in the ESS at the end of each day is shown in ascending order for the year 2012.

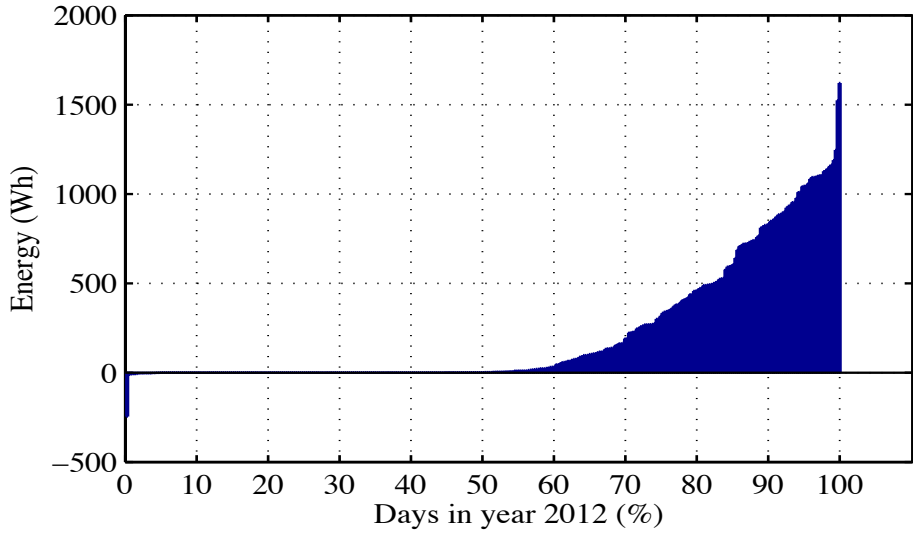

Figure 6.39: *Status of energy in the ESS at the end of each day in year 2012, shown in ascending order.*

Energy remained in the ESS at the end of daily operation in 55 % of the days, as can be seen in figure 6.39. Energy was deficient in the ESS in less than 5 % of the days. Zero energy remained in the ESS for about 40 % of the days.

Similar simulations of periodic ESS operations have been carried out for 245 days in the year 2013. Daily maximum energy charged by the ESS for 245 days in the year 2013 is shown in ascending order in figure 6.40.

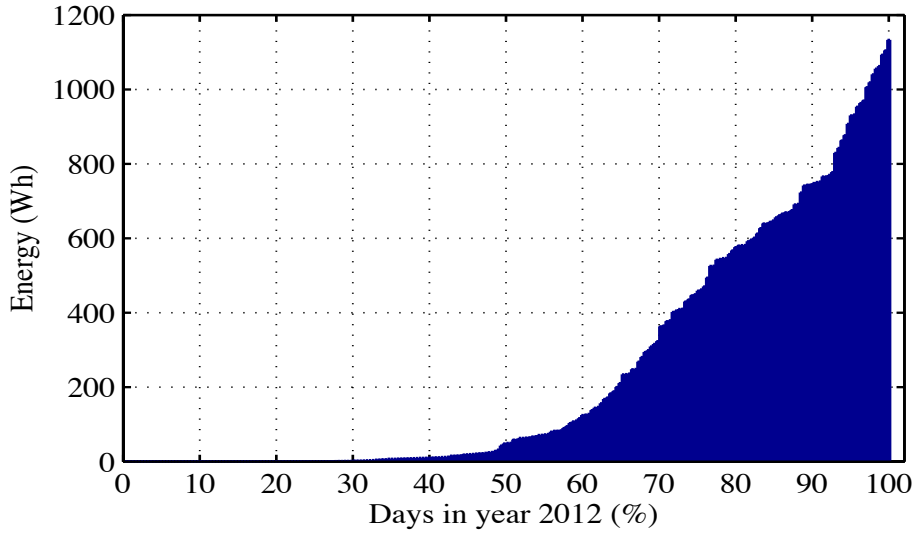

Figure 6.40: *Daily maximum energy charged by the ESS in each day of 8 months in 2013, shown in ascending order.*

Daily maximum energy charged by the ESS in year 2013 was 1133 Wh, as can be observed in figure 6.40. For 50 % of the days, the daily maximum energy charged by the ESS was less than 122 Wh. For 90 % of the days, the daily maximum energy charged by the ESS was less than 750 Wh. Daily maximum energy discharged by the ESS for 245 days in the year 2013 is shown in ascending order in figure 6.41.

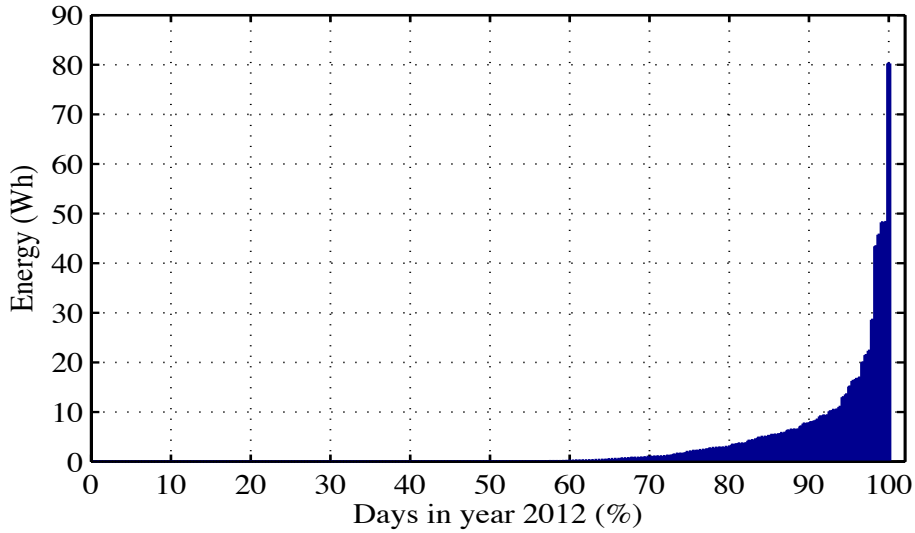

Figure 6.41: *Daily maximum energy deficiency in the ESS during 8 months of 2013, shown in ascending order.*

Maximum energy deficiency in the ESS was around 80 Wh, as shown in figure 6.41. The ESS did not discharge any energy during almost 40 % of the days. The maximum energy deficiency was less than 8 Wh for 90 % of the days. The status of energy in the ESS at the end of each day in 2013 is shown in ascending order in figure 6.42.

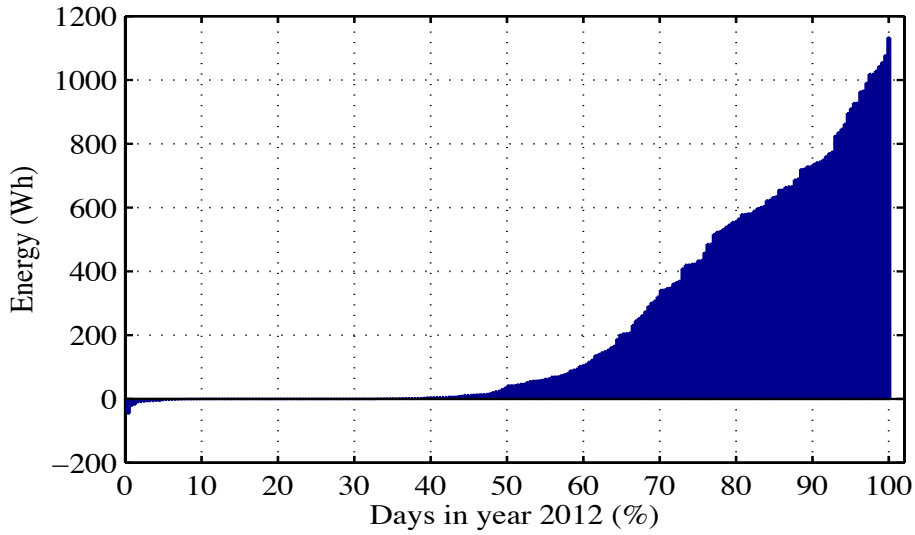

Figure 6.42: *Status of energy in the ESS at the end of each day of 8 months in the year 2013, shown in ascending order.*

From figure 6.42, it can be observed that energy remained in the ESS in almost 62 % of the days. The ESS was deficient in only 7 % of the days. The maximum deficiency in the ESS was 46 Wh and the maximum energy remaining in the ESS was 1133 Wh.

6.4.2 Continuous operation of the ESS

The ESS was operated for an entire year continuously without any recharging. Continuous operation of the ESS for the year 2012 is shown in figure 6.43. It can be observed from figure 6.43 that, the ESS continuously stores more energy than it discharges. At the end of the year 2012, the ESS had stored almost 77 kWh of energy.

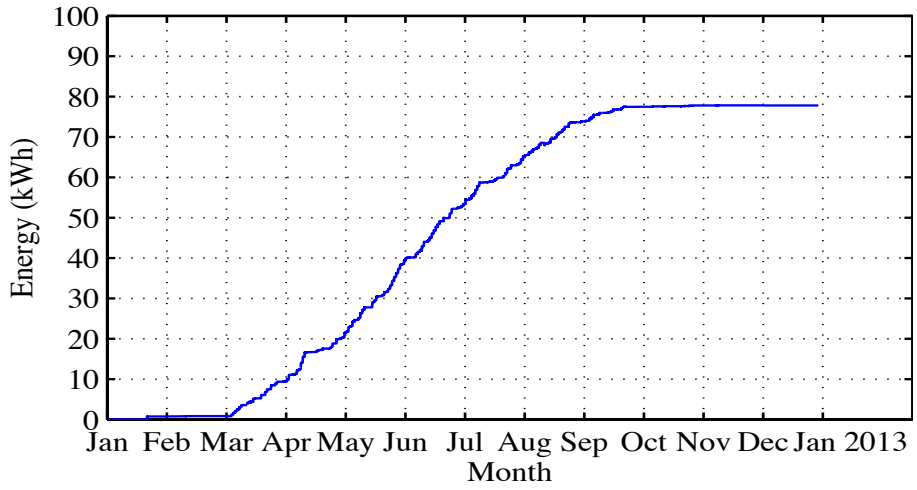

Figure 6.43: *Continuous operation of the ESS throughout the year 2012.*

In figure 6.44, continuous operation of the ESS throughout 8 months of the year 2013 is shown. It can be observed from figure 6.44 that the energy stored in the ESS steadily increases over time. Steady increase in stored energy continues until the end of September. At the end of the year 2013, the energy stored in the ESS was around 55 kWh.

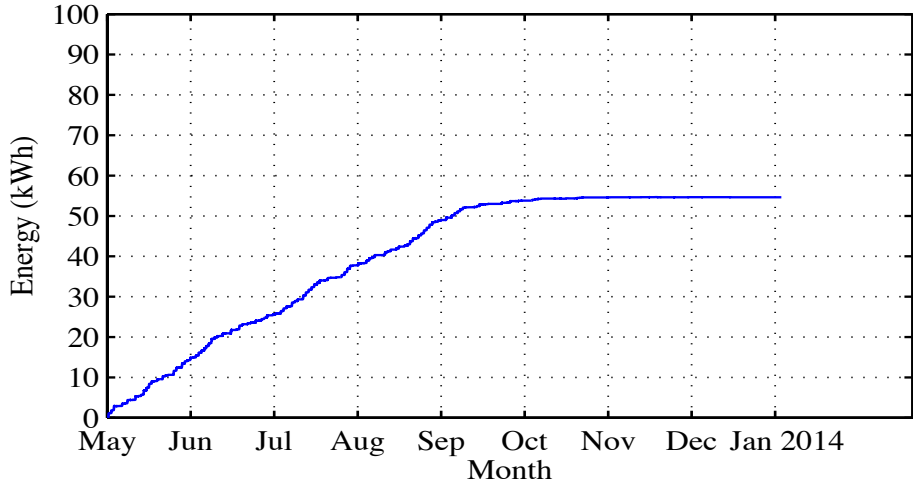

Figure 6.44: *Continuous operation of the ESS during 8 months of the year 2013.*

The ESS had 77 kWh of energy stored at the end of the year 2012. It also had 55 kWh of energy stored at the end of the year 2013 after 8 months of continuous operation. Besides controlling the ramp rates of the PV generated power, the energy storage can thus be used for many other grid-related applications and services. The charging and discharging powers of the ESS during the year 2012 are shown (in ascending order) in figure 6.45 and 6.46 respectively.

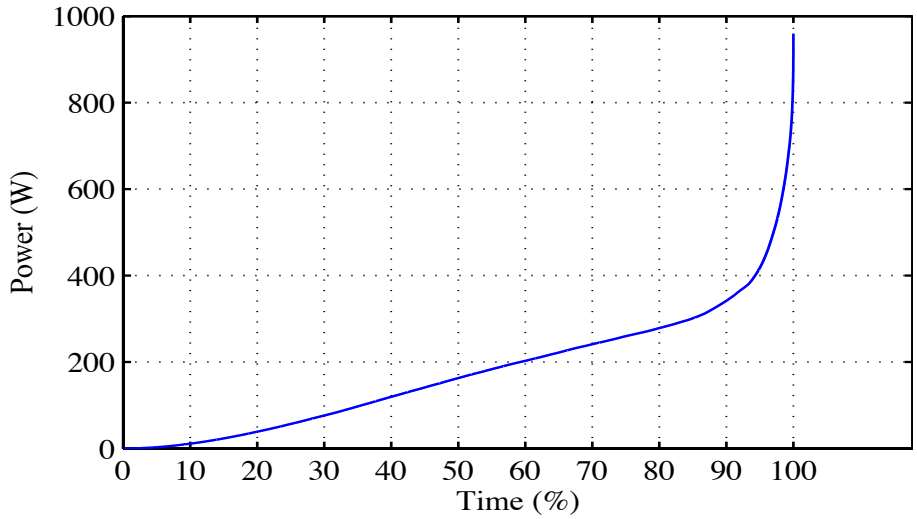

Figure 6.45: *Charging powers of the ESS, in the year 2012, shown in ascending order.*

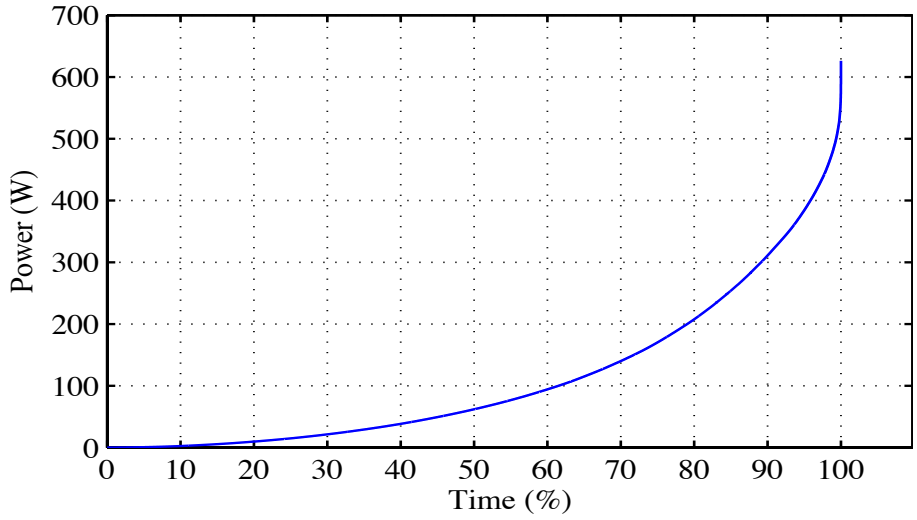

Figure 6.46: *Discharging power of the ESS, in the year 2012, shown in ascending order.*

During 2012, the ESS was charging for 590 hours. Maximum power during charging was around 960 W, as can be seen in figure 6.45. Average charging power was 175 W. The ESS was discharging for 228 hours. Maximum discharge power was 626 W. Average discharge power of the ESS was around 175 W. The maximum charging power was less than 400 W for around 95 % of the times, as can be observed in figure 6.45. The maximum discharging power was less than 300 W for around 90 % of the times, as can be seen in figure 6.46. The charging and discharging powers of the ESS during 245 days in the year 2013 are shown in ascending order, in figures 6.47 and 6.48 respectively.

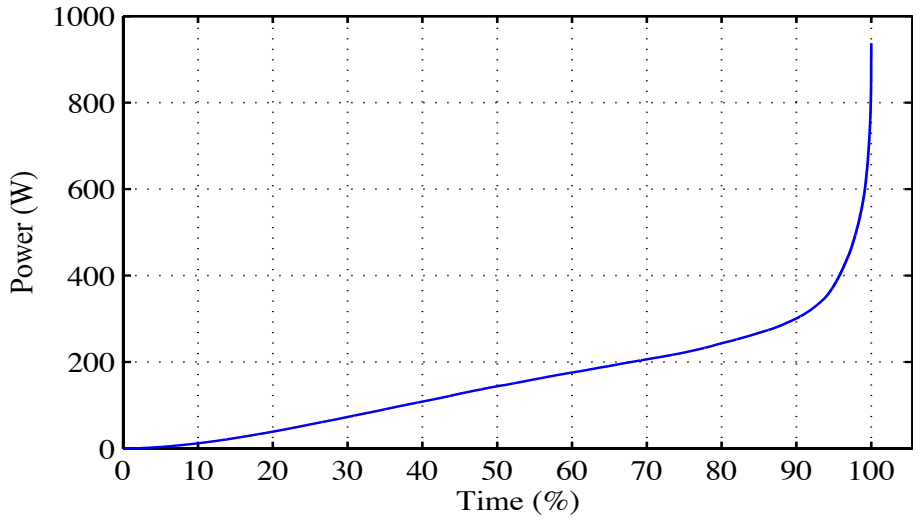

Figure 6.47: *Charging powers of the ESS, during 245 days in the year 2013, shown in ascending order.*

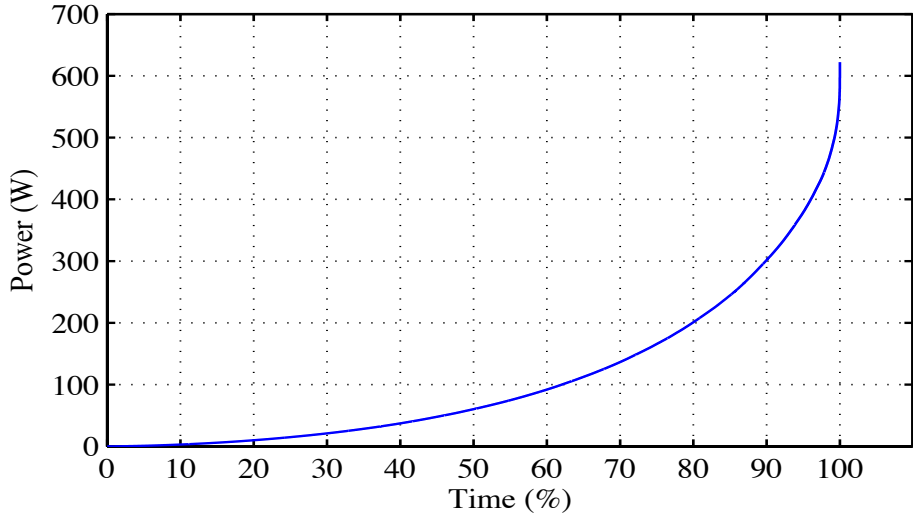

Figure 6.48: *Discharging powers of the ESS, during 245 days in the year 2013, shown in ascending order.*

During 8 months of operation in the year 2013, the ESS charged for 474 hours. The ESS discharged for 177 hours during the same period of operation. Maximum charging power was 938 W, as can be seen in figure 6.47. Average charging power was less than 156 W. Maximum discharging power was less than 622 W, as can be seen in figure 6.48. Average discharging power was less than 110 W. Maximum charging power was around 300 W for 90 % of the times. Maximum discharging power was also less than 300 W for 90 % of the times.

6.5 Assessment of ESS operations

In section 6.1, it was found that high ramp rates occurred for a total of 289 hours in the year 2012. It has also been observed that high ramp rates occurred for a total of 231 hours in 8 months of the year 2013. Three different operation scenarios of the ESS have been analyzed in the subsequent sections of this chapter. In section 6.2, the ESS operated to control the ramp rate of the PV generator, when the PV inverter was rated at 100 % of the PV generator capacity (category A). In section 6.3, the ESS operated to control the ramp rate of the PV generator, when the PV inverter was rated at 70 % of the PV generator capacity (category B). In section 6.4, automatic recharging of the ESS was enabled when the PV inverter was rated at 70 % of the PV generator capacity (category C). In table 6.1, the durations of active operation of the ESS in each operation category are presented.

Table 6.1: *Duration of active operation of the ESS.*

Category of ESS operation	Year of operation	Total time of charging (Hours)	Total time of discharging (Hours)	Total time of ESS operation (Hours)
(A) Inverter rated at 100 % of the PV generator capacity	2012	267	279	546
	2013	205	215	420
(B) Inverter rated at 70 % of the PV generator capacity	2012	216	228	444
	2013	168	177	345
(C) Automatic recharging of the ESS	2012	590	228	818
	2013	474	177	651

It can be observed from table 6.1 that the ESS operated for a total of 546 hours in 2012 when the PV inverter was rated at 100 % of the PV generator capacity (category A). The duration of ESS operation (444 hours) decreased in the same year of operation (year 2012), when the inverter was rated at 70 % of the PV generator capacity (category B). The duration of the ESS operation in 2012 increased to a total of 818 hours, when the ESS was automatically recharged using the excess energy (category C). It can also be observed from table 6.1 that the durations of discharging are generally higher than the durations of charging in operation category A and B. However, this trend is reversed in operation category C, where the charging durations of the ESS are more than double the durations of discharging in both years of operation. In table 6.2, the energy status of the ESS during operations analyzed in sections 6.2, 6.3 and 6.4 are summarized. The

maximum energy charged by the ESS during its daily operations is shown in table 6.2. Moreover, the maximum energy deficiency in the energy storage system during daily operations is also shown in table 6.2. Energy balance in the ESS at the end of each day is also shown.

Table 6.2: *Daily maximum charged energy, daily maximum energy deficiency and the energy balance at the end of each day's operations of the ESS are shown in table 6.2.*

Category of ESS operation	Year of operation	Maximum charged energy (Wh)	Maximum energy deficiency (Wh)	Energy balance in the ESS at the end of each day	
				Maximum remaining energy (Wh)	Maximum energy deficiency (Wh)
(A) Inverter rated at 100 % of the PV generator capacity	2012	197	568	156	411
	2013	237	383	132	370
(B) Inverter rated at 70 % of the PV generator capacity	2012	87	567	50	260
	2013	65	262	25	262
(C) Automatic recharging of the ESS	2012	1620	568	1622	246
	2013	1133	80	1133	46

In sections 6.2, 6.3 and 6.4, the periodic operations of the ESS were analyzed and discussed in detail. The ESS operated for each individual day in the year 2012 and in 8 months of the year 2013. The daily maximum energy states of the ESS were discussed in details. In table 6.2 above, the maximum energy states found in each category of operation are shown. For example, when the ESS was operated in operation category A, the maximum charged energy during a day was found to be 197 Wh in the year 2012. In the same category and in the same year of operation, the maximum energy deficiency in the ESS was found to be 568 Wh. The maximum energy remaining in the ESS at the end of a day's operation was 156 Wh. The maximum energy deficiency in the ESS was 411 Wh. The ESS generally discharged more energy than it charged during daily opera-

tions in category A and B. In operation category C, the ESS charged more energy than it discharged. It was found in sections 6.2 and 6.3 that the days where energy was deficient in the ESS at the end of daily operation were generally higher in number than the days where energy remained in the ESS at the end of daily operation. However, in section 6.3 (operation category C), it was found that, in more than 50 % of the days, energy remained in the ESS at the end of daily operation. Similar phenomena can also be observed from table 6.2, where the maximum remaining energy in the ESS at the end of a day was 1622 Wh in 2012 in operation category C. In comparison, the maximum remaining energy at the end of a day was only 50 Wh, in operation category B. In the following table 6.3, the maximum charging and discharging powers during the operations of the ESS are presented.

Table 6.3: *Summary of the observations made in sections 6.2, 6.3 and 6.4 regarding the charging and discharging powers of the ESS.*

Category of ESS operation	Year of operation	Maximum daily charging power (W)	Maximum daily discharging power (W)
(A) Inverter rated at 100 % of the PV generator capacity	2012	960	942
	2013	938	922
(B) Inverter rated at 70 % of the PV generator capacity	2012	578	626
	2013	698	622
(C) Automatic recharging of the ESS	2012	960	626
	2013	938	622

It can be seen from table 6.3 that the maximum charging power of the ESS was 960 W in operation category A and C. The inverter was rated at 70 % of the PV generator capacity in the operation category B, as a result, the maximum charging and discharging powers of the ESS were less than 700 W in operation category B. However, although power curtailment was active in category C, the ESS used the power cut off by the inverter to recharge itself. As a result, the maximum charging power was higher than 700 W in category C. The discharging power of the ESS was lower than 700 W in the operation category C.

In sections 6.2, 6.3 and 6.4, continuous operations of the ESS were discussed and analyzed. The ESS operated continuously for 366 days in the year 2012 without any recharge. In 2013, the ESS operated continuously for 245 days without being recharged. In table 6.4, the statuses of energy in the ESS at the end of the continuous operations are shown. Negative values of energy represent the deficiencies of energy.

Table 6.4: *Energy status of the ESS at the end of the continuous operations in each year.*

Category of ESS operation	Year of operation	Energy status of the ESS at the end of continuous operation (kWh)
(A) Inverter rated at 100 % of the PV generator capacity	2012	-6.12
	2013	-4.6
(B) Inverter rated at 70 % of the PV generator capacity	2012	-5.24
	2013	-4.34
(C) Automatic recharging of the ESS	2012	77
	2013	55

In operation category A, the ESS had an energy deficiency of 6.12 kWh at the end of the year 2012, as can be seen in table 6.4. The energy deficiency in the ESS at the end of the year 2012 decreased to a value of 5.24 kWh in operation category B. In addition, in operation category C, 77 kWh of energy was stored in the ESS at the end of the year 2012.

The objective of this thesis was to analyze the operations of a theoretical energy storage system (ESS), where the ESS controls the ramp rate of the PV generator output power. By analyzing the operations of the theoretical ESS, a suitable ESS of required energy capacity and power rating could be designed. The information gathered in this thesis can be used to design suitable energy storage systems for PV generators of any scale and size. Moreover, three different categories of ESS operation are analyzed in this thesis. The required capacity and power rating of the ESS can be determined for each operation scenarios portrayed in this thesis. Thus, the analyses presented in this thesis could help the continuous progression and development of PV power systems.

7 CONCLUSIONS

Photovoltaic (PV) power systems are considered a significant part of electricity generation paradigm of the future. Widespread implementation of PV systems is necessary to establish a sustainable and environmentally friendly energy production and consumption system. However, the inherent intermittency of the solar resource poses a significant challenge to the implementation of grid-connected PV power systems in mass scale. Rapid changes in PV generated power can cause serious problems for distribution systems containing a large quantity of PV generated power. Energy storage systems are increasingly being used to help integrate the PV power into the grid. Energy storage systems can mitigate issues such as ramp rate deviations, frequency and voltage deviations etc. Power quality, network reliability and economic values can be enhanced by using energy storage systems along with grid-connected PV systems.

The objective of this thesis was to study the applications of energy storage systems in grid-connected PV systems to balance the output power of the PV generators. Furthermore, by analyzing the operations of the energy storage systems, the storage systems could be suitably sized in terms of their energy capacity and power rating. A review of the energy storage systems has been presented in chapter 5, where applications and characteristics of various energy storage technologies were discussed. At the end of chapter 5, an assessment of the storage technologies, in regards to their suitability with renewable energy sources was presented. In chapter 6, applications of the energy storage system with grid-connected PV systems were discussed. An energy storage system (ESS) was used to control the rate of change of output power from a 1 kW rated PV generator. In all the cases, the ESS limited the rate of change of output power to 10 % of the PV generator capacity per minute (or similarly 1.6667 W/s). Three different operation scenarios of the ESS were analyzed. Firstly, the ESS controlled the rate of change of PV generator output power when the PV inverter operated at 100 % of the PV generator capacity. Secondly, the ESS controlled the rate of change of PV generator output power when the PV inverter operated at 70 % of the PV generator capacity. Thirdly, the ESS recharged automatically using the power cut off by the PV inverter (Inverter operated at 70 % of the PV generator capacity) while controlling the rate of change of PV generator output power. The ESS subtracted from the PV generated power (by charging itself) and added to the PV generated power (by discharging itself), whenever necessary, to control the ramp rates in the PV generated output power.

Periodic (daily) operation of the ESS in all application scenarios was analyzed. In daily operations, the status of the energy in the ESS was set to zero at the start of each day. The maximum energy stored in the ESS in each day of operation in the years 2012 and 2013 were presented. The maximum energy deficiency in the ESS in each day of

operation in 2012 and 2013 were also presented. The maximum stored energy at any time of operation was found to be 237 Wh, when the PV inverter was operating at 100 % of the PV generator capacity. The maximum stored energy was found to be 87 Wh, when the PV inverter was operating at 70 % of the PV generator capacity. The maximum stored energy was found to be 1620 Wh, when the ESS was automatically recharging using the power cut off by the inverter operating at 70 % of the generator capacity. The maximum energy deficiency at any time of operation was found to be 568 Wh, when the PV inverter was operating at 100 % of the PV generator capacity. The maximum energy deficiency was found to be 567 Wh, when the PV inverter was operating at 70 % of the PV generator capacity. The maximum energy deficiency was 568 Wh, when the ESS was recharging automatically using the power cut off by the inverter operating at 70 % of the generator capacity.

Continuous operation of the ESS throughout the year 2012 and for 8 months in 2013 was analyzed. The energy balance in the ESS at the end of the year 2012 was -6.12 kWh, when the PV inverter was operating at 100 % of the PV generator capacity. The energy balance in the ESS at the end of year 2012 was -5.24 kWh, when the PV inverter was operating at 70 % of the PV generator capacity. The energy balance in the ESS at the end of the year 2012 was 77 kWh, when the ESS was automatically recharging using the power cut off by the inverter operating at 70 % of the generator capacity. The maximum power either charged or discharged by the ESS was 960 W, when the PV inverter was operating at 100 % of the PV generator capacity. The maximum power either charged or discharged by the ESS was 698 W, when the PV inverter was operating at 70 % of the PV generator capacity. The maximum power either charged or discharged by the ESS was 960 W, when the ESS was automatically recharging using the power cut off by the inverter operating at 70 % of the generator capacity.

The ESS operated for a total of 546 hours (4.8 % of the total time) in the year 2012, when the PV inverter was rated at 100 % of the PV generator capacity. When the PV inverter was rated at 70 % of the PV generator capacity, the ESS operated for 444 hours (5 % of the total time) in 2012. The ESS operated for 818 hours (9.3 % of the total time) in 2012 when the ESS was automatically recharging during active power curtailment. It is worth mentioning that the total time of output power ramp rate deviations was 289 hours in the year 2012. The duration of ESS operation is quite short and the energy needed to recharge the storage after continuous operation is also quite low. For example, the energy balance in the ESS at the end of the year 2012 was -6.12 kWh, when the inverter was rated at 100 % of the PV generator capacity. In order to balance the deficiency in the storage, only 6.12 hours of the PV plant production is needed.

The studies conducted in this thesis could be used to determine capacity and power rating of energy storage systems suitable to be used with PV power systems of any size. It has also been observed that the ESS can contain a lot of energy, when it uses the cut

off power by the inverter operating at 70 % of the PV plant capacity, to recharge itself automatically. This operating scheme opens up many possibilities. Further studies regarding such integrated recharging methods may help to further enhance the values of PV power systems.

REFERENCES

[1] Twidell, J. & Weir, T. Renewable energy resources ED2. 2012, Taylor & Francis.

[2] Dincer, I. Renewable energy and sustainable development: a crucial review. Renewable and Sustainable Energy Reviews 4(2000)2, pp. 157-175.

[3] Hegedus, S. & Luque, A. Achievements and challenges of solar electricity from photovoltaics. Handbook of photovoltaic science and engineering (2011) pp. 2-38.

[4] World Energy Outlook 2013. European Union. [viitattu 5/28]. Saatavissa: http://www.iea.org/newsroomandevents/speeches/131112_WEO2013_Presentation.pdf.

[5] ROADMAP 2050. [viitattu 6/1]. Saatavissa: http://www.roadmap2050.eu/project/roadmap-2050.

[6] Solar (PV and CSP). [viitattu 5/28]. Saatavissa: http://www.iea.org/topics/solarpvandcsp/.

[7] Wind power. [viitattu 5/28]. Saatavissa: http://www.iea.org/topics/windpower/.

[8] Häberlin, H. Photovoltaics System Design and Practice. 1st ed. United Kingdom 2012, John Wiley & Sons, Ltd.

[9] Wenham, S.R., Green, M.A., Watt, M.E. & Corkish, R. Applied Photovoltaics. 2nd ed. UK, USA 2007, Earthscan.

[10] Messenger, R.A. & Ventre, J. Photovoltaic Systems Engineering. 2nd ed. 2005, CRC Press.

[11] Maki, A. & Valkealahti, S. Effect of Photovoltaic Generator Components on the Number of MPPs Under Partial Shading Conditions. Energy Conversion, IEEE Transactions on 28(2013)4, pp. 1008-1017.

[12] Lobera, D.T. & Valkealahti, S. Mismatch losses in PV power generators caused by partial shading due to clouds. Power Electronics for Distributed Generation Systems (PEDG), 2013 4th IEEE International Symposium on, 2013, pp. 1-7.

[13] Subudhi, B. & Pradhan, R. A Comparative Study on Maximum Power Point Tracking Techniques for Photovoltaic Power Systems. Sustainable Energy, IEEE Transactions on 4(2013)1, pp. 89-98.

[14] Nedumgatt, J.J., Jayakrishnan, K.B., Umashankar, S., Vijayakumar, D. & Kothari, D.P. Perturb and observe MPPT algorithm for solar PV systems-modeling and simulation. India Conference (INDICON), 2011 Annual IEEE, 2011, pp. 1-6.

[15] Femia, N., Petrone, G., Spagnuolo, G. & Vitelli, M. Optimization of perturb and observe maximum power point tracking method. Power Electronics, IEEE Transactions on 20(2005)4, pp. 963-973.

[16] Eltawil, M.A. & Zhao, Z. Grid-connected photovoltaic power systems: Technical and potential problems—A review. Renewable and Sustainable Energy Reviews 14(2010)1, pp. 112-129.

[17] Calais, M., Myrzik, J., Spooner, T. & Agelidis, V.G. Inverters for single-phase grid connected photovoltaic systems-an overview. Power Electronics Specialists Conference, 2002. pesc 02. 2002 IEEE 33rd Annual, 2002, pp. 1995-2000.

[18] Hadjipaschalis, I., Poullikkas, A. & Efthimiou, V. Overview of current and future energy storage technologies for electric power applications. Renewable and Sustainable Energy Reviews 13(2009)6–7, pp. 1513-1522.

[19] Alanne, K. & Saari, A. Distributed energy generation and sustainable development. Renewable and Sustainable Energy Reviews 10(2006)6, pp. 539-558.

[20] Korpaas, M., Holen, A.T. & Hildrum, R. Operation and sizing of energy storage for wind power plants in a market system. International Journal of Electrical Power & Energy Systems 25(2003)8, pp. 599-606.

[21] Chen, H., Cong, T.N., Yang, W., Tan, C., Li, Y. & Ding, Y. Progress in electrical energy storage system: A critical review. Progress in Natural Science 19(2009)3, pp. 291-312.

[22] Ibrahim, H., Ilinca, A. & Perron, J. Energy storage systems—Characteristics and comparisons. Renewable and Sustainable Energy Reviews 12(2008)5, pp. 1221-1250.

[23] Baker, J.N. & Collinson, A. Electrical energy storage at the turn of the Millennium. Power Engineering Journal 13(1999)3, pp. 107-112.

[24] Ritchie, A.G. Recent developments and future prospects for lithium rechargeable batteries. Journal of Power Sources 96(2001)1, pp. 1-4.

[25] Wakihara, M. Recent developments in lithium ion batteries. Materials Science and Engineering: R: Reports 33(2001)4, pp. 109-134.

[26] Scrosati, B. & Garche, J. Lithium batteries: Status, prospects and future. Journal of Power Sources 195(2010)9, pp. 2419-2430.

[27] Scrosati, B. Recent advances in lithium ion battery materials. Electrochimica Acta 45(2000)15–16, pp. 2461-2466.

[28] Chalk, S.G. & Miller, J.F. Key challenges and recent progress in batteries, fuel cells, and hydrogen storage for clean energy systems. Journal of Power Sources 159(2006)1, pp. 73-80.

[29] Weinmann, O. Hydrogen-the flexible storage for electrical energy. Power Engineering Journal 13(1999)3, pp. 164-170.

[30] Steinfeld, A. Solar thermochemical production of hydrogen—a review. Solar Energy 78(2005)5, pp. 603-615.

[31] Steinfeld, A. & Palumbo, R. Solar thermochemical process technology. Encyclopedia of physical science and technology 15(2001)1, pp. 237-256.

[32] Lovegrove, K., Luzzi, A., Mccann, M. & Freitag, O. Exergy analysis of ammonia-based solar thermochemical power systems. Solar Energy 66(1999)2, pp. 103-115.

[33] Joerissen, L., Garche, J., Fabjan, C. & Tomazic, G. Possible use of vanadium redox-flow batteries for energy storage in small grids and stand-alone photovoltaic systems. Journal of Power Sources 127(2004)1–2, pp. 98-104.

[34] Hasnain, S.M. Review on sustainable thermal energy storage technologies, Part I: heat storage materials and techniques. Energy Conversion and Management 39(1998)11, pp. 1127-1138.

[35] Wen, D.S., Chen, H.S., Ding, Y.L. & Dearman, P. Liquid nitrogen injection into water: Pressure build-up and heat transfer. Cryogenics 46(2006)10, pp. 740-748.

[36] Jacobi, J. Fast Response Energy Storage Devices. ScottMadden. January 2009, [viitattu 07/26]. Saatavissa: http://www.scottmadden.com/insight/259/fast-response-energy-storage-devices.html.

[37] Divya, K. & Østergaard, J. Battery energy storage technology for power systems—An overview. Electric Power Systems Research 79(2009)4, pp. 511-520.

[38] Poullikkas, A. A comparative overview of large-scale battery systems for electricity storage. Renewable and Sustainable Energy Reviews 27(2013) pp. 778-788.

[39] Hill, C.A., Such, M.C., Chen, D., Gonzalez, J. & Grady, W.M. Battery energy storage for enabling integration of distributed solar power generation. Smart Grid, IEEE Transactions on 3(2012)2, pp. 850-857.

[40] Marcos, J., Marroyo, L., Lorenzo, E. & García, M. Smoothing of PV power fluctuations by geographical dispersion. Progress in Photovoltaics: Research and Applications 20(2012)2, pp. 226-237.

[41] Marcos, J., Storkël, O., Marroyo, L., Garcia, M. & Lorenzo, E. Storage requirements for PV power ramp-rate control. Solar Energy 99(2014) pp. 28-35.

[42] Marcos, J., Marroyo, L., Lorenzo, E., Alvira, D. & Izco, E. Power output fluctuations in large scale PV plants: one year observations with one second resolution and a derived analytic model. Progress in Photovoltaics: Research and Applications 19(2011)2, pp. 218-227.